

AMERICAN UNIVERSITY OF BEIRUT

REGULATION OF CERAMIDE BY THE NOVEL  
SYNTHETIC RETINOID ST1926-INDUCED CELL DEATH  
IN HTLV-1 TRANSFORMED AND MALIGNANT T CELLS

by  
BOTHEINA KHALIL GHANDOUR

A thesis  
submitted in partial fulfillment of the requirements  
for the degree of Master of Science  
to the Department of Biochemistry and Molecular Genetics  
of the Faculty of Medicine  
at the American University of Beirut

Beirut, Lebanon  
May 2014

AMERICAN UNIVERSITY OF BEIRUT

REGULATION OF CERAMIDE BY THE NOVEL  
SYNTHETIC RETINOID ST1926-INDUCED CELL DEATH IN  
HTLV-1 TRANSFORMED AND MALIGNANT T CELLS

by  
BOTHEINA KHALIL GHANDOUR

Approved by:



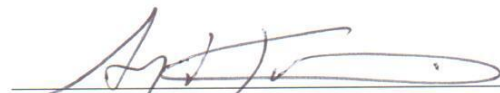
Dr. Nadine Darwiche, Professor  
Department of Biochemistry and Molecular Genetics

Advisor



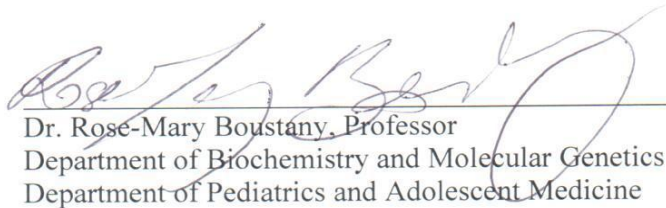
Dr. Ghassan Dbaibo, Professor  
Department of Biochemistry and Molecular Genetics  
Department of Pediatrics and Adolescent Medicine

Co-Advisor



Dr. Ayad Jaffa, Professor  
Department of Biochemistry and Molecular Genetics

Member of Committee



Dr. Rose-Mary Boustany, Professor  
Department of Biochemistry and Molecular Genetics  
Department of Pediatrics and Adolescent Medicine

Member of Committee

Date of thesis/dissertation defense: May 6, 2014

# AMERICAN UNIVERSITY OF BEIRUT

## THESIS, DISSERTATION, PROJECT RELEASE FORM

Student Name: Ghandour Botheina Khalil  
Last First Middle

Master's Thesis       Master's Project       Doctoral Dissertation

I authorize the American University of Beirut to: (a) reproduce hard or electronic copies of my thesis, dissertation, or project; (b) include such copies in the archives and digital repositories of the University; and (c) make freely available such copies to third parties for research or educational purposes.

I authorize the American University of Beirut, **three years after the date of submitting my thesis, dissertation, or project**, to: (a) reproduce hard or electronic copies of it; (b) include such copies in the archives and digital repositories of the University; and (c) make freely available such copies to third parties for research or educational purposes.

Botheina May 19, 2014  
Signature Date

This form is signed when submitting the thesis, dissertation, or project to the University Libraries

## ACKNOWLEDGEMENTS

I would like to thank all the people whose efforts led to the success of my Masters thesis.

First of all, Dr. Nadine Darwiche, you were more than an advisor to me. Even though the words cannot fairly describe it, I would like to thank you deeply for all the precious advice you offered all the way through.

My coadvisor Dr. Ghassan Dbaibo, thank you so much for making me learn that great results can be achieved while adopting a vigilant and discreet attitude.

I would also like to thank my committee members, Dr. Ayad Jaffa, and Dr. Rose-Mary Boustany, for their support and cooperation, as well as their understanding of my very tight deadline notices.

Finally, I would like to thank Dr. Darwiche's lab members, Bariaa, Melody, Raed, and Rana for their friendly attitude and support. Dr. Dbaibo's lab members, thank you for your help throughout my thesis.

It was my pleasure knowing every one of you.

## AN ABSTRACT OF THE THESIS OF

Botheina Khalil Ghandour for Master of Science;                      Major: Biochemistry

Title: Regulation of Ceramide by the Novel Synthetic Retinoid ST1926-Induced Cell Death in HTLV-1 Transformed and Malignant T Cells

Adult T cell Leukemia/lymphoma (ATL) is an aggressive malignancy caused by human T cell lymphotropic virus type 1 (HTLV-1). The oncoprotein Tax maintains viral persistence and pathogenesis and plays a crucial role in disease development. Because of resistance to chemotherapy, ATL carries a poor prognosis, which imposes a need for alternative therapies. ST1926 (E-3-(40-Hydroxy-30-adamantylbiphenyl-4-yl) acrylic acid) is a novel and orally bioavailable synthetic retinoid that has entered Phase I clinical trials. ST1926 has shown potent apoptotic activities and anticancer properties in several cancer models that are resistant to natural retinoids such as all-*trans* retinoic acid (ATRA). We demonstrated that pharmacologically achievable concentrations of ST1926 induced major cell growth inhibition in HTLV-1 positive and negative malignant T cells as well as in primary ATL cells, while no effect was detected in resting or activated normal lymphocytes. ST1926 induced massive apoptosis and upregulated p53 proteins in malignant T cells, while it caused an early reduction of Tax proteins in HTLV-1 positive cells.

Over the past two decades, studies have established ceramide as a potent lipid tumor-suppressor mediating multiple signaling pathways that ultimately determine cell fate response such as cell cycle arrest, apoptosis, and differentiation. The aim of the present study was to investigate the mechanism by which ST1926 regulates ceramide metabolism in HTLV-1 positive and negative malignant T cells. Interestingly, pharmacologically achievable concentrations of ST1926 caused early dose-dependent increases in ceramide levels in both cell types which preceded ST1926-induced growth suppression. ST1926 induced *de novo* ceramide synthesis in HTLV-1 positive and negative malignant cells and an earlier reduction of Tax protein levels in HTLV-1 positive cells. Most importantly, high-throughput sphingolipidomics analysis of ST1926-treated malignant T cells revealed pronounced accumulation of ceramide *versus* dihydroceramide species in both types of malignant T cells.

At the mitochondrial level, the intrinsic pathway of apoptosis is tightly regulated by the Bcl-2 family members and orchestrated by the bioactive sphingolipid ceramide. At this level, the pro-apoptotic ceramide was shown to antagonize the effects of Bcl-2 oncoprotein in a multitude of pathways. We dissected the interplay between the anti-apoptotic protein Bcl-2 and ceramide. We observed that Bcl-2 attenuated ST1926 growth-inhibitory response and interrupted both *de novo* ceramide accumulation and cell death in Molt-4 cells. Our results demonstrate the involvement of ceramide in ST1926-induced cell death effect.

Understanding ceramide metabolism and functions plays a crucial role in the development of novel therapeutic targets in cancer.

## CONTENTS

	Page
ACKNOWLEDGEMENTS.....	v
ABSTRACT.....	v
LIST OF ILLUSTRATIONS.....	vii
LIST OF TABLES.....	vii
LIST OF ABBREVIATIONS.....	viii
Chapter	
I.	
INTRODUCTION.....	1
A. Adult T cell Leukemia/Lymphoma.....	1
1. Historical Overview.....	1
2. Epidemiology and Routes of Transmission.....	2
3. Clinical Manifestation and Classification of ATL.....	3

B. Tax Oncogene Expression Dictates the Fate of HTLV- Infected Cells.....	3
C. Tax Promotes the Survival and Proliferation of HTLV-1 Infected Cells.....	5
1. Cell Cycle.....	7
2. Apoptosis.....	7
3. DNA Damage.....	8
4. Regulation of CREB and NF- $\kappa$ B pathway.....	9
D. Treatment Options of ATL.....	11
E. Retinoids.....	14
1. Overview.....	14
2. Retinoids Mechanism of Action.....	15
3. Retinoids in the Treatment of Leukemias.....	16
F. Synthetic Retinoids.....	17
1. HPR.....	17
2. CD437.....	18
G. ST1926: A Potent Analogue of CD437 with Promising Anti-tumor Activities.....	18
1. Overview.....	18

2. ST1926 Mechanism of Action.....	20
3. Antitumor Activities of ST1926 in Different Malignancies.....	20
a. APL Treatment.....	20
b. Neuroblastoma.....	21
c. Ovarian Carcinoma.....	22
H. Ceramide.....	22
1. Introduction.....	22
2. Ceramide Biosynthesis and Degradation.....	23
3. Ceramide Accumulation and Apoptosis.....	26
4. Mitochondrial Ceramide and Apoptosis.....	28
5. Ceramide and the synthetic retinoids, HPR and CD437.....	32
I. Aim of the Study.....	33
<b>I. MATERIALS AND METHODS.....</b>	<b>34</b>
A. Cell Culture.....	34
1. HTLV-1 Positive and Negative Malignant T-cell Lines.....	34
2. Isolation of Peripheral Blood Mononuclear Cells.....	35
3. Primary ATL Cells.....	35
B. Cell Growth and Treatment.....	36
1. Cell Passaging.....	36
2. Preparation of ST1926.....	37
C. Cell Growth Assays.....	37
D. Cell Cycle Analysis.....	38
E. TUNEL.....	38
F. Immunoblot Assays.....	39
1. Protein Extraction.....	39



2. Gel Casting.....	39
3. Gel Running and Protein Transfer.....	40
4. Hybridization and Protein Detection.....	41
G. Determination of Ceramide Levels.....	42
1. Lipid Extraction.....	42
2. Ceramide Measurement.....	42
3. Lipid Phosphate Measurement.....	43
H. <i>De Novo</i> Ceramide synthesis.....	44
I. Liquid Chromatography-Mass Spectrometry (LC-MS).....	44
1. Sample Preparation.....	44
2. Liquid Chromatography-Mass Spectrometry (LC-MS).....	45
a. Mechanism of Electropray Ionization Mass Spectrometry (ESI-MS).....	45
b. Cer, dhCer Molecular Species Identification.....	46
3. Quantitation.....	46
J. Densitometric Analysis.....	47
K. Statistical Analysis.....	47
<b>III. RESULTS.....</b>	<b>48</b>
A. ST1926 Induces Growth Inhibition in Malignant T Cells, Primary ATL Cells, but not Normal Lymphocytes.....	48
1. HTLV-1 Positive are Sensitive to ST1926.....	48
2. HTLV-1 Negative are Sensitive to ST1926.....	50
3. ST1926 Induces Growth Inhibition in Primary ATL Cells.....	50
4. Normal Lymphocytes are Resistant to ST1926.....	52
B. ST1926 Induces Cell Cycle Arrest and Apoptosis in HTLV-1 Transformed and Malignant T Cells.....	54
1. Treatment with ST1926 Causes G <sub>1</sub> Arrest and Accumulation of Cells in the PreG <sub>1</sub> Region.....	54
2. ST1926 Induces Massive Apoptosis in all Tested Malignant T Cells.....	57
C. ST1926 Reduces Oncoprotein Tax Levels	

and Induces p53 Activity.....	59
1. ST1926 Treatment Results in Reduced Levels of Oncoprotein Tax.....	59
2. ST1926 Upregulates Total and Phosphorylated p53 Protein Levels in HTLV-1 Transformed and Malignant T Cells, While Maintaining a p53-independent Growth-Suppressive Effect.....	60
D. ST1926 Induces an Early Time-dependent Accumulation of Ceramide in Both HTLV-1 Transformed and Negative Malignant T Cells.....	64
E. ST1926 Stimulates a Dose-dependent Accumulation of Ceramide in HTLV-1 Transformed and Malignant T Cells.....	68
F. ST1926 Induces Early De Novo Ceramide Synthesis in HTLV-1 Positive and HTLV-1 Negative Malignant T Cells.....	71
G. Ceramide, but not Dihydroceramide Species, Predominantly Accumulate in Response to ST1926 Treatment in HTLV-1 Positive and HTLV-1 Negative Cells.....	73
H. Bcl-2 Attenuates ST1926-Induced Cell Growth Arrest in Molt-4 cells.....	80
I. Bcl-2 Delays Cell Death Response and Interferes with Ceramide Generation Mediated by ST1926 in Molt-4 Cells.....	82
J. Bcl-2 Inhibits De Novo Ceramide Synthesis in Response to ST1926 in Molt-4 Cells.....	85

## IV. DISCUSSION

## REFERENCES

## ILLUSTRATIONS

Figure

Page

1. The natural history of HTLV-1 infection.....	4
2. The various functional domain found in Tax.....	6
3. Chemical structures of CD437 and ST1926.....	19
4. Metabolic pathways of ceramide.....	25
5. Compartmentalized pathways of ceramide signaling.....	31
6. ST1926 treatment of HTLV-1 positive cells causes a concentration- and time-dependent growth suppression.....	49
7. ST1926 treatment of HTLV-1 negative cells causes a concentration and time-dependent growth suppression.....	51
8. Primary ATL cells are sensitive to ST1926.....	52
9. Resting and Activated T-lymphocytes are resistant to suprapharmacological concentrations of ST1926.....	53
10. ST1926 induces cell cycle arrest in HTLV-1 positive and HTLV-1 negative human T Cells.....	55
11. Histogram analysis of the effects of ST1926 on the cell cycle distribution of HuT-102, MT-2, Jurkat, and Molt-4 cells .....	56
12. ST1926 induces apoptosis at 24 h by TUNEL positivity in all tested HTLV-1 positive and negative malignant T-cells.....	58
13. ST1926 degrades Tax protein in HuT-102 and MT-2.....	60
14. ST1926 upregulates p53 and its phosphorylated form in HTLV-1 positive cells and HTLV-1 negative cells.....	62
15. ST1926 growth-suppressive effect is p53-independent in Molt-4 cells.....	63
16. ST1926 treatment causes early accumulation in ceramide levels in HTLV-1 positive (HuT-102 and MT-2) human T-cell lines.....	65

17. ST1926 treatment causes early accumulation in ceramide levels in HTLV-1 negative malignant cells (Jurkat and Molt-4).....	67
18. Dose-response to ST1926 treatment in HTLV-1 positive human T cells.....	69
19. Dose-response to ST1926 treatment in HTLV-1-negative human T cells.....	70
20. A. ST1926 induces <i>de novo</i> ceramide synthesis in HTLV-1 positive (HuT-102) and HTLV-1 negative malignant T-cells.....	72
B. ST1926 causes early degradation of Tax oncoprotein levels in HuT-102 cells.....	72
21. Medium-chain dihydroceramide/ceramide species levels in HTLV-1 positive and HTLV-1 negative cells in response to ST1926.....	76
22. Long-chain dihydroceramide/ceramide species levels in HTLV-1 positive and HTLV-1 negative cells in response to ST1926.....	76
23. Very long-chain dihydroceramide/ceramide species levels in HTLV-1 positive and HTLV-1 negative cells in response to ST1926.....	76
24. Bcl-2 attenuates ST1926-induced growth suppression in Molt-4 cells.....	81
25. A. Bcl-2 interrupts ST1926-induced cell death and ceramide accumulation in Molt-4 Cells.....	84
B. Bcl-2 interferes with ceramide generation mediated by ST1926 in Molt-4 cells.....	84
26. Bcl-2 inhibits ST1926-induced <i>de novo</i> synthesis of ceramide in Molt-4 cells.....	86

## TABLES

Table

Page

1. Chain length specific effects of ceramides on tumor growth and apoptosis.....	28
2. Percent increase in total ceramide and dihydroceramide species in HuT-102 and Molt-4 Cells.....	79
3. Percent Increase of medium long chain (MLC), long chain (LC), and very long chain (VLC) ceramide and dihydroceramide species in HuT-102 and Molt-4 cells.....	79

## ABBREVIATIONS

Allo-HSCT transplantation	allogeneic hematopoietic stem cell
AML	acute myeloid leukemia
APL	acute promyelocytic leukemia
AsO <sub>3</sub>	arsenic trioxide
ATF	activating transcription factor
ATL	adult T-cell leukemia/lymphoma
ATM	ataxia telangiectasia mutated
ATRA	all- <i>trans</i> retinoic acid
AZT	zidovudine
Bcl	B cell lymphoma
Bp	base pair
BPR	base excision repair
C	carbon
Ca	Calcium
cAMP	cyclic adenosine monophosphate
CBP	CREB binding protein
CD437	6-[3-(1-adamantyl)-4-hydroxyphenyl] -2- naphthalene carboxylic acid
CDK	cyclin dependent kinase

CDKI	cyclin dependent kinase inhibitor
Cer	ceramide
CerS	ceramide synthase
Chk	Checkpoint
CoA	Coenzyme A
c-RA	<i>cis</i> retinoic acid
CRE	cyclic AMP response element
CREB	cyclic AMP response element binding protein
ddH <sub>2</sub> O	double distilled water
DGK	diacylglycerol kinase
dhCer	dihydroceramide
DMSO	dimethylsulfoxide
DNA	deoxyribonucleic acid
DR	death receptor
DSB	double strand breaks
DSBR	double strand break repair
EGFR	endothelial growth factor receptor
ELISA	enzyme-linked immuno-sorbent assay
ESI-MS	electrospray ionization-mass spectrometry
FBS	fetal bovine serum
FACS	fluorescence activated cell sorter
HAT	histone acetylase transferase
HDAC	histone deacetylase

HPR	N-(4-hydroxyphenyl)retinamide
HPV	human papilloma virus
hTert	human telomerase
HTLV-1	human T-cell lymphotropic virus type-1
H <sub>2</sub> O <sub>2</sub>	hydrogen peroxide
HO·	hydroxyl radical
IAP	inhibitor of apoptosis protein
IFN	interferon
IκB	inhibitor of kappa b
IL-2	interleukin 2
IL-2	interleukin 2 receptor
IKK	inhibitor of IκB
KIX	kinase inducible domain interacting
LC	long-chain
LC/MS	liquid chromatography/mass spectrometry
LDH	lactate dehydrogenase
LIC	leukemia initiating cells
LTR	long terminal repeat
μM	micromolar
MAPK	mitogen activated protein kinase
MDC1	mediator of DNA damage checkpoint 1
MLC	medium long-chain



MMR	mismatch repair
MN	micronuclei
MPP	mitochondrial permeability potential
MRM	multiple-reaction-monitoring
m/z	mass/charge
NB	neuroblastoma
Nbs	Nijmegen breakage syndrome
NEMO	NF- $\kappa$ B essential modulator
NER	nuclear excision repair
NES	nuclear export signal
NF $\kappa$ B	nuclear factor kappa b
NK	natural killer
Nmol	nanomole
OD	optical density
O <sub>2</sub> <sup>-</sup>	superoxide anion
PARP	Poly (ADP-ribose) polymerase
PCNA	proliferating cell nuclear antigen
PBMC	peripheral blood mononuclear cells
PBS	phosphate-buffered saline
PHA	phytohemagglutinin
P <sub>i</sub>	inorganic phosphate
PI	propidium iodide
Pmol	picomol

PML	promyelocytic leukemia
PP1	protein phosphatase 1
PP2A	protein phosphatase 2A
PS341	proteasome inhibitor
c-RA	<i>cis</i> -retinoic acid
RAR	retinoic acid receptor
RARE	retinoic acid response element
RB	retinoblastoma
RNA	ribonucleic acid
ROS	reactive oxygen species
RRM	retinoid related molecules
RXR	retinoid X receptor
RXRE	retinoid X response element
R123	rhodamine 123
SCID	severe combined immunodeficiency
SD	standard deviation
SDS	sodium dodecyl sulfoxide
Ser	serine
SR	serine-arginine
SRF	serum response factor
ST1926	E-4-(4'-hydroxy-3'-adamantyl biphenyl-4-yl) acrylic acid
TEMED	N,N,N',N'-tetramethylethylenediamine

TLC	thin layer chromatography
TNF	tumor necrosis factor
TRAIL	tumor necrosis factor-related apoptosis inducing ligand
TSP/HAM	tropical spastic paraplegia/HTLV-1 associated myelopathy
TUNEL	dUTP nick end labeling
VEGF	vascular endothelial growth factor
VLC	very long-chain

# CHAPTER I

## INTRODUCTION

### **A. Adult T Cell Leukemia/Lymphoma**

#### *1. Historical Overview*

HTLV-1 associated adult T cell leukemia/lymphoma (ATL) is an aggressive and fatal neoplasm of CD4<sup>+</sup> T lymphocytes (Baydoun 2008). First described in 1977 by Uchiyama and Takatsuki as a progressive peripheral T lymphocytic malignancy, ATL emerged as unusual clusters in specified areas of Japan suggesting a transmissible mediator of the disease (Baydoun 2008, Tsukasaki 2013). Successively, in the late 1970s, a novel viral etiology of the disease was resolved based on the presence of antibodies against HTLV-1 antigens in the sera of ATL patients; in addition to the isolation of HTLV-1 from a cell line established by Minna and Gazdar from a patient with cutaneous T cell lymphoma (Gallo 2005). Consequently, HTLV-1 was recognized as the first retrovirus associated with human disease (Matsuoka 2003).

Besides being included among human carcinogenic pathogens, HTLV-1 is also the causative agent of a neurological disease called HTLV-1 associated myelopathy/tropical spastic paraplegia (TSP/HAM) (Bazarbachi 2004). TSP/HAM is characterized by the continuous demyelination of long motor neurons of the spinal cord that leads to a debilitating inflammatory disease of the central nervous system (Nasr 2011). Meanwhile, HTLV-1 is also an important risk factor for opportunistic infections such as the parasite

*Strongyloides stercoralis* because of the subsequent severe immunosuppression caused by the disease (Carvalho 2004).

## ***2. Epidemiology and Routes of Transmission***

HTLV-1 can be transmitted mainly by three routes which are mother-to-child *via* breast-feeding, blood transfusions, and sexual intercourse (Tsukasaki 2012). HTLV-1 causes T cell transformation and development of ATL after a mean latency period of over 50 years in 3-5% of the approximate 10-20 million HTLV-1 asymptomatic carriers (Marcais 2013). The incidence and frequency vary by country and there have been a worldwide collection of data related to prevalence, geographic distribution, clinical features, biologic variability and outcomes of ATL. ATL usually appears in individuals from HTLV-1-endemic areas such as Japan, the Caribbean, inter-tropical and South Africa, Central and South America, some regions of Romania, northern Iran, and the Middle East (Bazarbachi 2011, Nasr 2011).

Bitar *et al* reported the presence of the first two ATL cases in Lebanon (Bitar 2009). The first patient of Lebanese origin presented with acute ATL and the second patient of Romanian origin developed early relapse after autologous transplantation for ATL. Both patients had similar clinical manifestations such as lymphocytosis, severe hypercalcemia, and CD25<sup>+</sup> T-cell immunophenotype on peripheral blood. After serological examination, both patients tested positive for HTLV-1 as evidenced by enzyme-linked immunosorbent assay (ELISA). Strikingly, seven family members of the first patient were also carriers of HTLV-1 upon screening, while four of them were regular blood donors.

### ***3. Clinical Manifestation and Classification of ATL***

ATL is classified into four subtypes defined by diverse diagnostic criteria based on the complications of organ involvement, LDH, as well as  $\text{Ca}^{2+}$  levels (Tsukasaki 2012). The most commonly involved organs are lymph nodes, spleen, liver, and skin (Tsukasaki 2013). Thus, these sub-categories are now identified as: acute (60% of cases), chronic (15%), smoldering (5%) and adult T-cell lymphoma (20%) based on their different clinical presentations and prognosis, and these are essential for assigning treatment strategies (Bazarbachi 2004, Tsukasaki 2013). Well known as “flower cells”, ATL cells can be easily detected in the blood of patients except for the smoldering type (Tsukasaki 2013). These malignant activated lymphocytes are presented with convoluted nuclei and basophilic cytoplasm as shown by the histological and cytological infiltrations in the lung and skin of infected patients (Bazarbachi 2004).

#### **B. Tax Oncogene Expression Dictates the Fate of HTLV- Infected Cells**

The long latency period which precedes the onset of ATL suggests a multistep process in the development and oncogenesis of the disease (Figure 1). However, a clear elucidation of the overall cellular and molecular mechanisms still lags behind. Meanwhile, HTLV-1 infection appears to be responsible for the first events that enhance carcinogenesis of ATL. Moreover, it is proposed that multiple factors, such as the involvement of viral proteins in the genetic and epigenetic alterations of host genome, and immune status of the hosts, could be implicated in leukemogenesis of ATL (Yasunaga 2007). Based on this insight, one of these viral regulatory proteins, Tax, has proven to exert critical pleiotropic actions that induce transformation of HTLV-1 infected cells, and lead to cell cycle

progression, cell death, and angiogenesis *in vivo* (Kfoury 2005). Once cell-to-cell transmission occurs, HTLV-1 increases its copy number by the oligoclonal expansion of infected cells. In this respect, the viral transactivator protein Tax plays a crucial role in this initial stage of infection, ultimately enhancing proliferation and inhibiting apoptosis (Taylor 2005).

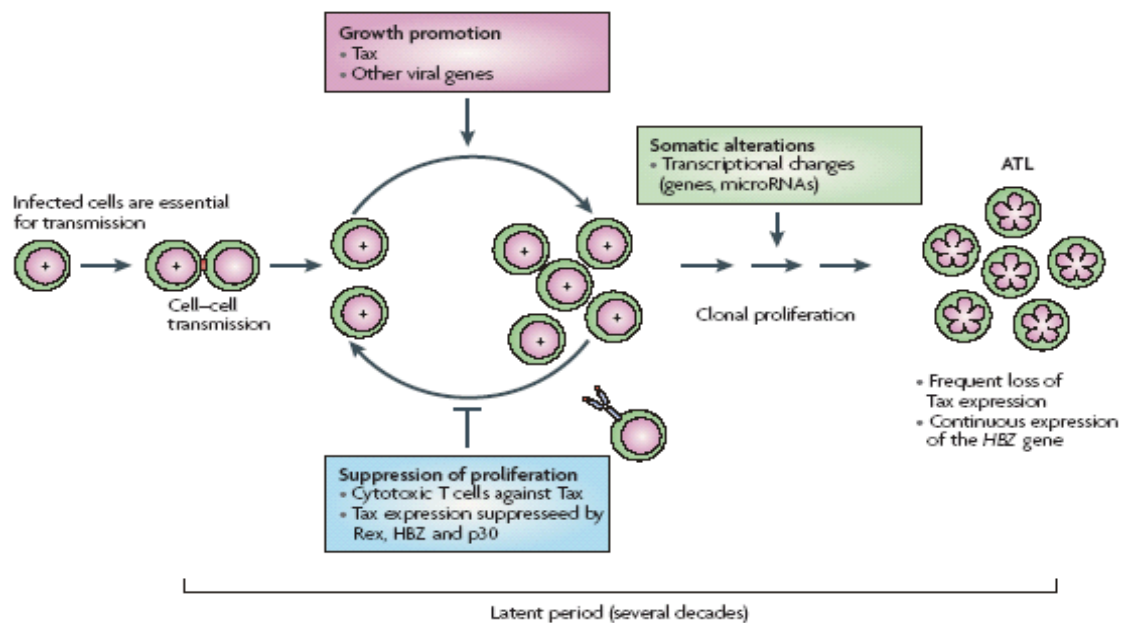


Figure 1. The natural history of HTLV-1 infection.

Source: Matsuoka, M., & Jeang, K. T. 2007. Human T-cell leukemia virus type 1 (HTLV-1) infectivity and cellular transformation. *Nature Reviews Cancer*, 7(4): 270-280

Tax is a moderately small phosphoprotein (40 kDa) and is encoded by the pX region of viral genome, and it predominantly localizes to the nucleus of infected cells. However, it can also shuttle to the cytoplasm using nuclear export signals (NES) (Kfoury 2005). There is accumulating evidence owing to the oncogenic potential of Tax. Tax expression in rat fibroblasts and primary T cell lines was shown to induce their

transformation and immortalization *in vitro*. Indeed, *tax*-transgenic mice recapitulate a leukemia/lymphoma disease with prominent ATL features. Furthermore, modification of NOD-SCID mice with HTLV-1 *tax*-transduced human CD34<sup>+</sup> cells results in CD4<sup>+</sup> lymphomas progression (Nasr 2011). Accordingly, this holds the premise that Tax alone is sufficient to initiate and drive the leukemogenesis of ATL. However, given the fact that ATL only occurs in 3-5% of infected individuals and Tax is mostly undetectable *in vivo*, this raises a controversy whether Tax is required for the maintenance of this aggressive phenotype (Nasr 2011).

### **C. Tax Promotes the Survival and Proliferation of HTLV-1 Infected Cells**

HTLV-1 is a retrovirus that gets integrated into the host genome after the reverse transcription of its RNA into a double-stranded DNA. Tax expression powers the transcription of viral structural genes that are needed for cell-to-cell mediated *de novo* infection and expansion (Satou 2012) (Figure 2). It has been reported that HTLV-1 persistence can only be efficiently mediated through cell-to-cell communication *via* virological synapses, rather than by free virions. In this regard, Tax plays an integral role in the oligoclonal proliferation of CD4<sup>+</sup> T cells and enhances infectivity, such that living infected cells are crucial for the maintenance and persistence of the disease (Taylor 2005).



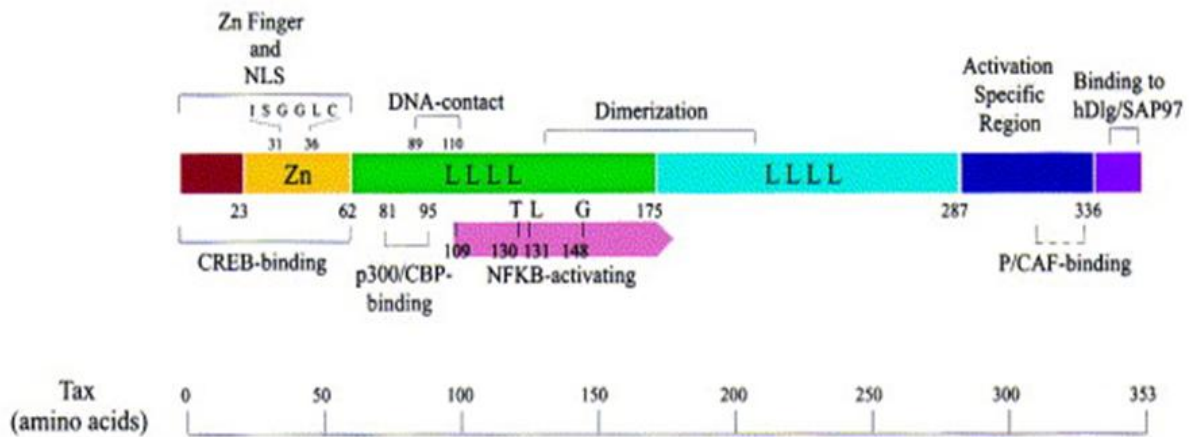


Figure 2. The various functional domains found in Tax.

Source: Jeang KT. 2001. Functional activities of the human T-cell leukemia virus type 1 Tax oncoprotein: cellular signaling through NF kappa B. *Cytokine Growth Factor Reviews*, 12: 207-217

Moreover, Tax is at the root of numerous cellular-transforming effects, such as interfering with cell cycle progression, activation of different cellular transcription factor pathways, and resisting apoptosis (Yoshida 2001). Likewise, it impacts the microenvironment through promoting angiogenesis, metalloproteinases, and gap junction-mediated communication between infected and endothelial cells, thus contributing to tumor dissemination *via* extravasation and invasiveness of ATL cells (Kfoury 2005). Moreover, Tax has pleiotropic functions that include the activation of a set of critical transcription factors such as the nuclear factor kappa-light-chain-enhancer of activated B cells (NF-κB), cyclic AMP response element-binding protein (CREB), serum responsive factor (SRF), and activated protein 1 (Nasr 2011).

## ***1. Cell Cycle***

A multitude of deregulated cell cycle control checkpoints in transformed T-cells are targeted by Tax. One of its mitogenic activities is particularly implicated in the G<sub>1</sub>/S transition, whereby it triggers various cellular responses. For instance, Tax mediates the inactivation of CDK4 by forming a complex with two cell cycle inhibitors, p16INK4a and p15INK4b, that inhibit CDK4 and result in the phosphorylation of retinoblastoma (Rb). This releases the breaks on the transcription factor E2F and facilitates the cell cycle transition from G<sub>1</sub> to S phase. Whereas Tax indirectly interferes with Rb inactivation, it forms a complex with other cell cycle regulators such as cyclin D3 at its post-translational level, inducing its phosphorylation. Furthermore, Tax can also interfere with the cell cycle progression through the transcriptional activation or repression of p18INK4c, cyclins: A, C, D2 and E, CDK2, and p21 (CIP1/WAF1) (Jeang 2004). Tax inhibits the function of tumor suppressor proteins such as p53 and p16 (Pise-Masison 1998, Suzuki 1997).

## ***2. Apoptosis***

Tax expression dictates protection from both spontaneous and chemotherapy-induced apoptosis. One of Tax anti-apoptotic functions is mediated through activation of NF-κB and cAMP pathways, and the resulting overexpression of Bcl-xL (Mori 2001, Brauweiler 1997). Furthermore, Tax blocks the transcription of the pro-apoptotic *Bax* gene and inhibits the caspase cascade *via* the NF-κB pathway which induces the expression of the inhibitors of apoptosis: X-IAP, cIAP-1, and c-IAP-2 (Kawakami 1999). Furthermore, p53 expression is elevated in several HTLV-1 transformed lymphocytic cell lines, but is sometimes mutated and in most times is functionally inactive because of the inhibitory role

of Tax. Indeed, one of the cellular effects of Tax is activation of the NF- $\kappa$ B pathway which plays a critical role in the inhibition of p53 transactivation functions (Pise-Masison 2000). Moreover, Tax alone is capable of repressing the transcriptional activity of p53 and can abrogate G<sub>1</sub> arrest and apoptosis induced by p53 (Menard 1999). Finally, Tax mediates p53 inhibition through the phosphorylation of p53 on Ser 15 and Ser 392.

### ***3. DNA Damage***

Other potential targets of the viral oncogene Tax is the DNA repair machinery of the infected T cell checkpoints. In order to conserve the integrity of genetic material, DNA repair and cell cycle progression have several mechanisms in common and may often be redundant (Pryor 2013). In response to different types of DNA damage, DNA repair occurs mainly through four overlapping mechanisms; the mismatch repair (MMR), base excision repair (BPR), nucleotide excision repair (NER), and double strand break repair (DSBR). Tax suppresses the transcription of DNA polymerase- $\beta$ , which is involved in base excision repair of DNA cuts that result from reactive oxygen species and increased mutagenesis (Pryor 2013). It also represses the nucleotide excision repair *via* p53 inactivation and transcriptional up-regulation of PCNA (Pryor 2013).

As tumor suppressor proteins, p53 and p16 inactivation by Tax interferes with the cell cycle checkpoints and increase the accumulation of mutations in HTLV-1 infected cells by repressing DNA repair (Pise-Masison 1998, Suzuki 1997, Afonso 2007). It is noteworthy that Tax inactivation of p53 does not involve direct binding to p53, but rather includes a constitutive phosphorylation of p53 at Ser 15 and Ser 392 (Pise-Masison 2000). In response to double- strand DNA breaks (DSBs), ataxia telangiectasia mutated (ATM)

phosphorylates target DNA damage regulator proteins, H2AX, Chk2, p53, Nbs1, and MDC1 that cooperate to arrest the cell cycle and repair DNA (Driscoll 2006). However, it has been found in Tax-expressing cells these ATM targets show reduced phosphorylation, thus releasing breaks from the S-phase checkpoint, while maintaining the DSBs (Chandhasin 2008, Majone 2000). Present as markers for genome instability, Tax-expressing cells form micronuclei (MN) during mitosis because of the persistence of DSBs (Majone 1993). Furthermore, Tax represses the expression of human telomerase (hTert); thus, it interferes with protective mechanisms used to prevent inappropriate breakages fusion (Jeang 2004).

Tax has also been found to bind and thus impair the function of Mad1, a mitotic spindle checkpoint constituent which is reflected as chromosomal instabilities in ATL cells (Gabet 2003, Matsuoka 2003). Altogether, these multiple activities of Tax stimulate infected T-cell proliferation, produce cellular defects, and consequently lead to transformation.

#### ***4. Regulation of CREB and NF- $\kappa$ B pathway***

Since numerous studies have underscored the sufficient role of Tax in HTLV-1 mediated lymphomagenesis (Pryor and Marriott 2013), much effort has been spent to identify the molecular mechanisms of Tax alteration of normal cellular responses, and the mediation of cellular transformation and tumorigenesis. Beside microarray analysis that has shown changes in proliferation, cell cycle, apoptosis, a multitude of genome-wide modifications also highlight the discernible influence of Tax on potential targets of several cellular pathways (Pise-masison 2001). Moreover, accumulating evidence revealed the

presence of nuclear localization and export signals, as well as activation domains specific for two essential pathways for Tax-mediated transformation, NF- $\kappa$ B, and CREB pathways (Adya 1995, Yoshida 2001). Tax modulation of these transcription factor pathways is indirect acting on proteins that interact with NF- $\kappa$ B and CREB transcription factors rather than binding DNA.

One of the notable cellular outcomes of Tax is the activation of NF- $\kappa$ B pathway, which induces the activation of a wide array of signals that are involved in immune response, inflammation, apoptosis, and angiogenesis (Sun 2003). Once sequestered in the cytoplasm, NF- $\kappa$ B family members are kept inactive by the I $\kappa$ B family of inhibitory proteins. Subsequently, their control of gene expression can only be mediated by their free translocation to the nucleus. Tax regulation of NF- $\kappa$ B pathway is maintained by several mechanisms. First, in the cytoplasm, Tax increases the phosphorylation of I $\kappa$ B by I $\kappa$ B kinase (IKK), leading to their ubiquitination and proteasomal degradation (Suzuki 1995, Chu 1998, Fu 2003). Tax-induced phosphorylation and degradation is also retained through forming a complex with NF- $\kappa$ B essential modulator (NEMO), IKK $\gamma$ , Tax, and PP2A that inhibits IKK deactivation. Second, in the nucleus, the interaction of Tax with NF- $\kappa$ B on promoters activates cellular genes that are involved in cell proliferation and resistance to apoptosis, thus maintaining the malignancy of the disease (Brockman 1995). Many of these up-regulated genes include T-cell activator genes, such as *IL-2*, *IL-2R $\alpha$*  subunit, and *IL-15*, which execute essential functions in HTLV-1 transformation and immortalization of normal T-cells. These genes are also involved in HTLV-1-infected cell proliferation and growth both *in vivo* and *in vitro* (Matsuoka 2003, Pryor 2013).

Meanwhile, Tax regulation of CREB pathway is crucial for the induction of viral gene expression through the transcriptional activation of HTLV-1 promoter long terminal repeat (LTR) which contains a Tax-responsive element of three non-palindromic 21-bp repeats (Pryor 2013). In normal cells, growth factor stimulation recruits CREB activation through the phosphorylation of CREB's kinase inducible domain, subsequent dimerization of CREB, and the resulting recruitment of CREB binding protein (CBP), forming CREB-CBP complex. As such, this complex binds CRE sequence, which is essential for Tax-mediated transactivation, leading to the expression of CREB-dependent genes (Chrivia 1993). This system is highly controlled by Tax which enhances the binding affinity of CREB for the viral TRE by increasing its dimerization (Pryor 2013). Alternatively, even in the absence of CREB phosphorylation, Tax has the ability to interact with KIX domain of CBP to augment its stabilization of Tax-CBP-TRE complex, thereby favoring CREB binding to viral LTR instead of cellular CRE, eventually bypassing the activation of CBP by cAMP signaling pathway (Chen 2004, Pryor 2013).

#### **D. Treatment Options of ATL**

Different treatment options are suggested based on the clinical subtype classification and prognostic features (Bazarbachi 2011, Tsukazaki 2013). These include “watch and wait policy”, conventional combined chemotherapy, antiretroviral therapy such as interferon alfa (IFN), zidovudine (AZT), arsenic trioxide (AsO<sub>3</sub>), allogeneic hematopoietic stem cell transplantation (allo-HSCT), monoclonal antibody, and other treatment modalities.

Patients with the indolent form of ATL (smoldering or favorable chronic subtypes) show better prognosis than acute or lymphoma subtype, so therapy is approached by watchful waiting policy or with chemotherapy until the disease progresses into a poor prognosis state (Takasaki 2010, Tsukazaki 2009).

Knowing that ATL is an aggressive neoplastic disease of mature T cells, chemotherapeutic approaches were similar to those for non-Hodgkin's Lymphoma (Yasunaga 2007). The standard treatment for ATL subtype was CHOP therapy, consisting of a combination of cyclophosphamide, hydroxydoxorubicin, vincristine, and prednisolone. It has also been shown that other powerful chemotherapeutic combinations improve prognosis of ATL, such as VCAP (vincristine, cyclophosphamide, doxorubicin, and prednisolone), AMP (doxorubicin, ranimustine, and prednisolone), and VECP (vindesine, etoposide, and carboplatin).

Nevertheless, results are still unsatisfactory because of the intrinsic resistance of ATL against chemotherapeutic drugs, consistent with overexpression of multidrug resistant genes (Gartenhaus 1996, Lau 1998), *p53* gene mutations (Sakashita 1992, Kuwazuru 1990). In addition to chemoresistance, multiple clinical effects such as immunosuppression render patients having poor prognosis with no complete remission and survival (Bazarbachi 2004).

Bazarbachi *et al* showed a very effective treatment of ATL with AZT/IFN combination especially with previously untreated acute form of the disease (Bazarbachi 1996). While the first treatment option of the acute, chronic and smoldering subtypes is a combination therapy of AZT/IFN, patients of ATL lymphoma show better outcomes with chemotherapy (Marcais 2012).

The mechanism of action of antiretroviral therapy is still not well-elucidated, but *in vitro* studies suggest AZT's inhibitory role for HTLV-1 replication (Bazarbachi 2000, Isono 1990). As part of its antiviral activities, IFN interferes with the targeting of Gag viral protein into plasma membrane lipid rafts, consequently the assembly of HTLV-1 virus. (Feng 2003). As a modulator of the immune system, IFN stimulates antigen presentation to lymphocytes, activates natural killer cells and macrophages, therefore, it boosts the resistance of host cells to viral infection and alternatively, represses tumor cell growth. (Goodbourn 2000). In addition to its safety profile, the high and complete response in patients lasts for several years (Bazarbachi 2004). However, patients very often relapse, which necessitates the need for other combined targeted therapies such as AsO<sub>3</sub>/IFN or monoclonal antibodies.

Besides being an effective treatment against acute promyelocytic leukemia (APL), the combined targeted therapy of AsO<sub>3</sub>/IFN has shown promising results with the treatment of ATL by producing cell cycle arrest in HTLV-1 positive and malignant T cells (Bazarbachi 2004). Interestingly, the combination of AsO<sub>3</sub>/IFN results in Tax proteasomal degradation, followed by reversing the constitutive activation of NF-κB pathway, as well as delayed shut off of cell cycle genes after proteasomal degradation of Tax (El-Sabban 2000, Nasr 2003). Indeed, more promising results were reported by El Hajj *et al* showing that the mentioned combination treatment selectively targets leukemia initiating cells (LIC) activity (El Hajj 2010).

Meanwhile, aggressive chemotherapy followed by the anti-retroviral therapy is affective against the lymphoma subtype to achieve a complete response and avoid chemo-resistance or relapse (Bazarbachi 2004). In addition, allogenic bone marrow transplantation



is taken into consideration with young patient, although the median age of the onset is 60 years (Marcais 2012). Patients with the smoldering and chronic subtypes are often administered with monoclonal antibodies such as antibodies against IL-2R (Bazarbachi 2011). Another monoclonal antibody against CD2 is in preclinical murine model of ATL.

Other approaches include kinase inhibitors used to inhibit angiogenesis by targeting the interaction of ATL cells with endothelial cells. This interaction triggers HTLV-1 infected cells to over-secrete vascular endothelial growth factor (VEGF) and heparin-binding growth factor to promote angiogenesis (El Sabban 2002).

Finally, the use of both natural and synthetic retinoids in several hematological malignancies is documented. For instance, although the natural retinoid all *trans*-retinoic acid (ATRA) has been used as the standard treatment for APL, HTLV-1 transformed cells show resistance due to their lack of the retinoic acid receptor  $\alpha$  (RAR  $\alpha$ ), through which ATRA exerts its antitumor effects (Darwiche 2001). However, the use of synthetic retinoids bypasses this limitation by inducing apoptosis in HTLV-1 infected cells *via* both receptor-dependent and -independent fashion (Darwiche 2004).

## **E. Retinoids**

### ***1. Overview***

The term retinoids refers to natural or synthetic derivatives of vitamin A exhibiting vitamin A activities (Chamboun 2005). As an important mediator of essential biological processes, retinoids exert their crucial role as early as during embryonic development and organogenesis, and later in adult life, as in reproduction, cell growth arrest, apoptosis, differentiation, and immune response (Chambon 2005, Freemantle 2003).

ATRA and 9-*cis* retinoic acid (c-RA) are natural derivatives of vitamin A (Germain 2006). ATRA, an endogenous metabolite of retinoids, is used to treat APL patients (De The 1990, Degos and Wang 2001, Lin 1999).

## ***2. Retinoids Mechanism of Action***

Retinoids act through binding and activating the RARs and retinoid X receptors (RXRs), which are members of the steroid/thyroid nuclear receptors, each having three subtypes ( $\alpha$ ,  $\beta$ , and  $\gamma$ ) (Fontana 2002). Differential splicing and promoter usage produce are responsible for producing the different isoforms of these three subtypes. RARs and RXRs act as ligand-dependent transcription factors via heterodimerization, which is required for their activation (Tang 2011). Unlike RARs, only RXRs can homodimerize, thus, promoting a distinct retinoic acid signaling pathway through binding to RXR response elements (RXREs) in the promoter region of target genes. Moreover, RXRs can dimerize with vitamin D, thyroid hormone, and with orphan receptors as well (Fontana 2002).

Since RAR/RXR dimers are dependent on ligands to regulate the expression of RA target genes, in the absence of ligands, they recruit co-repressors, such as histone deacetylases (HDAC) or DNA methyltransferases that condense the chromatin and prevent transcription activation. Once RAR binds to a ligand, the RAR/RXR heterodimers bind with higher affinity to co-activators instead and activate the expression of RA target genes (Tang 2011).

### ***3. Retinoids in the Treatment of Leukemias***

Interestingly, natural retinoids, such as ATRA, are shown to affect normal hematopoietic differentiation, which was reflected by their efficiency in treating several leukemias and lymphomas (Collins 2008). Particularly, ATRA is used for treatment of APL (Khanna-Gupta 2007) and ATL (Maeda 2008).

As a differentiating agent, ATRA is used for the treatment of APL cells at pharmacologically achievable concentrations (De The 1990, Degos and Wang 2001, Fenaux 2007). Indeed, ATRA induces complete remission and increases the survival of more than 90% of APL patients within 40 to 60 days (de The 1990). However, the duration of complete remission induced by ATRA is brief (3-6 months) and relapse is often associated with acquired resistance to ATRA-mediated differentiation, whose etiology appears to be multi-factorial (Freemantle 2003). Although ATL cells were found to be resistant to ATRA (Darwiche 2001, Darwiche 2004), it triggers growth arrest of LICs in mouse models (Nasr 2007, Nasr 2008).

Meanwhile, classical retinoids have limited potential in the treatment of neoplastic diseases which is attributed to their acquired resistance after long term therapy and toxic side effects, such as teratogenicity, bone toxicity, and elevation of serum triglycerides (Germain 2006). To overcome these limitations, pharmaceutical companies have developed a series of synthetic retinoids with increased specificity and decreased toxicity which mediate their action through receptor-dependent and -independent mechanisms, thus, bypassing ATRA resistance due to mutations in the retinoid receptor signaling pathway (Holmes 2003, Cincinelli 2003, Pisano 2007). However, only few of these synthetic retinoids showing anticancer properties have reached clinical trials (Crowe 2002).

## **F. Synthetic Retinoids**

Atypical or synthetic retinoids demonstrate promises in cancer treatment, particularly in hematological malignancies (Fontana 2002). Although the exact mechanism of action of these retinoids is not fully elucidated, their anti-proliferative and pro-apoptotic activities are attributed to their ability to mediate both receptor-dependent and -independent mechanisms of action. In particular, synthetic retinoids or so called retinoid related molecules (RRMs), such as N-(4-hydroxyphenyl) retinamide (HPR) and 6-[3-(1-adamantyl)-4-hydroxyphenyl]-2-naphthalene carboxylic acid (CD437) have shown interesting anti-neoplastic activities, and are the most promising synthetic retinoids used in clinical trials now.

### ***1. HPR***

Also called fenretinide, HPR was synthesized in 1978 (Gander 1978), and was shown to mediate its effect through both receptor-dependent and -independent pathways. Interestingly, HPR hinders proliferation and induce cell death in several ATRA-resistant T lymphoma cells and ATL (Darwiche 2001, Darwiche 2004). Contrary to HTLV-1 positive cells, we showed that HPR induces major loss of mitochondrial membrane potential, ceramide accumulation, activation of caspase cascade, including caspase 3, 8, 9, and complete PARP cleavage only in HTLV-1 negative T cells (Darwiche 2004). The increase in intracellular reactive oxygen species (ROS) levels results in ceramide accumulation, cell cycle arrest, cytochrome c release, caspase activation, and caspase-dependent apoptosis (Darwiche 2007). HPR-induced cell death is also observed in other human cancer cell lines including breast carcinoma, prostate adenocarcinoma, ovarian carcinoma, cervical

carcinoma, head and neck squamous cell carcinoma, small-cell lung cancer, neuroblastoma, lymphomas, and leukemias (Fontana 2002).

## **2. CD437**

CD437 exerts its effects through retinoid receptor-dependent and -independent pathways (Fontana 2002). It selectively binds to RAR $\gamma$  receptor though it can bind RAR $\beta$  and minimally RAR $\alpha$  (Bernard 1992, Chao 1997). Depending on the cancer cell type, CD437 may induce cell cycle arrest at different stages (Zhang 2000, Li XS 1996). In ATL, CD437 induces growth arrest with similar sensitivity in HTLV-1 positive and negative cells (unpublished data).

## **G. ST1926: A Potent Analogue of CD437 with Promising Anti-tumor Activities**

### **1. Overview**

ST1926 or E-4-(4'-hydroxy-3'-adamantyl biphenyl-4-yl)acrylic acid (Figure 3) is prepared in a high yielding three-step sequence where CD437 was used as the reference compound, while replacing naphthalene ring in CD437 by styrene moiety in ST1926 (Cincinelli 2003). As we have discussed earlier, HPR and CD437 have potential roles in mediating anti-tumor activities in various cancer models. Unfortunately, these synthetic retinoids have a narrow window between therapeutic and toxic doses and relatively unfavorable pharmacokinetic profile (Grattini 2004).

For these reasons, researchers have developed a new synthetic retinoid, ST1926, an adamantly derivative of CD437, with increased specificity and bioavailability (Cincinelli 2003). ST1926 has promising anti-tumor potential with broad spectrum of activity in a

large panel of cancer cell lines (Cincinelli 2003). Of particular interest, ST1926 is effective against tumor models that are resistant to ATRA (Valli 2008) and is now in Phase I clinical trials in patients with ovarian cancer (Sala 2009).

Given its potential role in cancer therapeutic field, its unique pharmacokinetic profile, and *in vivo* tolerance after oral administration, ST1926 shows promising results in several solid tumors and hematological malignancies (Garattini 2004). Most importantly, ST1926 is pharmacologically achievable in plasma of patients at micromolar ( $\mu\text{M}$ ) concentrations (Cincinelli 2003); meanwhile, it has no effect on normal resting and activated lymphocytes from normal donors (data not shown).

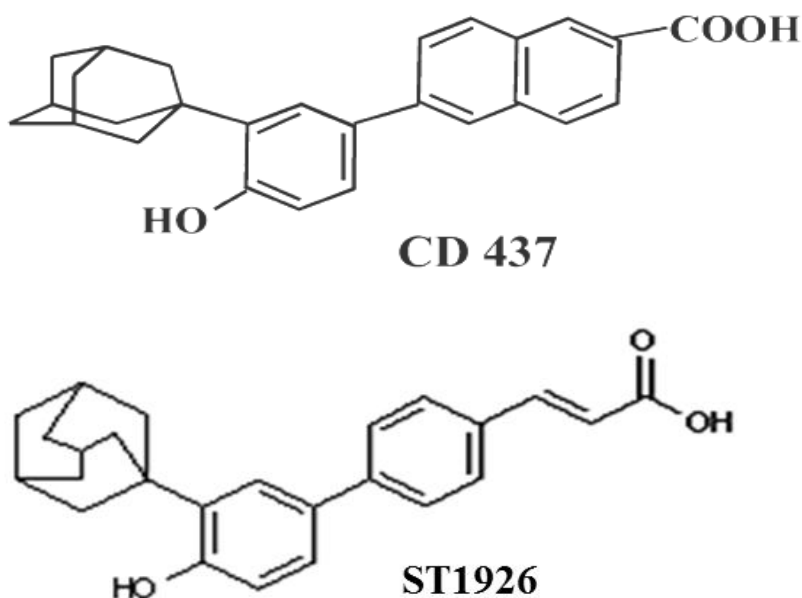


Figure 3. Chemical structures of CD437 and ST1926

## **2. *ST1926 Mechanism of Action***

Previous studies have shown that ST1926 binds to RAR $\gamma$  receptors with low affinity; on the contrary, others have demonstrated that it binds and transactivate RAR $\gamma$  (Parella 2006).

As an effective inducer of apoptosis, ST1926 mediates its action mainly through inducing several patterns of genotoxic stress and DNA damage, inducing cell death through mitochondrial pathways of apoptosis (Valli 2008). However, ST1926 causes G<sub>1</sub>/S (Pisano2004) and G<sub>2</sub>/M cell-cycle arrest prior to apoptosis (Parella 2006).

It is established that ST1926 exerts its anti-proliferative effects through p53-independent mechanisms in a variety of cell lines (Cincinelli 2003). Moreover, ST1926 induces p21 and Bax upregulation, in addition to activation of p53, and caspase 3, 8, and 9 (Grattini 2004). Moreover, compared to CD437, ST1926 induces a more powerful Ca<sup>2+</sup> mobilization from the mitochondria resulting in more potent apoptotic stimulation (Garattini 2004). ST1926 also maintains the function and increases the number of B and T cells, increases the percentage of Natural Killer (NK) cells in tumor nodules, increases TRAIL concentrations in plasma, and up-regulates FAS-ligand expression in lymphocytes (Sun 2000).

## **3. *Antitumor Activities of ST1926 in Different Malignancies***

### **a. APL Treatment**

The anti-cancer activity of ST1926 in APL has been well established.

Interestingly, ST1926 causes down-regulation of a large number of ribosomal, mitochondrial, and translation-related proteins as revealed by microarray analysis of NB4

treated cells. Therefore, *de novo* protein synthesis is not required for apoptosis induction (Garattini 2004). ST1926 causes an increase in cytosolic  $\text{Ca}^{2+}$  levels in a dose-dependent manner *via* inhibition of the energy-dependent uptake of  $\text{Ca}^{2+}$  into the mitochondria (Grattini 2004). Most importantly, orally administered ST1926 shows promising anti-leukemic activities *in vivo*. In combination with ATRA, ST1926 was markedly effective against the aggressive SCID mice transplanted with NB4 cells, which implicates the potential future use of ST1926 in combination therapy in myeloid leukemia (Garattini 2004).

New insights about the role of ST1926 in acute myeloid leukemia (AML) indicates a potential role of histone H2A.Z, cAMP-dependent protein kinase A, and the proteasome in the mechanisms underlying sensitivity/resistance to ST1926 (Fratelli 2013). Moreover, ST1926 induces DNA DSB; the underlying mechanism by which ST1926 induces its anti-leukemic effects (Valli 2008). Remarkably, DSBs were maximal during cell cycle S phase. Most importantly, DSBs are observed early after treatment and are not secondary to apoptosis (Valli 2008).

b. Neuroblastoma

In an *in vitro* neuroblastoma model (NB), Dri Fransecso *et al*, showed that ST1926 induces apoptosis independent of p53 or caspases. Of great importance, ST1926 oral administration caused tumor reduction in NB xenograts. Since all studied NB cell lines are ATRA-resistant, ST1926 provides great promise in treating NB patients, either administered alone or in combination with ATRA (Di Franseco 2007).



Di Franseco *et al* showed that combined ATRA and ST1926 boost G<sub>2</sub>/M arrest and accumulate cells in the PreG<sub>0</sub>/G<sub>1</sub> phase. In addition, this co-treatment induces apoptosis as evidenced by PARP cleavage, caspase 3, 8, and 9 activation, and modulation of death receptor 5 (DR5) and FAS (Di Franseco 2011).

c. Ovarian Carcinoma

In Ovarian carcinoma, Zuco *et al* showed that ST926 causes p53 activation and early upregulation of p53 target genes. This indicates a p53-dependent and DNA damage response in ST1926-induced apoptosis in IGROV-1 ovarian carcinoma cell line (Zuco 2004). Moreover, IGROV-1 cells revealed G<sub>1</sub> cell cycle arrest which provides evidence for the role of genotoxic stress in p53-dependent apoptosis in these cells (Zuco 2010).

Moreover, ST1926 was used in combination with HDAC inhibitor, which modulate the chromatin structure, and show enhanced DNA response that sensitize cells to apoptosis in IGROV-1 (Zuco 2010). This also emphasizes the role of DNA damage in ST1926 antiproliferative activities (Zuco 2003).

## **H. Ceramide**

### ***1. Introduction***

Sphingolipids are a class of lipids which have a backbone of sphingoid base in common. Sphingolipids were first discovered by the German biochemist, Thudichum in 1884, and the term derives its name from the Great Sphinx because of its mysterious (“Sphinx-like”) properties (Merill 1997). It has been long thought that sphingolipids play merely structural role in the regulation of plasma membrane fluidity and lipid rafts

(Ogretmen and Hannun 2004). However, there have been emerging evidence that shows sphingolipids act as effector molecules and play a crucial role in several biological processes (Ponnusamy 2010). In particular ceramide, the central molecule of sphingolipid metabolism, functions as a lipid tumor suppressor that regulates cancer cell growth, cell cycle, apoptosis, stress response, differentiation, senescence, and inflammation (Hannun 2002, Ogretmen and Hannun 2004). The anti-cancer effects of ceramide have been elucidated in studies that utilize exogenous C2- and C6-ceramides, and/or generation of endogenous ceramide *via de novo* synthesis or hydrolysis of sphingomyelin upon apoptotic stimuli combined with the use of inhibitors of the enzymes of ceramide metabolism (Huang 2011).

## ***2. Ceramide Biosynthesis and Degradation***

Ceramide or N-acylsphingosine consists of a C18-sphingoid base (C18-SB) backbone with an amino group to which a fatty acid chain, 14 to 26 C (carbons), is bound (Reynold 2004). Ceramides are present with mono-unsaturated or saturated fatty acid chains with various lengths that dictate their different physical properties (Antoine 2010). The most commonly found ceramides in mammalian cell membranes are with C16-C24 fatty acyl chains (Morad 2013). A number of specialized enzymes with different compartment localizations regulate the levels of ceramide. Based upon the cell type and stimulus, endogenous levels of ceramide can be induced *via* three main metabolic pathways.

First in the endoplasmic reticulum (ER) and in the mitochondria (Hannun and Obeid 2008, Bartke and Hannun 2009), ceramide can be generated *de novo* by the

condensation of L-serine and palmitoyl-CoA, catalyzed by serine palmitoyl transferase (SPT) to form 3-ketosphinganine, which is then reduced into sphinganine (dihydrosphingosine) by the action of 3-ketosphinganine reductase (Figure 4). Then, (dihydro)ceramide synthase enzyme, of which there are six isoforms, acylates dihydrosphingosine to produce dihydroceramide (Taha 2006, Hannun 2011). Different ceramide synthases (CerS) attach a relatively specific range of fatty acyl chain lengths to form dihydroceramide (s). In a final step, dihydroceramide is converted to ceramide by an oxidation reaction catalyzed by the enzyme dihydroceramide desaturase (Figure 4). Subsequently, a double bond is introduced across C4 and C5 of the sphingosine backbone, which is essential for its activity, such that dihydroceramide which lacks this double bond is biologically inactive (Ogretmen and Hannun 2004). ER-generated ceramide is then transported to the Golgi *via* the ceramide transfer protein (CERT), or through vesicular trafficking (Hanada 2003) (Figure 5).

Alternatively, ceramide can be produced from the hydrolysis of sphingomyelin at the cell membrane by the action of neutral, acidic, or alkaline sphingomyelinase (Mullen 2011) (Figure 4). Finally, ceramide can be generated through the salvage pathway, which accounts for 50% to 60% of sphingolipid biosynthesis. This pathway occurs in acidic compartments of the cell, such as late endosomes and lysosomes, wherein complex sphingolipids are degraded into sphingosine (Bankeu 2010, Mullen 2011). In addition, ceramide is hydrolyzed by the action of lysosomal ceramidase into sphingosine and a free fatty acid (Figure 4), which unlike ceramide, can be released from the lysosome (Heinrich 2004). Free sphingosine released from lysosome are probably trapped by CerS family

members at the surface of the ER and in its associated membranes (Bankeu 2010, Mullen 2011).

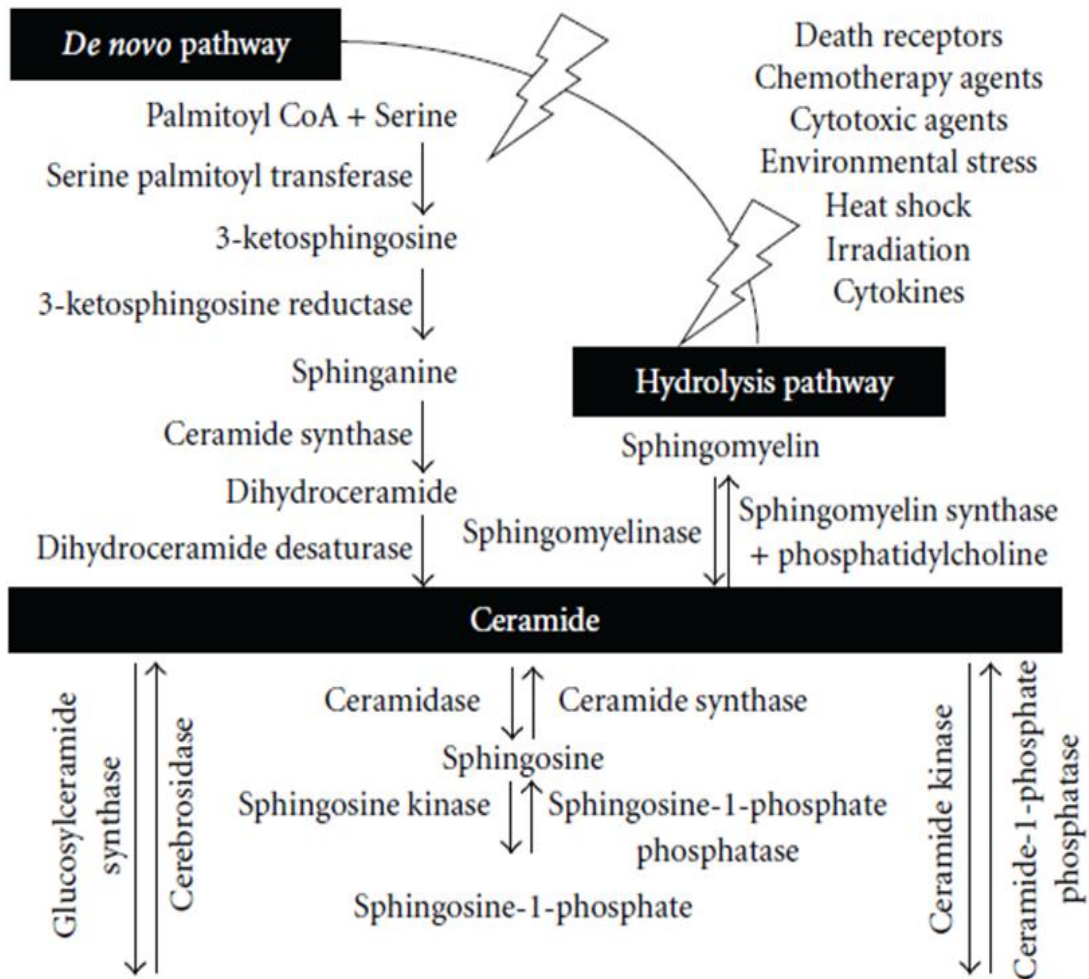


Figure 4. Metabolic pathways of ceramide.

Source: Huang *et al.* 2011. Apoptotic Sphingolipid Ceramide in Cancer Therapy. *Journal of Lipids*, 2011

### 3. *Ceramide Accumulation and Apoptosis*

The regulation of apoptotic pathways by ceramide has been extensively explored over the past years. Studies have shown that endogenous levels of ceramide are accumulated prior to the activation of apoptotic cascade (Dbaibo 1998). Many of the apoptotic stimuli including chemotherapeutic drugs, UV radiation, hypoxia, CD95, tumor necrosis factor-1 (TNF-1), and DNA damage lead to the production of ceramide suggesting a role for ceramide in apoptosis (Pettus 2002).

Based on cell type and stimuli, ceramide accumulation seems to be highly compartmentalized which dictates the subsequent response. In the ER, *de novo* ceramide is elevated in response to chemotherapeutic agents such as etoposide, daunorubicin, gemcitabine, cannabinoids, Fas ligand, and HPR (Chalfant 2001, Wang 2001, Chalfant 2002). For instance, daunorubicin induces ceramide by activation of dihydroceramide synthase (Bose 1995), and etoposide increases serine palmitoyltransferase (SPT) activity in leukemic Molt-4 cells (Perry 2002). Moreover, HPR enhances *de novo* ceramide synthesis *via* activation of serine palmitoyltransferase and/or (dihydro) ceramide synthase, with simultaneous inhibition of (dihydro) ceramide desaturase (Valsecchi 2010). Kroesen *et al.* found that B cell receptor (BcR)-induced apoptosis of lymphoma cells implicates a highly selective production of C16-ceramide specifically through the *de novo* pathway. Interestingly, inhibition of ceramide generation prevents BcR-induced apoptosis which preceded mitochondrial changes of apoptosis, such as loss of membrane potential and activation of executioner caspases (Kroesen 2001). In LNCaP prostate cancer cells, Eto *et al* showed that androgen ablation also results in selective accumulation of *de novo*-generated C16-ceramide, which is blocked by fumonisin B<sub>1</sub>, an inhibitor of the *de novo*

pathway. The accumulated ceramide leads to G<sub>0</sub>/G<sub>1</sub> arrest followed by apoptosis in these cells (Eto 2003).

Interestingly, C16-ceramide has been identified, by the emerging use of liquid chromatography-mass spectrometry (LC-MS), to be a possible marker of *de novo* pathway that plays a pivotal role in apoptosis (Chalfant 2001, Kroesen 2001, Grösch 2012). Specifically, this pathway induces the dephosphorylation of SR proteins, a family of serine/arginine-domain proteins and known modulators of mRNA splicing, which causes the alternative splicing of the genes encoding BCL-X and caspase 9 by activation of protein phosphatase 1 (PP1) (Figure 5). This suggests the contribution of specific ceramide synthase subtypes in apoptosis and cancer suppression (Grösch 2012). Table 1 summarizes the effect of fatty acyl chain length and/or involvement of their associated CerS on tumor growth and apoptosis in several cancer types.

Alternatively, enhanced elevation of ceramide can be attained through sphingomyelin hydrolysis or catabolism of more complex sphingolipids (Reynold 2004). Endogenous levels of ceramide can also be induced by inhibiting several enzymes involved in its clearance, such as glucosylceramide synthase (GCS), sphingomyelin synthase (SMS) or ceramidases (CDases) (Ogretmen and Hannun 2004).

In most cases, ceramide accumulation involves contribution of more than one pathway and enzymes which are often deregulated in cancer cells (Radin 2003). Indeed, defects in ceramide production result in increased resistance to anticancer drugs (Cai 1997, Chmura 1997, Michael 1997), while chemotherapeutic agents that induce ceramide accumulation lower the threshold of tumor cell apoptosis (Michael 1997, Lavie 1997).

Ceramide Synthase/Ceramide	Cell type	Treatment	Effect
Overexpression CerS1 + CerS6	HeLa	IR	No effect
Overexpression CerS2/C24:0-, C24:1-Cer]	HeLa	IR	Anti-apoptotic
Overexpression CerS5/C16-Cer]	HeLa	IR	Pro-apoptotic
C16:0-, C24:1-, C24:0-Cer]	Baby mouse kidney cells	UV-C radiation	Pro-apoptotic
C16:0-, C18:0-, C20:0-Cer]	Hematopoietic cells	IL3 starvation	Pro-apoptotic
C16:0-, C18:0-Cer]	Hematopoietic cells	Cisplatin	Pro-apoptotic
C16:0-Cer]	Jurkat cells	IR	Pro-apoptotic
C16:0-Cer]	Primary Hepatocytes	TNF $\alpha$	Pro-apoptotic
C16:0-Cer]	LNcaP prostate cancer cells	Androgen ablation	Pro-apoptotic
C16:0-Cer]	Human Leukemia cells	ZnCl <sub>2</sub>	Pro-apoptotic
C16:0-Cer]	Human B-cells	BcR-crosslinking	Pro-apoptotic
C16:0-, C24:0-Cer]	Human blood neutrophils	-	Pro-apoptotic
C16:0-Cer]	HCT-116	Celecoxib	Pro-apoptotic
Cers3,CerS6/ C16-, C18-, C24:0-, C24:1-Cer]	Rec-1	R(+)-methanandamide	Induction of cell death
Overexpression CerS6	SW620	Sorafenib/Vorinostat	Increase cell death
Overexpression CerS6	SW620	TRAIL	Increase cell death
Overexpression CerS1, C18:0-Cer]	HNSCC	-	Pro-apoptotic
CerS1], C18-Cer], C16-, C24:0-, C24:1-Cer]	HNSCC	-	Pro survival, enhanced metastasis
CerS1 and C18-Cer]	HNSCC	Gemcitabine/Doxorubicin	Pro-apoptotic
CerS1 and C18-Cer]	HNSCC	Cisplatin	Pro-apoptotic
CerS6 and C16-Cer]	HNSCC	-	Anti-apoptotic
C22:0-, C24:0-, C24:1-Cer]	Osteoblasts	Sodium nitroprusside	Pro-apoptotic

Table 1. Chain length specific effects of ceramides on tumor growth and apoptosis. *Source: Grösch S. et al. 2012. Chain length specific properties of ceramide. Progress in Lipid Research 51: 50-62*

#### 4. Mitochondrial Ceramide and Apoptosis

Accumulating evidence shows that ceramide plays an integral role in the intrinsic mitochondrial pathway and extrinsic pathway of cell death (Kroemer 2007). Indeed, ceramide accumulation occurs prior to mitochondrial pathway of apoptosis. In the intrinsic pathway, mitochondria can be targeted directly or through signaling transduction pathways via Bcl-2 pro-apoptotic members, Bax and Bak, which release cytochrome c and lead to caspase activation and apoptosis (Amaral 2010). Moreover, ceramide was shown to be intimately linked to mitochondria-mediated apoptosis. ER-generated ceramide translocates

to the mitochondria along with another pool generated in the mitochondria, where it activates protein phosphatase 2A (PP2A) (Siskind 2005). PP2A then phosphorylates and inhibits the anti-apoptotic Bcl-2 protein (Figure 5). Meanwhile, Bax activates CerS in outer mitochondrial membrane (Siskind 2005). Mitochondrial ceramides form large stable barrel-like channels either alone or with Bax (Colombini 2010). These channels allow cytochrome c release into the cytosol, and activation of executioner caspases, such as caspase 3 (Colombini 2010).

Indeed, cellular ceramide accumulation occurs prior to mitochondrial apoptosis (Kroesen 2001). Furthermore, Ardail *et al* have shown that mitochondrial outer membrane contains at least three fold ceramide levels than the inner membrane. Interestingly, mitochondria isolated from normal rat liver had more dihydroceramide (nonapoptotic) than ceramide (apoptotic) (Ardail 2001). In fact, enzymes involved in ceramide biosynthesis and hydrolysis, such as CerS and ceramidase, are present in the mitochondria (Bionda 2004). Apoptotic stimuli such as TNF $\alpha$ -radiation, UV, and CD95 induce increase mitochondrial ceramide levels, which is the case in TNF-treated MCF7 breast cancer cells (Dai 2004).

In the mitochondria, ceramide has various effects, including the release of mitochondrial intermembrane space proteins, cytochrome c, generation of ROS, and alteration of calcium homeostasis of mitochondria and the endoplasmic reticulum (Pinton 2001, Siskind 2002, Di Paola 2000) (Figure 5). Overexpression with Bcl-2 or Bcl-xl prevents ceramide channel formation and cytochrome c release (Gottschalk 1994, Wiesner 1997). It has been observed that Bcl-2 inhibits ceramide-induced apoptosis without blocking ceramide generation (Zhang 1996, Allouche 1997, Birbes 2001), which indicates



that ceramide acts upstream of Bcl-2. However, conflicting studies have shown that Bcl-2 prevents ceramide-induced apoptosis by inhibiting ceramide accumulation (Yoshimura 1998, Tepper 1999, Kawatani 2003). On the other hand, treatment of MCF7 cells with TNF resulted in enhanced mitochondrial ceramide levels that were associated with Bax translocation to mitochondria (Birbes 2005). Moreover, addition of C16-ceramide to isolated mitochondria stimulates Bax translocation to mitochondria and subsequent cytochrome *c*/Smac release (Kashkar 2005).

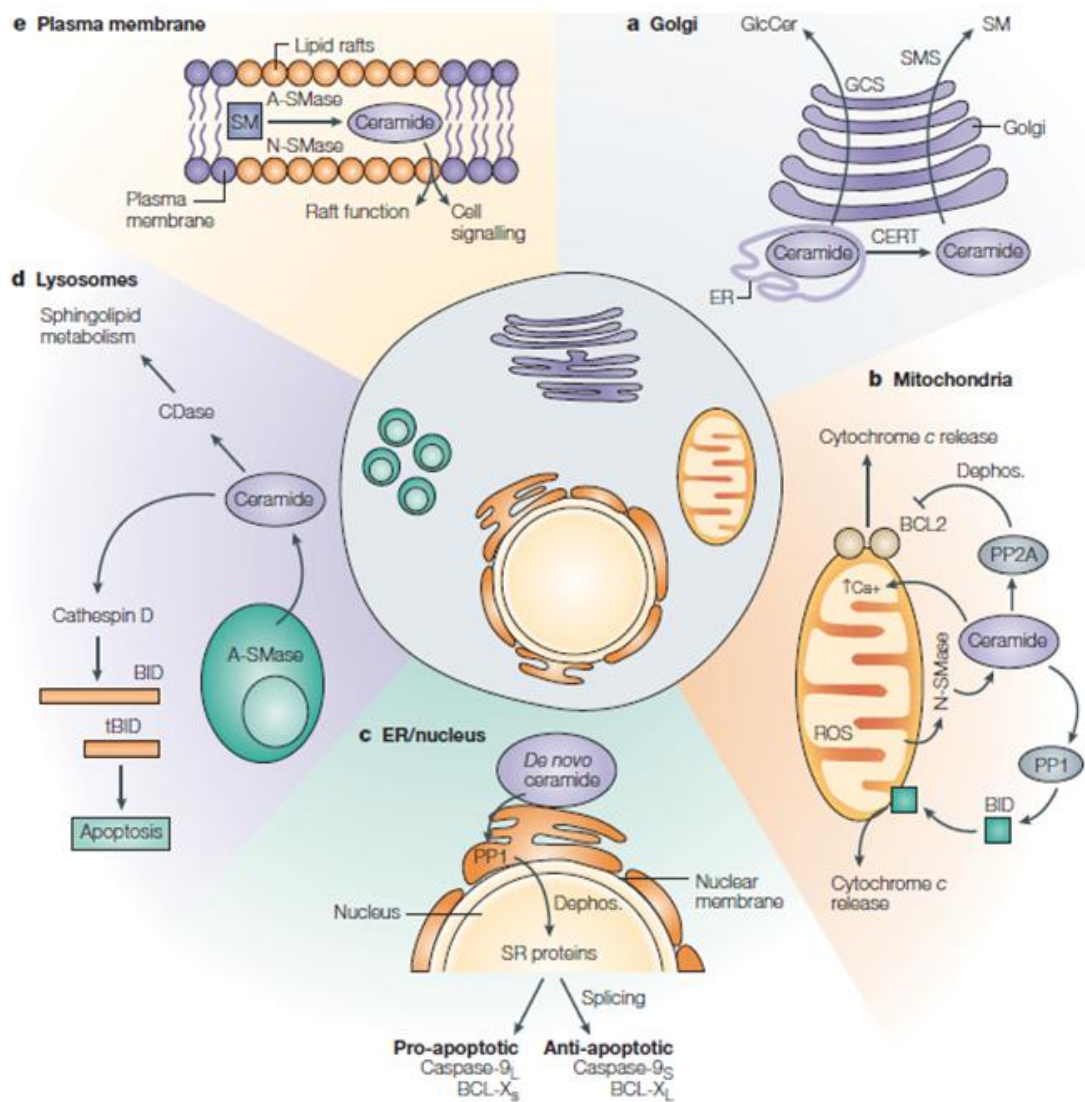


Figure 5. Compartmentalized pathways of ceramide signaling.

Source: Ogretmen & Hannun 2004. Biologically Active Sphingolipids in Cancer Pathogenesis and Treatment. *Nature Reviews Cancer*, 4(8), 604-616.

## 5. *Ceramide and the synthetic retinoids, HPR and CD437*

As we have discussed earlier, several anticancer agents, including HPR exert tumor suppressive role, at least in part, by increasing ceramide levels through activation of *de novo* ceramide pathway. Importantly, HPR is now under clinical trials for the treatment of ovarian, prostate, neuroblastoma, and lymphoma cancers (Valsecchi 2010). Treatment of human NB and prostate cancer with HPR results in time- and dose-dependent enhanced activity of serine palmitoyltransferase and (dihydro)CerS (Wang 2001). This activation occurs parallel to inhibition of dihydroceramide desaturase enzyme, which increases dihydroceramide levels (Valsecchi 2010). The increase in dihydroceramide was also observed in breast and colon carcinoma and leukemia cells (Wang 2008). Although dihydroceramide is not considered to have apoptotic functions, its role in autophagic cell death has been explicitly studied (Zheng 2006).

We have shown that HPR increases ceramide levels in HTLV-1 negative malignant cells, but not in HTLV-1 transformed cells, concomitant with lower sensitivity of HTLV-1 positive cells to treatment with exogenous C2- and C6-ceramide. Moreover, this was attributed to a defect in *de novo* ceramide synthesis in HTLV-1 positive cells treated with HPR (Darwiche 2005). Similar to HPR, CD437 elicits ceramide accumulation in HTLV-1 negative cells only (data not shown).

Analysis of sphingolipid metabolism has long used with thin layer chromatography (TLC) and does not provide a clear identification of dihydroceramide *versus* ceramide. However, the emergence of LC-MS analysis allowed researchers to distinguish and quantify dihydroceramide and ceramide species and to study their particular roles in cancer prevention and treatment.

## **I. Aim of the Study**

Using *in vitro* models of ATL and peripheral T lymphomas, we aim to investigate the effect of ST1926 on cell cycle progression, cell death mechanisms, and regulation of ceramide signaling. We will use HTLV-1 positive cells (HuT-102, MT-2 and C81) and HTLV-1 negative cells (CEM, Jurkat and Molt-4). Our specific aims are:

- 1- Test the effect of ST1926 on the growth of ATL and malignant T-cell lines, primary ATL cells, and normal resting and activated lymphocytes
- 2- Determine the effect of ST1926 on cell cycle and apoptosis
- 3- Determine whether ST1926-induced apoptosis involves p53 activation
- 4- Investigate ST926 mechanism of action on ceramide metabolism/biosynthesis
- 5- Analyze the effect of Bcl-2 protein on ST1926-induced growth-suppression
- 6- Investigate whether Bcl-2 inhibits ceramide generation upon ST1926 treatment.

Understanding the mechanism of action of ST1926 in ATL and malignant T-cells will hopefully support a potential therapeutic role of this synthetic retinoid in ATL and peripheral T-lymphomas. Moreover, understanding ceramide metabolism and functions plays a crucial role in the development of novel therapeutic targets in cancer.

## CHAPTER II

### MATERIALS AND METHODS

#### A. Cell Culture

##### 1. HTLV-1 Positive and Negative Malignant T-cell Lines

CEM, Jurkat, and Molt-4 are HTLV-1 negative CD4<sup>+</sup> malignant T-cell lines, whereas, C8166, HuT-102, and MT2 are HTLV-1 transformed CD4<sup>+</sup> T-cell lines. The HTLV-1 transformed ATL cell lines are infected with the HTLV-1 retrovirus and transformed by the oncoprotein and transactivator, Tax, that is produced by the pX region of the HTLV-1 transcriptome. CEM cells are T-lymphoblastoid cells derived by Foley *et al*, (Foley 1965) from peripheral blood of a 4-year-old Caucasian female with acute lymphoblastic leukemia (ALL). Jurkat cells were originally established by Schneider *et al*, (Schneider 1977), from the peripheral blood of a 14-year-old with ALL in relapse. Molt-4 cells were first identified as rosette-forming human lymphoid thymus-derived T-cell line. Molt-4 cells were extracted from a patient with ALL in relapse and who had received prior multi-drug chemotherapy. Molt-4E6 lacks a functional p53 due to transfection with E6 protein of human papilloma virus. Molt- 4LXSN is the control cell line used for Molt-4E6, being transfected with an empty vector. Molt-4 cells transfected with p-MEP4 with (Molt4-Bcl2) or without (Molt4-MEP4) full length murine *bcl-2* gene. C8166 cells are immortalized, non-producer, human umbilical cord blood lymphocyte cultures developed by cocultivation or fusion of fresh cells with T- cells cultured from leukemia-lymphoma patients. These transformed neonatal leukocytes exhibit morphological, cytochemical, and

other phenotypic characteristics similar to those of other HTLV-1 infected cells. However, in contrast to the usual productive infection seen, these cells contain only low amounts of viral proteins and do not release virus particles, thus, they are defective for viral replication. In addition, viruses in C8166 cells have other defects in their transcriptional machinery. HuT-102 cells were originally derived from the peripheral blood of a 26 year old Black male patient with cutaneous T-cell lymphoma and were found to contain type C retrovirus particles (Poiesz 1980). MT2 cells are similar to HuT-102 cells.

## ***2. Isolation of Peripheral Blood Mononuclear Cells***

Peripheral blood mononuclear cells (PBMC) were collected from healthy HTLV-1 negative donors after obtaining their informed consent (American University Hospital, AUB). Venous blood was collected into heparinized syringes using uniform standards. The heparinized blood was diluted 1:2 with phosphate buffered saline (PBS) (Gibco, Invitrogen, Paisley, UK), pH 7.2, and layered on a Ficoll-Hypaque gradient (Lymphoprep, Nyegaard, Norway). The gradient was centrifuged at 800 x *g* for 30 minutes at room temperature and the PBMC band was collected and washed twice in PBS. Before ST1926 addition, resting PBMC were cultured for 24 hours at  $1 \times 10^5$  cells/ml in RPMI-1640 medium containing 10% heat inactivated FBS) and antibiotics. Activated PBMC were grown in Ham's F10 medium (Gibco) supplemented with 2% PHA (Gibco).

## ***3. Primary ATL Cells***

Primary ATL cells were collected from PBMC which were isolated from HTLV-1 positive donors and centrifuged over Ficoll-Hypaque. Before ST1926 addition, cells were

grown for three days in 10% Rec IL-2, 20% heat inactivated FBS, and a ratio of 1:400 PHA. At this stage, the cells can be frozen for future use. When needed, cells are thawed and cultured in 20% heat inactivated FBS and 10% Rec IL-2.

**B. Cell Growth and Treatment** All HTLV-1 positive and negative cells were cultured in RPMI 1640 medium (Gibco) containing 10% heat inactivated FBS, 25 mM Hepes buffer, 1% L-glutamine, 1% penicillin-streptomycin antibiotics, 1% kanamycin solution, and 1% sodium pyruvate (Gibco). All cells were grown in a humidified incubator (95% air, 5% CO<sub>2</sub>). Molt4-LXSN and Molt4-E6 were clonally selected for once per week and before each experiment with (Geneticin Gibco, Life Technology) (500 µg/ml). Molt4-MEP4 and Molt4-Bcl2 were clonally selected for once per week and before each experiment with Hygromycin B1 (Invitrogen) (500 µg/ml).

### *1. Cell Passaging*

Cells were passaged or fed for maintenance and expanded before an experiment. To feed or passage the HTLV-1 positive and negative cells, around 75% of the cell suspension volume is discarded, followed by the addition of RPMI 1640 medium three times the volume of the remaining cells. Cells were usually fed every two to three days depending upon the rate of growth of the cell lines. To expand the number of cells (before an experiment), RPMI 1640 medium was added to the cells to increase volume of cells three fold. For experimentation, cell number was calculated using a hemocytometer according to the following formula: cells/ml = average number of cells x dilution factor x volume of suspension x 10<sup>4</sup>. Cells were counted using trypan blue dye exclusion using 0.4% trypan

blue solution. For most experiments, cells were seeded at a density of  $2 \times 10^5$  cells/ml. Tissue culture flasks were purchased in a variety of sizes from the Falcon division of Becton, Dickinson and Co. (Cockeysville, MD).

## **2. Preparation of ST1926**

ST1926 was obtained from Sigma TAU (Rome, Italy) and was reconstituted in 0.1% dimethylsulfoxide (DMSO) at a concentration of  $1 \times 10^{-2}$  M and  $3.3 \times 10^{-2}$  M, respectively under amber light, aliquoted, stored at  $-80^\circ\text{C}$ , and used for up to six months. For use in experimentation, an aliquot of stock ST1926 ( $1 \times 10^{-2}$  M) was either applied directly on cells, or serially diluted under amber light in 0.1% DMSO to produce stock dilutions ranging in concentration from  $5 \times 10^{-8}$  M to  $5 \times 10^{-6}$  M ST1926. These stocks of diluted ST1926 were thawed twice and then discarded.

## **C. Cell Growth Assays**

All cell lines were seeded into 96-well plates at a density of  $2 \times 10^5$  cell/ml. Cells were, then, treated with 0.1% DMSO or varying concentrations of ST1926 ( $5 \times 10^{-8}$ -  $5 \times 10^{-6}$  M). Medium containing the appropriate treatment was kept for three days, and viability at days 1, 2, or 3 post-ST1926 treatments was assayed using the CellTiter 96<sup>®</sup> non-radioactive cell proliferation assay kit (Roche, Mannheim, Germany) according to manufacturer's instructions. Relative MTT dye uptake is assessed by optical density (OD) measurement at 595 nm using an ELISA microplate reader. Results are expressed as growth relative to DMSO-treated controls and are derived from the mean of quadruplicate wells.



#### **D. Cell Cycle Analysis**

Cells were cultured in 25 cm<sup>2</sup> flasks (Falcon) and collected at 24 or 48 hours after ST1926 treatment. Cells were, then, washed twice with cold PBS, fixed in ice cold 100% ethanol, and stored for 24 hours at -20°C. Subsequently, cells were rinsed with PBS, incubated for one hour in PBS containing 50 units RNaseA (Roche, Mannheim, Germany) and then stained with propidium iodide (PI) (50 µg/ml) (Sigma). Cell cycle analysis was performed using a FACS scan flow cytometer (Becton Dickinson). Each sample was collected as 10,000 ungated events and the corresponding cell cycle distribution was determined using Cell Quest software (Becton-Dickinson).

#### **E. TUNEL Assay**

The TUNEL assay is a measure of apoptosis through detection of DNA strand breaks (a late apoptotic event). DNA strand breaks contain free 3'-OH termini which may be conjugated to dUTP-fluorescein through the enzymatic action of terminal deoxynucleotidyl transferase. Fluorescein fluorescence is detected by flow cytometry and serves as a measure of apoptosis. In brief, cells are seeded (10x10<sup>6</sup> cells/condition) and treated with 0.1% DMSO for control or 1x10<sup>-6</sup> M ST1926. Two extra control flasks, one for positive and one for negative controls, are prepared from any cell line used in the experiment. Cells are washed and fixed with 4% formaldehyde solution for 15 min at room temperature, and then the dry pellet is stored at -20 °C for not more than one week. Cells are then washed with 1X PBS and incubated with 250 µl permeabilization solution (0.1% triton X-100 in 0.1% sodium- citrate) on ice for 4 min. Only the positive control cells are

then incubated in 200  $\mu$ l of 1mg/ml DNase (prepared in 50 mM Tris pH 7.5) for 15 min at room temperature, then washed twice with 1X PBS. Other samples are washed once with 1X PBS, and pellets are re-suspended and incubated for 60 min at 37<sup>0</sup> C in an incubator in the dark in TUNEL reagents: 50  $\mu$ l Label solution for negative control tube, 50  $\mu$ l TUNEL reaction mixture for other samples (TUNEL reaction mixture: 50  $\mu$ l enzyme + 450  $\mu$ l label solution). Cells are then washed twice with 1X PBS, re-suspended in 1 ml PBS, and transferred into polystyrene falcon round bottom tubes for flow cytometry analysis (with the excitation wavelength set at 470–490 nm and the emission wavelength at 505 nm).

## **F. Immunoblot Assays**

### ***1. Protein Extraction***

Total cellular protein extracts were prepared from cultured cells washed twice with ice-cold 1x PBS and lysed with SDS-lysis buffer (0.25 M Tris-HCl pH 6.8, 20% glycerol, 4% SDS, 0.002% bromophenol blue, 10%  $\beta$ -mercaptoethanol). Protein concentrations were determined using the DC Protein Assay from Bio-Rad (Hercules, CA) according to the manufacturer's instructions.

### ***2. Gel Casting***

Denaturing polyacrylamide gels were cast in two layers according to the following procedure. Using the Bio-Rad electrophoresis cell, the gel casting stand was assembled according to manufacturer's instructions. A 12% separating gel was prepared by combining 3 ml of 30% acrylamide/0.8% N'N'-bis-methylene-acrylamide solution, 2 ml of

4x separating gel buffer (1.6 M tris-HCl pH 8.8, 10% (w/v) SDS) and 2.5 ml ddH<sub>2</sub>O. A 10% gel was prepared in the same way except 2.5 ml acrylamide solution and 3 ml ddH<sub>2</sub>O were used. Before pouring the separating gel, 45 µl 10% APS (freshly prepared) and 12 µl N,N,N',N'-Tetramethylethylenediamine (TEMED) were added. The gel was poured to ~3 cm below the top of the smaller glass plate and water-saturated isobutanol was layered atop the gel to allow for a level upper surface. After polymerization of the separating gel (~10-15 min), the water-saturated isobutanol was rinsed off three times using a 1x separating gel buffer solution. The stacking gel was then prepared by combining 1 ml of 30% acrylamide / 0.8% N'N'-bis-methylene-acrylamide solution, 1.7 ml of 4x stacking gel buffer (0.5 M tris-HCl pH 6.8, 0.4% (w/v) SDS), and 4 ml ddH<sub>2</sub>O. Before pouring the gel, 40 µl 10% APS (freshly prepared) and 10.6 µl TEMED were added. The gel solution was poured to the top of the smaller glass plate and a comb was inserted between the plates. After polymerization of the stacking gel (30-60 min), the comb was gently withdrawn and the wells were rinsed with 1x electrophoresis buffer (prepared from a 5x solution containing 120 mM tris base, 1 M glycine, 0.5% (w/v) SDS, pH to 8.3).

### ***3. Gel Running and Protein Transfer***

After the gels were cast, cellular protein extracts (25-100 µg) were loaded and run in 1x electrophoresis buffer at 74 Volts for ~1.5 h using the Mini-PROTEAN II electrophoresis cell unit. After the run, gel sandwiches were disassembled and gels were set up for transfer in the Bio-Rad Trans-Blot<sup>®</sup> Electrophoretic Transfer Cell according to manufacturer's instructions. Proteins were transferred onto nitrocellulose membranes

(Biolab) in transfer buffer [(50mM tris base, 77 mM glycine, 0.04% SDS (w/v), 20% methanol (v/v)] under 30 Volts overnight at 4°C while stirring.

#### ***4. Hybridization and Protein Detection***

Hybridization conditions for Bax, Bcl2, caspase 3, PARP, p21, Tax, p53, phosphorylated p53, and GAPDH (Santa Cruz) are similar. Briefly, membranes were incubated in TBS (10 mM tris-HCl pH 8.0, 150 mM NaCl) containing 5% dry milk and 0.05% tween 20 for 1 hour at room temperature while shaking. Membranes were then incubated with the primary antibody for either 2 hours at room temperature or overnight at 4°C. Membranes were then washed 3 times (10 min per wash) in TBS containing 0.05% tween 20 and placed in the secondary antibody (Santa Cruz, horseradish peroxidase-conjugated anti-rabbit, anti-mouse, or anti-goat) at a dilution of 1:5000 for 1 hour at room temperature while shaking. Finally, membranes were washed 3 times (10 min per wash) with TBS containing 0.05% tween 20 before protein detection.

Proteins were detected by enhanced chemiluminescence using the ECL system (Santa Cruz) in conjunction with horseradish peroxidase-conjugated secondary antibodies. Membranes were then exposed to x-ray films for varying time periods (10 sec-15 min). Equal protein loading and quality were verified using GAPDH staining and parallel gel staining (20 min) with a filtered coomassie blue solution (2.5 g coomassie blue, 454 ml methanol, 92 ml glacial acetic acid, 454 ml ddH<sub>2</sub>O) followed by 3 washes (10 min per wash) in a high methanol destain solution (45.4% methanol, 7.5% glacial acetic acid) and

one overnight wash in a low methanol destain solution (5% methanol, 7.5% glacial acetic acid) at room temperature. Coomassie-stained gels were then dried at 70°C for 1 hour.

## **G. Determination of Ceramide Levels**

### ***1. Lipid extraction***

Lipids were extracted by the method of Bligh and Dyer (Bligh 1959). Briefly, cell membranes were extracted with 3 ml of chloroform/methanol (1/2). The monophasic mixture was mixed, then water was added and the samples rested for 10 min. The organic and aqueous phases were subsequently separated by addition of 1 ml of chloroform and 1 ml of water followed by vigorous shaking and centrifugation at 200xg. The organic phase was carefully removed and transferred to a new tube and the sample dried under nitrogen. Lipids were then resuspended in 1 ml of chloroform.

### ***2. Ceramide Measurement***

Cells were seeded at  $3.5 \times 10^5$  cells/ml. Ceramide levels were measured using a modified diacylglycerol kinase assay and external ceramide standards as described previously (Bielawska 2001). 80% of sample lipids were dried under N<sub>2</sub>. Dried lipids were solubilized in 7.5% octyl- $\beta$ -D-glucoside, 25 mM dioleoyl phosphatidylglycerol solution *via* several cycles of sonication in a bath sonicator. The reaction buffer was prepared as 2x solution, containing 100 mM imidazole HCl (pH 6.6), 100 mM LiCl, 25 mM MgCl<sub>2</sub> and 2 mM EGTA. To the lipid micelles, 50  $\mu$ l of 2X reaction buffer were added, 0.2  $\mu$ l of 1M

dithiothreitol, 5 µg of diglycerol kinase membranes and dilution buffer (10 mM imidazole, pH 6.6, 1 mM diethylenetriaminepenta- acetic acid, pH 7) to a final volume of 90 µl. The reaction was started by adding [ $\gamma$ - $^{32}$ P] ATP solution and allowed to proceed at 25°C for 30 min.

Extracted lipids in the 1.8 ml of the organic phase were nitrogen dried, then resuspended in 50 µl of methanol/chloroform (1:9, v/v). An aliquot of 25 µl was spotted on to a 20 cm silica gel thin layer chromatography (TLC) plates. Plates were developed using chloroform: acetone: methanol: acetic acid: H<sub>2</sub>O (50:20:15:10:5, by vol), air-dried and subjected to autoradiography. The radioactive spots corresponding to phosphatidic acid and ceramide-phosphate, the phosphorylated products of diacylglycerol and ceramide, respectively, were identified by comparison with known standards. Spots were scraped into a scintillation vial containing 4 ml of scintillation fluid and counted on a scintillation counter. Linear curves of phosphorylation were produced over a concentration range of 0-960 pM of external standards (dioleoyl glycerol and CIII-ceramide, Sigma). Ceramide levels were constantly normalized to cellular phospholipids. It is important to note that under these conditions, there was a total conversion of ceramide and diacylglycerol into their phosphorylated products, and there was no change in the specific activity of the diacylglycerol kinase (DGK) enzyme.

### ***3. Lipid phosphate measurement***

Lipid phosphates were measured according to the method of Rouser *et al* (Rouser 1970). Briefly, 20% of the lipid sample was dried under nitrogen and oxidized with 70%

perchloric acid on a heating block at 160°C for 45 minutes. The tubes were allowed to cool then water was added, followed by 2.5% ammonium molybdate, and 10% ascorbic acid with vortexing after each addition. The tubes were then incubated at 50°C for 15 mins, allowed to cool, and absorbency read at 820 nm. Linear curves of known phosphate concentrations were produced over a concentration of 0-80 nM of external standards.

## **H. *De novo* Ceramide Synthesis**

At initiation of treatment, [<sup>3</sup>H]palmitic acid (1 μCi/mL medium) purchased from Perkin Elmer was added to treated and control samples. Then, lipids were extracted according to Bligh and Dyer method (Bligh and Dyer 1959), N<sub>2</sub> dried, and resuspended in 60 μL chloroform:methanol (2:1); 40 μL were spotted on 20 cm silica gel TLC plates. Plates were developed with ethylacetate:isooctane:acetic acid (90:50:20, v/v), air dried, and sprayed lightly with En3hance® (Perkin Elmer) to enhance tritium readings. [<sup>3</sup>H] ceramide spots were visualized by iodine vapor mark. Radioactivity was visualized by autoradiography after 96 h at 80 °C and the [<sup>3</sup>H] ceramide spots were scraped into scintillation vials containing 4 ml of scintillation fluid and counted on a Packard scintillation counter. [<sup>3</sup>H] ceramide counts were normalized to lipid phosphate levels.

## **I. Liquid Chromatography-Mass Spectrometry (LC-MS)**

### ***I. Sample Preparation***

Cells were seeded at a density of  $3.5 \times 10^5$  cells/ml. Cells were harvested at the indicated time points, and cell pellets were washed twice with 1X PBS, left for 24 hours at -80°C. The following day, cell pellets were lyophilized, kept for up to one week at 4°C, and sent to the Medical University of South Carolina (MUSC) for sphingolipidomics analysis

(LC-MS) performed by Dr. Jacek Bielwaski as described (Bielawski 2010). Briefly, Samples were fortified with internal standards and lipids were extracted using one-phase extraction with ethyl acetate/isopropanol/water (60:30:10 by volume), evaporated to dryness and reconstituted in 100  $\mu$ l of methanol. This provides a safe and neutral condition that maintains the parent sphingolipid and assures quantitative extraction of sphingolipids from biological samples.

## ***2. Liquid Chromatography-Mass Spectrometry (LC-MS)***

Samples are introduced into an LC device to separate total lipid extracts into either various lipid subclasses and/or individual molecular species within the class, using MS highly selective detection modes. Mass spectrometry (MS) is a powerful detection technique that enables separation and characterization of compounds according to their mass-to-charge ratio ( $m/z$ ). Its essential components include a sample inlet, ion source, mass analyzer, detector and data handling system. The LC-MS instrumentation was used with the MRM scanning mode where each target analyte is uniquely identified by the Precursor-Product ion mass transition and the specific retention time. Analysis was performed using electrospray ionization MS/MS analysis on a Thermo Finnigan TSQ 7000 triple quadrupole mass spectrometer, operating in multiple-reactions-monitoring (MRM) positive-ionization mode.

### **a. Mechanism of Electrospray Ionization Mass Spectrometry (ESI-MS)**



ESI-MS involves transformation of ions from the liquid to the gas phase. It is a method that operates at atmospheric pressure and ambient temperature. Initially, a solution containing the analytes of interest is introduced to the ESI ion source through capillary tubing. The narrow orifice at the end of the capillary and the dynamic forces facilitate formation of sprayed small droplets in the ionization chamber. Application of electric potential (approximately 2-5 kV) causes ionization, consequently the droplets carry a net charge. The charged droplets are then directed into the mass analyzer/detector by the applied electric field. This cycle is repeated until molecular ions are generated prior to their entrance into the mass analyzer.

b. Cer, dhCer molecular species Identification

This is established by the Precursor Ion Scan, performed for the common Product Ion ( $m/z$ ) 264.2 and 266.1 for Sphingosine and dihydrosphingosine derivatives, respectively at the high collision energy (35-55 eV), operating in positive ionization mode. A representative sample extract is infused directly into ESI source and it is then scanned for molecular ions of the potential sphingolipids. Further confirmation of identity is achieved through MRM analysis with “soft” fragmentation (15-30 eV). Running sample through the LC system also confirms a reasonable retention time. Only sphingolipids that satisfy identification criteria in both analyses should be considered truly present in the sample.

### ***3. Quantitation***

Selection of internal standards is used as a reference for both the determination and quantitation of the corresponding species. Internal standards should be as close as

possible from the target analyte, such as having similar MS fragmentation pattern as well as physicochemical properties reflected by similar solubility, extraction efficiency and mobile-stationary phase relationship during the LC separation. Therefore, internal standards for particular sphingolipid classes (Cers and dhCers) synthesized from C17-sphingoid base as the closest “unnatural” sphingoid base to the natural C18-sphingoid base counterpart.

Results from the MS analysis represent the mass level of particular ceramide/dihydroceramide species (in pmols) per total sample used for lipid extract preparation and quantitative analysis, represented by total phospholipid contents Pi ( $\mu\text{mol}$ ).

All mentioned steps of LC-MS analysis and quantitation were done by Dr. Jacek Bielawski at MUSC.

#### **J. Densitometric Analysis**

Bands were quantified using Image J software (National Institutes of Health, Maryland, USA).

#### **K. Statistical Analysis**

Data presented are the means  $\pm$  SD of n assays as noted in the figure legends. Significant differences were determined using the Independent T-test. Significance was set at differences of  $p \leq 0.05$ ,  $p \leq 0.01$ , or  $p \leq 0.001$ .

## CHAPTER III

### RESULTS

#### **A. ST1926 Induces Growth Inhibition in Malignant T Cells, Primary ATL Cells, but not Normal Lymphocytes**

We used three HTLV-1 positive cell lines, HuT-102, MT-2, and C8166; and three HTLV-1 negative cell lines, Molt4, Jurkat, and CEM. Darwiche *et al* have shown that all mentioned cell lines, except for C8166 are resistant to ATRA at pharmacologically achievable concentrations up to 5  $\mu\text{M}$  (Darwiche 2001, Darwiche 2004). Meanwhile, treatment with the synthetic retinoids, HPR and CD437, at concentrations ranging from 0.5  $\mu\text{M}$  to 10  $\mu\text{M}$ , induced growth inhibition,  $G_0/G_1$  arrest, and apoptosis in all tested HTLV-1 transformed and malignant T cell lines (Darwiche 2004; unpublished results). Therefore, our purpose was to test the effect of ST1926 on the growth and viability of these cell lines and to determine its relative potency to the other mentioned synthetic retinoids in eradicating ATL (HTLV-1 positive) and T-lymphoma cells (HTLV-1 negative cells).

##### ***1. HTLV-1 Positive Cells are Sensitive to ST1926***

We tested the effect of ST1926 on cell growth and viability of three HTLV-1 transformed cell lines: HuT-102, MT-2, and C8166. Pharmacologically achievable levels of ST1926 were used ranging from 0.05  $\mu\text{M}$  up to 5  $\mu\text{M}$  (Valli 2008). Submicromolar concentrations of ST1926 resulted in a time-dependent growth suppression in all tested cell lines (Figure 6). At 0.5  $\mu\text{M}$  concentration, treatment with ST1926 showed a threshold level

that is similar to the effect of a ten-fold higher concentration, except for C8166. At 24 hours post treatment, 1  $\mu$ M ST1926 inhibited growth of HuT-102, MT-2, and C8166 by 69%, 41%, and 48%, respectively, and resulted in the total loss of cells at 72 hours. Similar trends were observed using the trypan blue exclusion assay (data not shown).

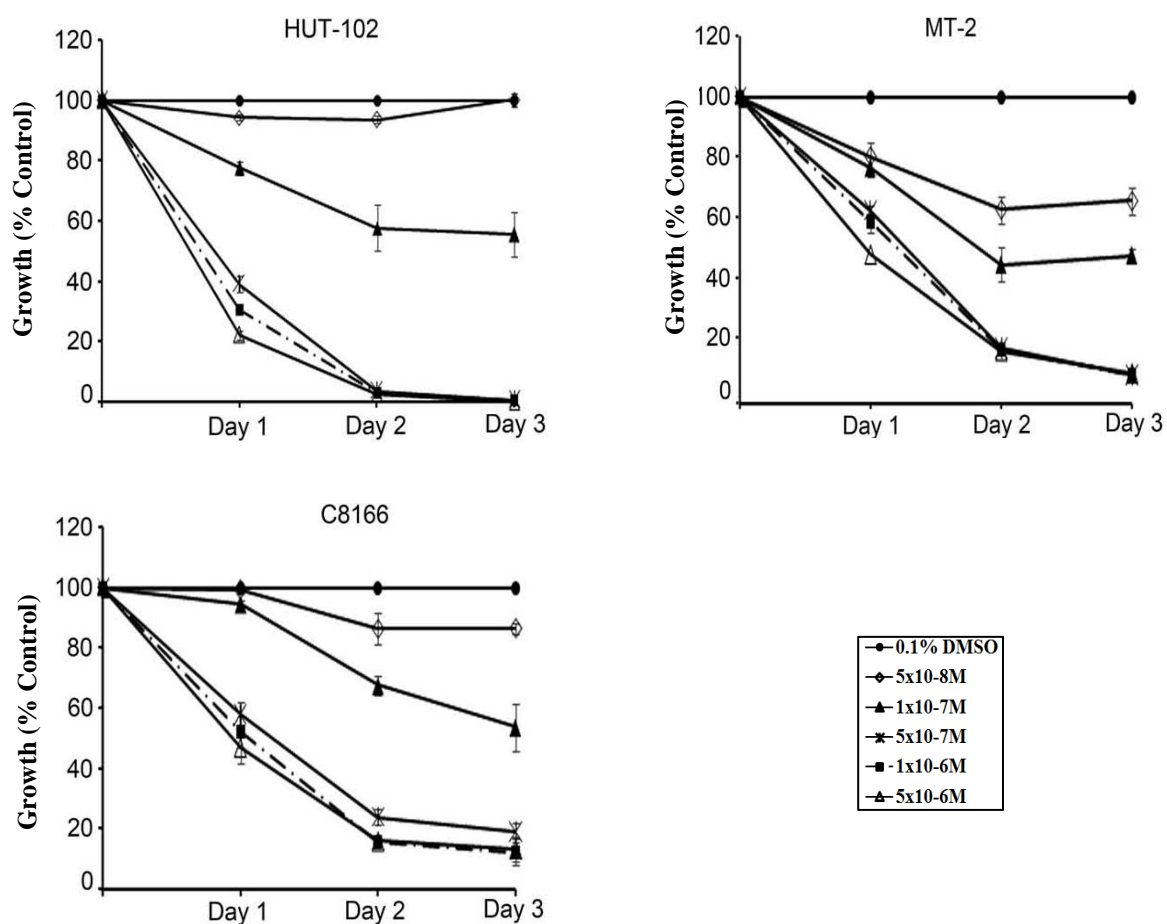


Figure 6. ST1926 treatment of HTLV-1 positive cells causes a concentration - and time-dependent growth suppression. HuT-102, and MT-2, and C8166 were seeded at a density of  $2 \times 10^5$  cells/ml. Cell growth was assayed in quadruplicate wells with the CellTiter 96® nonradioactive cell proliferation kit. The results are expressed as percentage of control (0.1% DMSO), and represent the mean of the results obtained in at least three independent experiments ( $\pm$ ) SE.

## ***2. HTLV-1 Negative Cells are Sensitive to ST1926***

We used three HTLV-1 negative cell lines (Jurkat, Molt-4, and CEM) to test for the growth and viability of these cell lines upon treatment with ST1926. Concentrations of ST1926 that range from 0.05  $\mu\text{M}$  to 5  $\mu\text{M}$  were used, and these have shown similar growth-inhibitory effects in all tested cell lines (Figure 7). At 24 hours post treatment, 1  $\mu\text{M}$  ST1926 inhibited growth by 78% of control in Jurkat and by 83% of control in Molt-4, and 61% in CEM and completely eradicated growth at 72 hours. We have also observed similar trends with trypan blue exclusion assay (data not shown).

In conclusion, we have shown that both HTLV-1 positive and negative malignant cells have comparable sensitivity to ST1926.

## ***3. ST1926 Induces Growth Inhibition in Primary ATL Cells***

We also determined the effect of ST1926 on peripheral blood mononuclear cells (PBMC) isolated from three patients; two with newly diagnosed acute ATL and one with chronic ATL which relapsed treatment (Bitar 2009; unpublished results). Cells were treated with 1  $\mu\text{M}$  and 5  $\mu\text{M}$  ST1926 up to 96 hours. Interestingly, 1  $\mu\text{M}$  ST1926 completely inhibited the growth of primary ATL cells from the newly diagnosed acute ATL patients and more than 60% in a relapsed ATL patient (Figure 8).

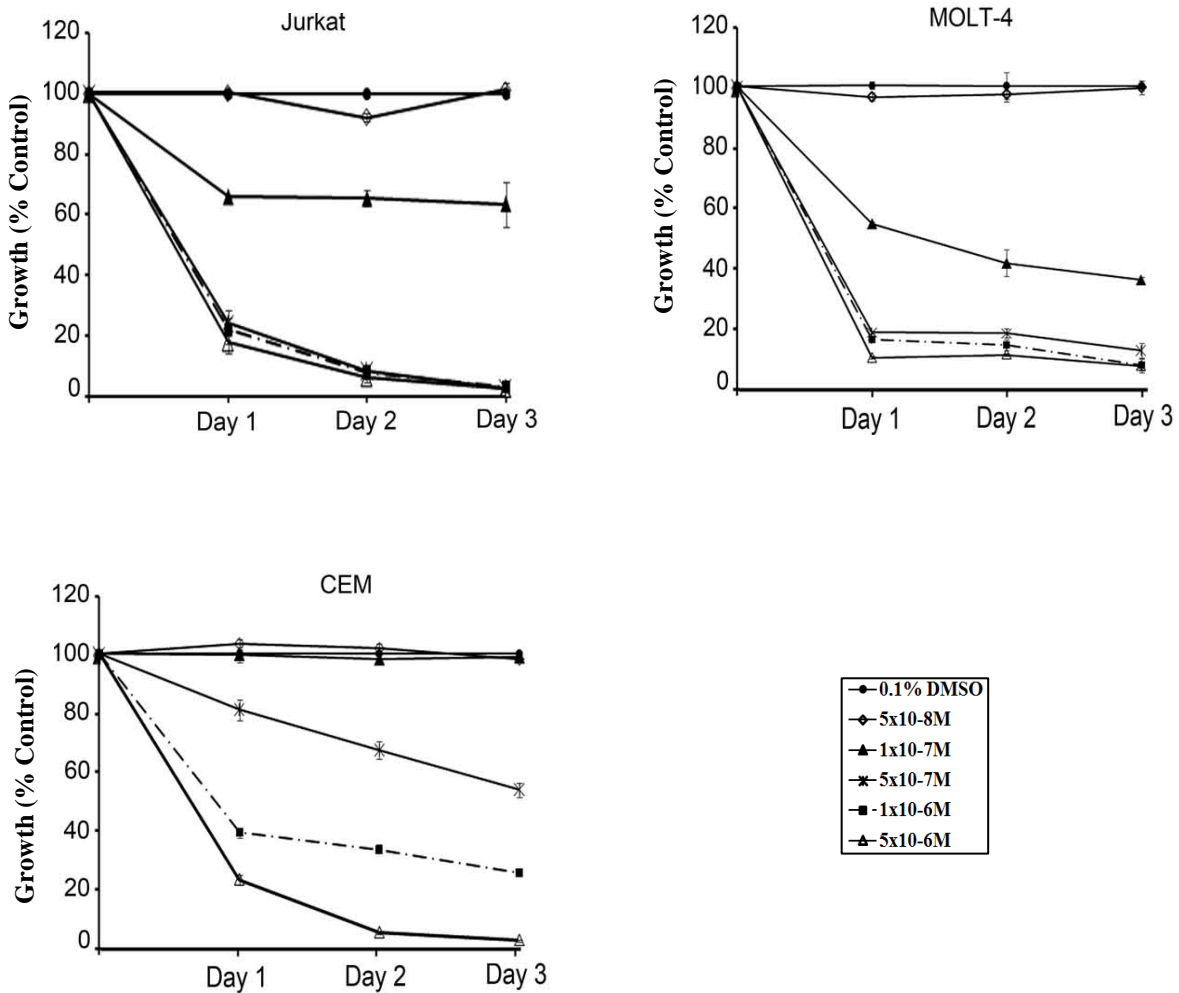


Figure 7. ST1926 treatment of HTLV-1 negative cells causes a concentration and time-dependent growth suppression. CEM, Jurkat, and Molt-4 were seeded at a density of  $2 \times 10^5$  cells/ml. Cell growth was assayed in quadruplicate wells with the CellTiter 96® nonradioactive cell proliferation kit. The results are expressed as percentage of control (0.1% DMSO), and represent the mean of the results obtained in at least three independent experiments ( $\pm$ ) SE.

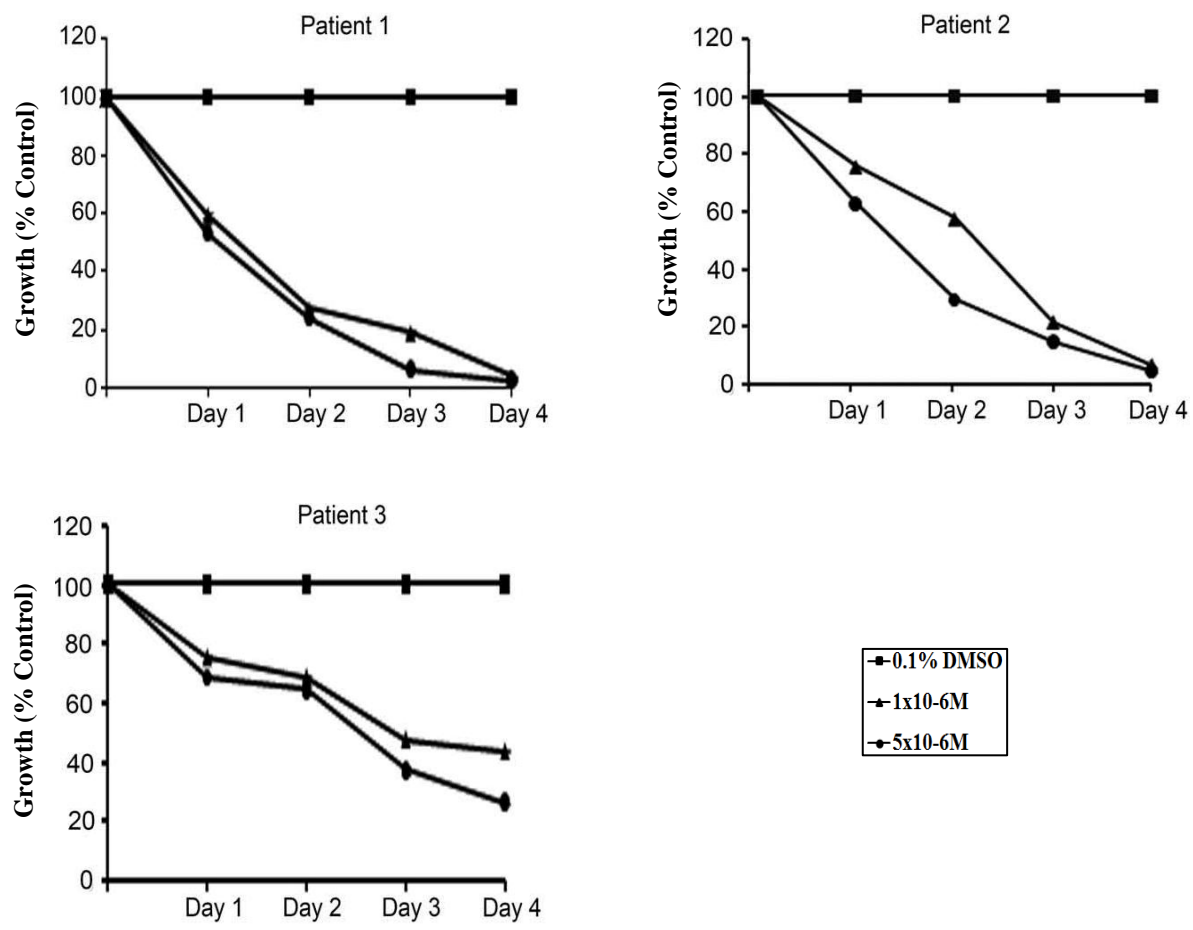


Figure 8. Primary ATL cells are sensitive to ST1926. Before treatment. Cells were cultured for a maximum of three days in 10% Rec IL-2, 20% FBS, and 2% PHA. Cell growth was assayed in quadruplicate wells with the CellTiter 96® non-radioactive cell proliferation kit. The results are expressed as percentage of control (0.1% DMSO) from three ATL patients.

#### 4. Normal Lymphocytes are Resistant to ST1926

Most importantly, resting and PHA-stimulated normal lymphocytes from three healthy donors were resistant to ST1926 treatment up to 10  $\mu$ M suprapharmacological concentrations (Figure 9). We observed less than 10 % decrease in growth of normal

resting or activated PBMCs after 48 hours of treatment with 10  $\mu$ M ST1926 (Bariaa Khalil, MS Biology, AUB 2012).

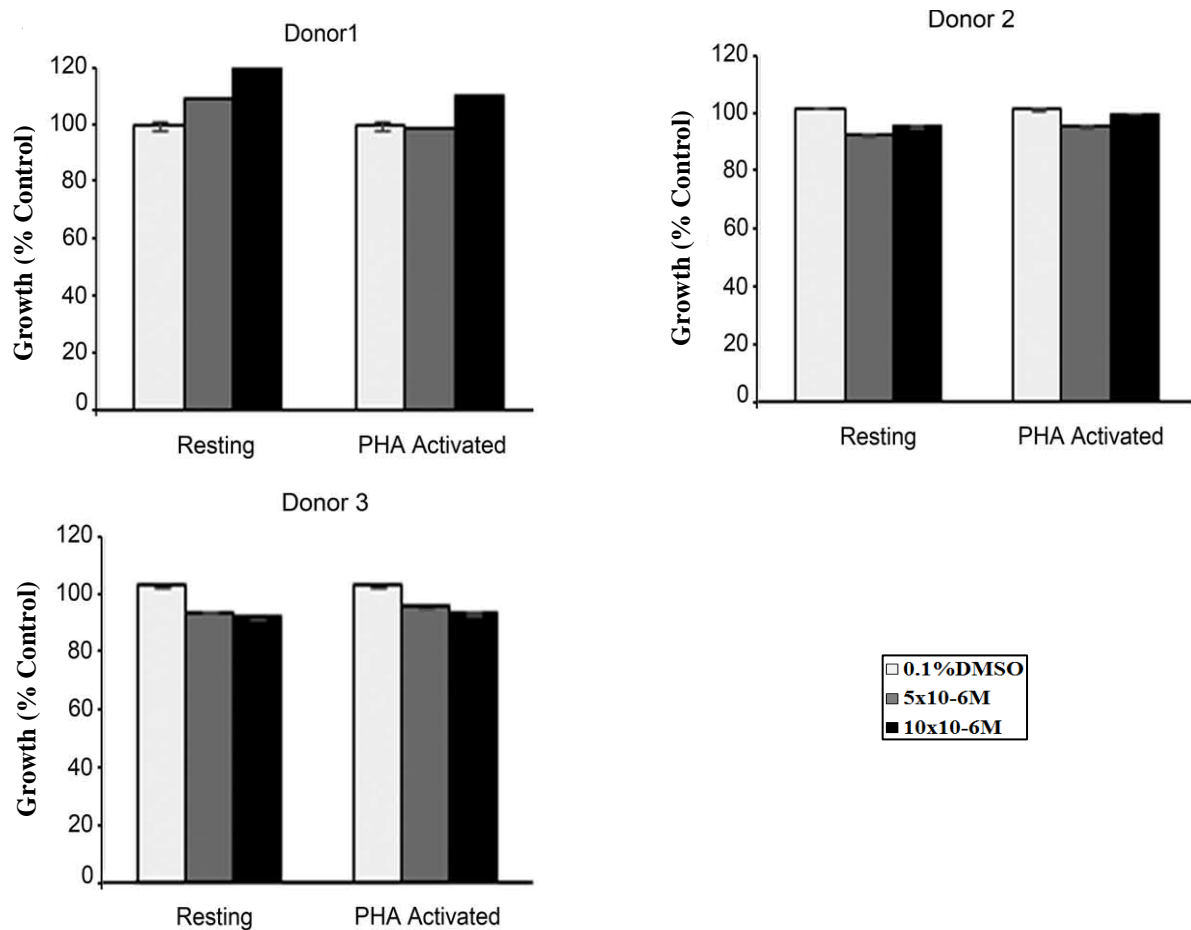


Figure 9. Resting and Activated T-lymphocytes are resistant to suprapharmacological concentrations of ST1926. PBMC were collected from three healthy donors after their informed consent. Activated PBMC were supplemented with 2% PHA. Cells were seeded at a density of  $2 \times 10^5$  cell/ml in 24-well plates and treated with 0.1% DMSO or  $10 \times 10^{-6}$  M ST1926 up to 48 h. Cell growth was assayed in triplicate wells using the Cell Titer 96® non-radioactive cell proliferation kit. Results are representative of three donors and expressed as percentage of control (0.1% DMSO) ( $\pm$  SD).



## **B. ST1926 Induces Cell Cycle Arrest and Apoptosis in HTLV-1 Transformed and Malignant T Cells**

Since 1  $\mu$ M ST1926 is pharmacologically achievable, we decided to use this concentration to decipher the mechanisms of ST1926-induced growth suppression and cell death; whereby at 48 hours, it caused at least 90 % growth inhibition in the HTLV-1 representative cell lines (HuT-102 and MT-2), and HTLV-1 negative cells (Jurkat and Molt-4). Cells treated with ST1926 and control cells (0.1%DMSO) were stained with PI (50  $\mu$ g/ml), and further cell cycle analysis was performed using FACScan flow cytometer. The cell cycle distribution among the untreated HuT-102, MT-2, Jurkat, and Molt-4 showed no variation (Figures 10 and 11).

### ***1. Treatment with ST1926 Causes G<sub>1</sub> Arrest and Accumulation of Cells in the PreG<sub>1</sub> Region***

Treatment with 1  $\mu$ M ST1926 caused a moderate G<sub>1</sub> cell cycle arrest after 24 hours of treatment which is reflected by a decrease in the percentage of cycling cells by 59% and 21% in HuT-102 and MT-2 cells, respectively, and by 27% in Molt-4 cells (Figures 10 and 11). Meanwhile, at 24 hours post-treatment with the same concentration there was a profound cell accumulation in the presumably apoptotic preG<sub>1</sub> region of 25% and 20% in HuT-102 and MT-2, respectively, and 40% and 20% in Jurkat, and Molt-4 cells, respectively (Figures 10 and 11).

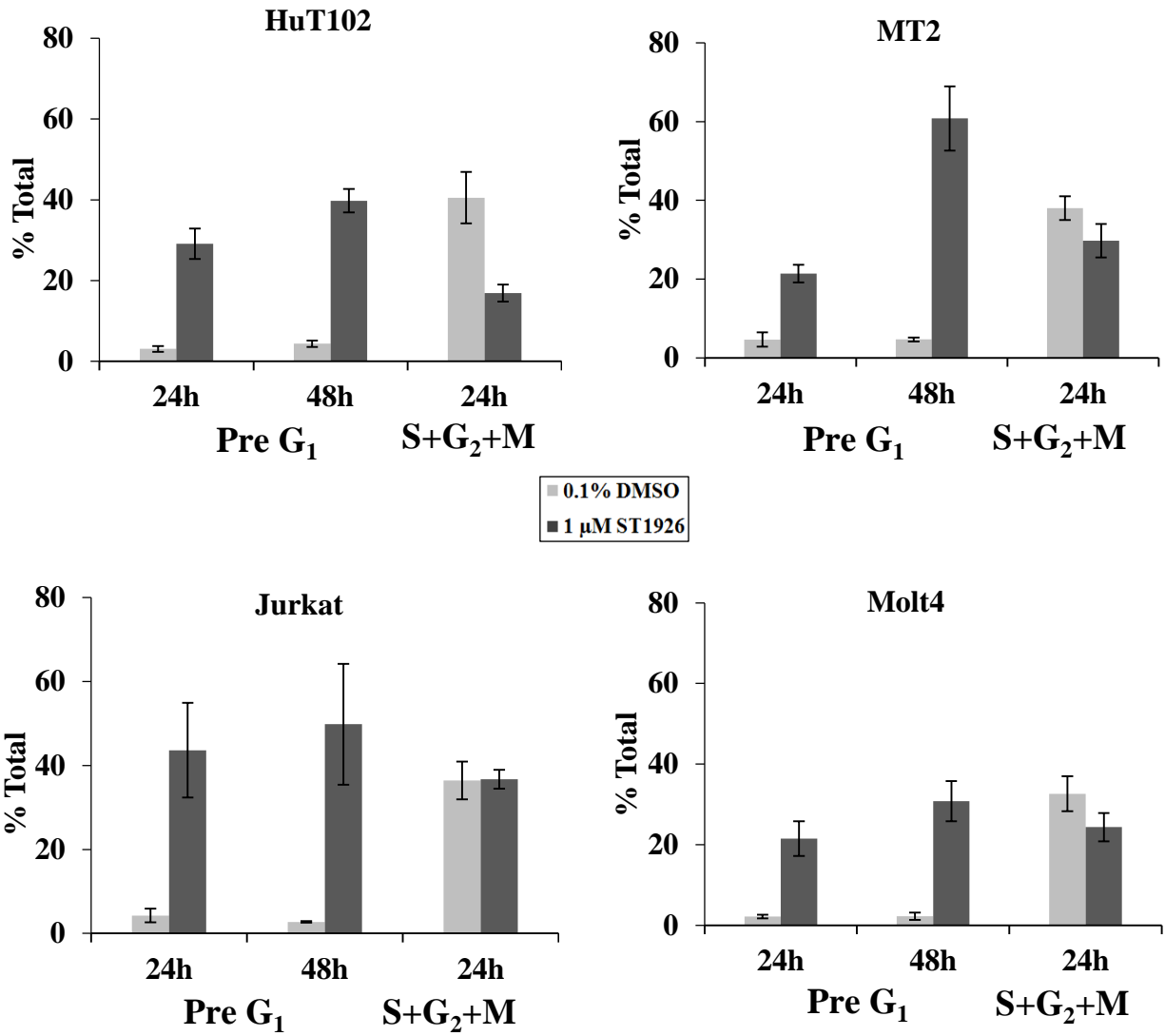


Figure 10. ST1926 induces cell cycle arrest in HTLV-1 positive and HTLV-1 negative human T-cells. HTLV-1 positive (HuT102 and MT-2), and HTLV-1 negative (Jurkat and Molt-4) cells were treated with 1 μM ST1926 up to 48 h while control cells were treated with 0.1% DMSO. Cells were stained with PI (50 μg/ml) and the cell cycle analysis was performed using a FACScan flow cytometer. The pre G<sub>1</sub> percentage represents apoptotic cells. Cycling cells, the sum of (S+G<sub>2</sub>/M) phases, are a percentage of nonapoptotic cells. Percentage of cells in G<sub>1</sub> phase is calculated as 100 minus (S+G<sub>2</sub>+M). The results represent the average of three independent experiments (±) SE.

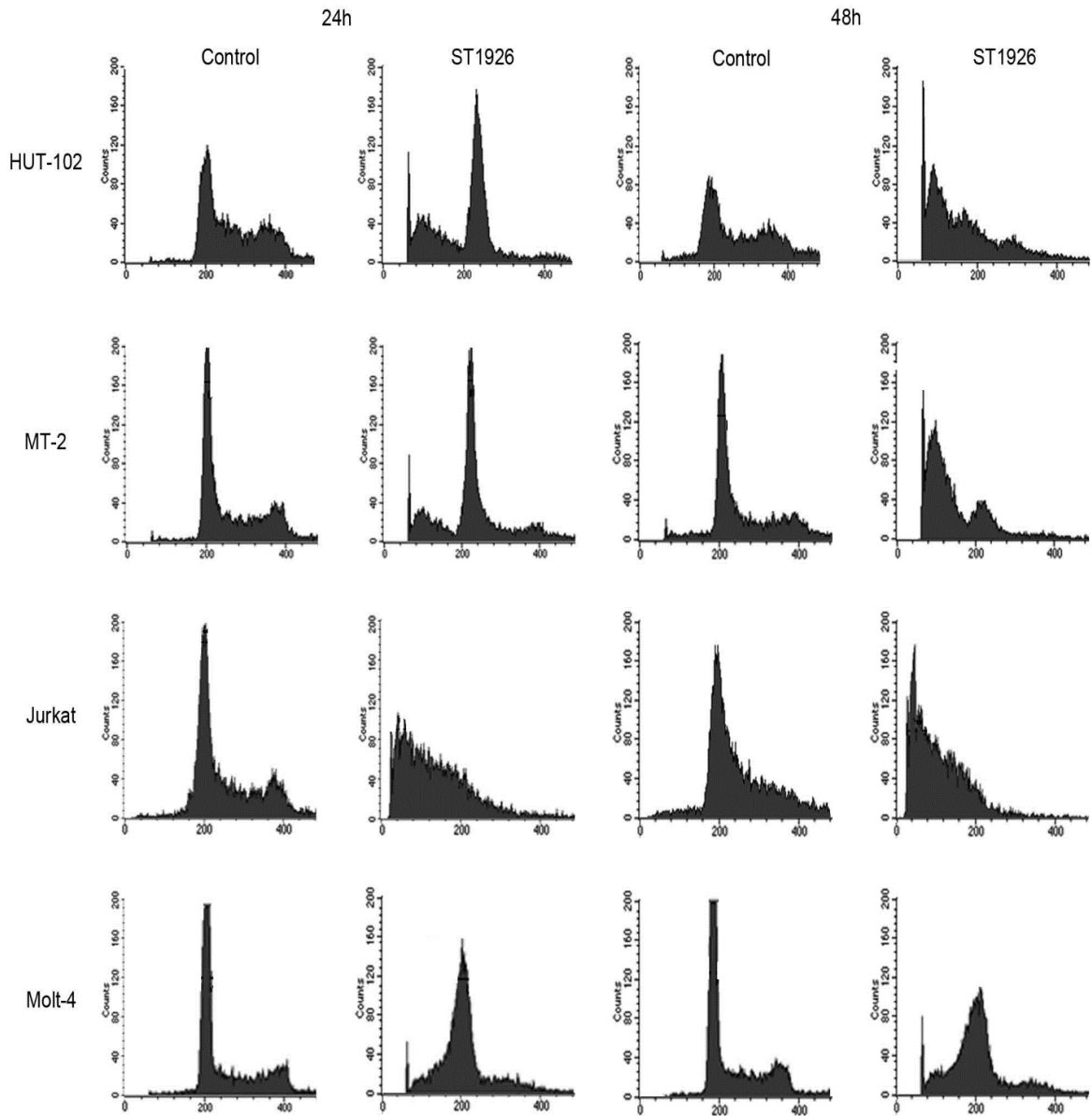


Figure 11. Histogram analysis of the effects of ST1926 on the cell cycle distribution of HuT-102, MT-2, Jurkat, and MOLT-4 cells. Cells were treated with 1  $\mu$ M ST1926 up to 48 h and stained with PI (50  $\mu$ g/ml) and the cell cycle analysis was performed using a FACScan flow cytometer. Results are representative of three independent experiments.

## ***2. ST1926 Induces Massive Apoptosis in all Tested Malignant T Cells***

Since all tested cells accumulate in the presumably apoptotic preG<sub>1</sub> phase upon 1  $\mu$ M treatment with ST1926, we used this concentration to confirm ST1926-induced apoptosis up to 48 hours using the TUNEL assay which shows DNA cleavage by labeling free 3'OH ends. The percentage of cells showing TUNEL positivity was markedly increased in all tested cell lines after treatment, as clearly as reaching 78% by 24 hours (Figure 12).

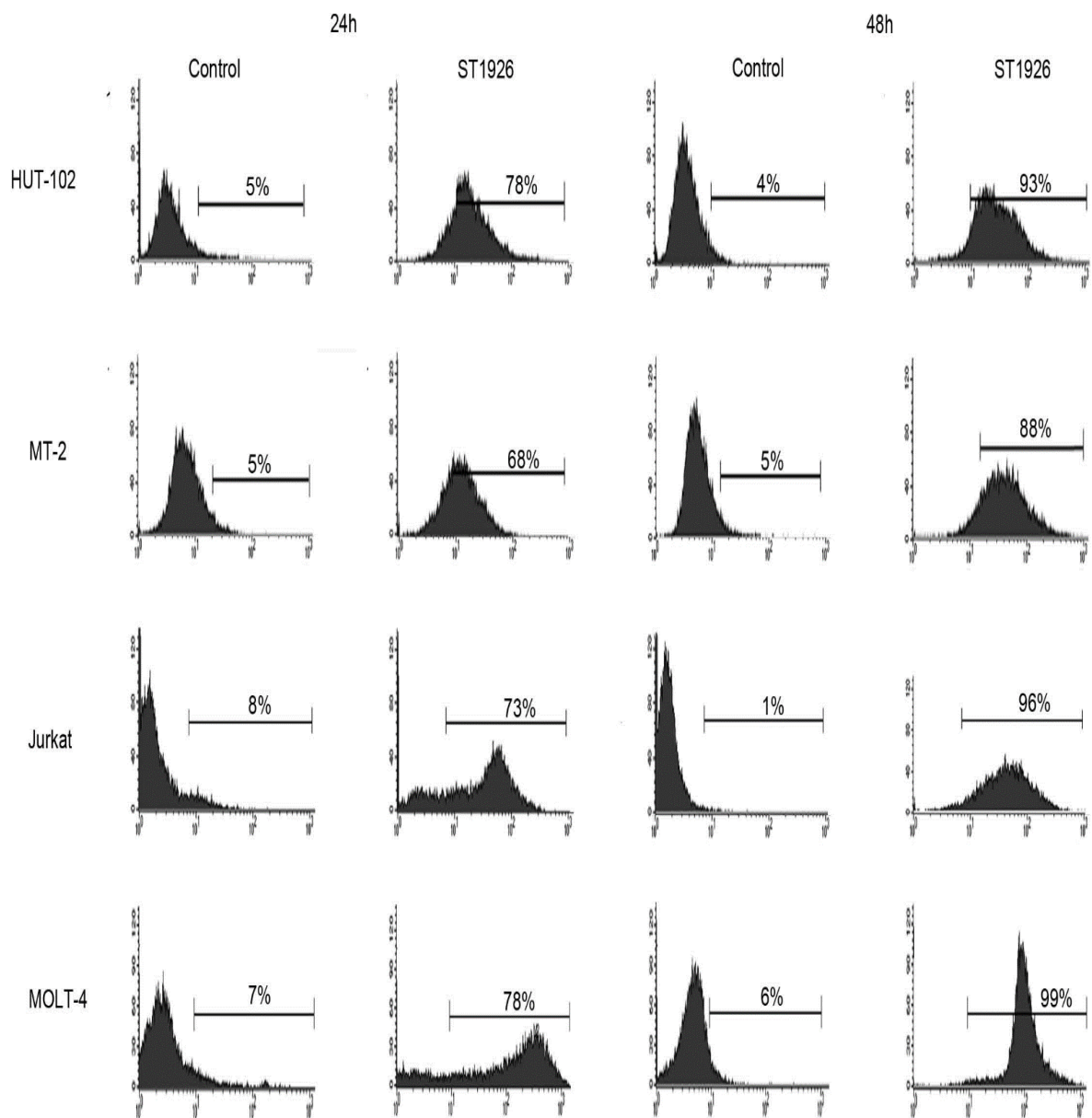


Figure 12. ST1926 induces apoptosis at 24 h by TUNEL positivity in all tested HTLV-1 positive and negative malignant T-cells. TUNEL analysis in HuT-102, MT-2, Jurkat, and Molt-4 treated with 1  $\mu$ M ST1926 for 24 h and 48 h. The results are representative of two independent experiments.

### **C. ST1926 Reduces Oncoprotein Tax levels and Induces p53 Activity**

To further investigate the different players in the ST1926-induced apoptosis, we used two HTLV-1 positive (HuT102 and MT-2), and two HTLV-1 negative (Jurkat and Molt-4) cell lines treated with 1  $\mu$ M ST1926 up to 24 hours. We have previously shown that ST1926-induced apoptosis was associated with caspase activation, detected by PARP cleavage as early as 12 hours in HuT-102 and MT-2 treated cells, and as early as 2 hours in Jurkat and Molt-4 treated cells. Caspase 3 was also cleaved in tested malignant T cells, and ST1926 induced-cell death was partially caspase-dependent (Bariaa Khalil, MS Biology, AUB 2012).

#### ***1. ST1926 Treatment Results in Reduced Levels of Oncoprotein Tax***

To investigate the effect of ST1926 on Tax oncoprotein, we treated malignant T cells with 1  $\mu$ M concentrations for 2, 12, and 24 hours. Notably, Tax protein levels were significantly reduced by 12 hours, and disappeared completely by 24 hours in both HuT-102 and MT-2 cells (Figure 13). Since Tax is known to transactivate the *p21* promoter, *p21* expression at both the transcript and protein levels, is found to be upregulated in HTLV-1 infected cells (Grassmann 2005). Therefore, we examined whether ST1926 modulates *p21* levels in HuT102 and MT-2 cells at 2, 12, and 24 hours. Similarly, *p21* levels were reduced as early as 12 hours in both cell lines (Bariaa Khalil, MS Biology, AUB 2012).

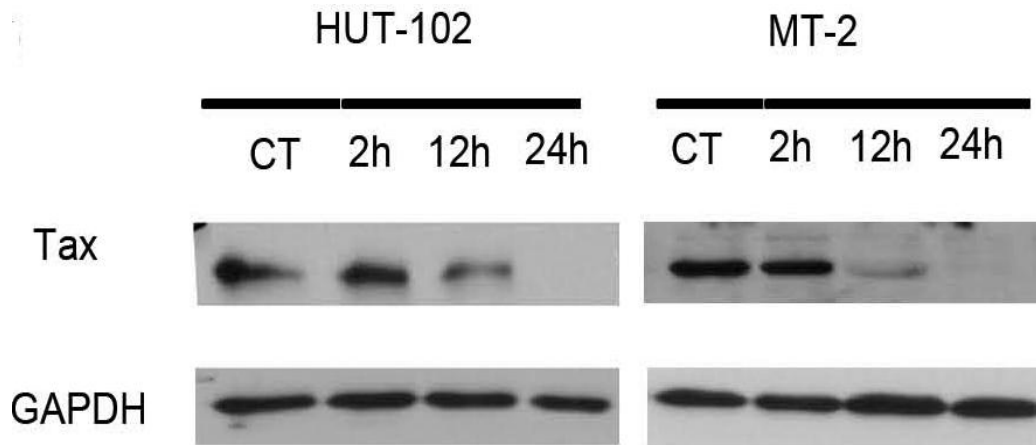


Figure 13. ST1926 degrades Tax protein in HuT-102 and MT-2. Cells were seeded at a density of  $2 \times 10^5$  cells/ml and treated with  $1 \times 10^{-6}$  M ST1926 for 2, 12 and 24 h. Whole SDS protein lysates (50  $\mu$ g/lane) were prepared and immunoblotted against Tax antibody. All blots were re-probed with GAPDH antibody to ensure equal protein loading. Similar trends in protein levels were observed in three independent experiments.

***2. ST1926 Upregulates Total and Phosphorylated p53 Protein Levels in HTLV-1 Transformed and Malignant T Cells, While Maintaining a p53-Independent Growth-Suppressive Effect***

The tumor suppressor gene, *p53*, which plays important roles in cell cycle arrest and apoptosis, is mutated in various human tumors (Levine, 1997). Many DNA viral oncoproteins including SV40 T antigen, human papillomavirus (HPV) E6, and adenovirus E1B and adenovirus E4orf6 oncoproteins inhibit p53 function through direct binding (Bargonetti 1992). Mutated *p53* genes have been found in only 25% of ATL cases (Nagai 1991, Yamato 1993). Moreover, Tax was shown to be involved in the inactivation of p53 function (Pise-Masison 1998). We monitored the total levels of p53 protein at 2, 12, and 24

hours post-treatment with 1  $\mu$ M ST1926. Total p53 protein levels, its phosphorylated active form, as well as the ratio of phosphorylated over unphosphorylated form, has substantially increased as early as 2 hours in HuT-102, MT-2, and Molt-4 (Figure 14, Bariaa, Khalil, MS Biology, AUB 2012). Meanwhile, both phosphorylated and unphosphorylated protein levels of p53 did not increase in Jurkat cells, since these cells possess a mutant form of p53 (Cheng 1990).

To further investigate the role of p53 in the growth-inhibitory response to ST1926, we have studied its anti-proliferative effect on Molt-E6, a p53-null cell line, and compared it to Molt4-LXSN with wild type *p53* (Dbaibo 1998). We observed a similar trend of dose- and time-dependent response in both cell lines irrespective of *p53* status, which rules out the role of p53 in ST1926 growth-suppressive response, at least in Molt-4 cells (Figure 15).



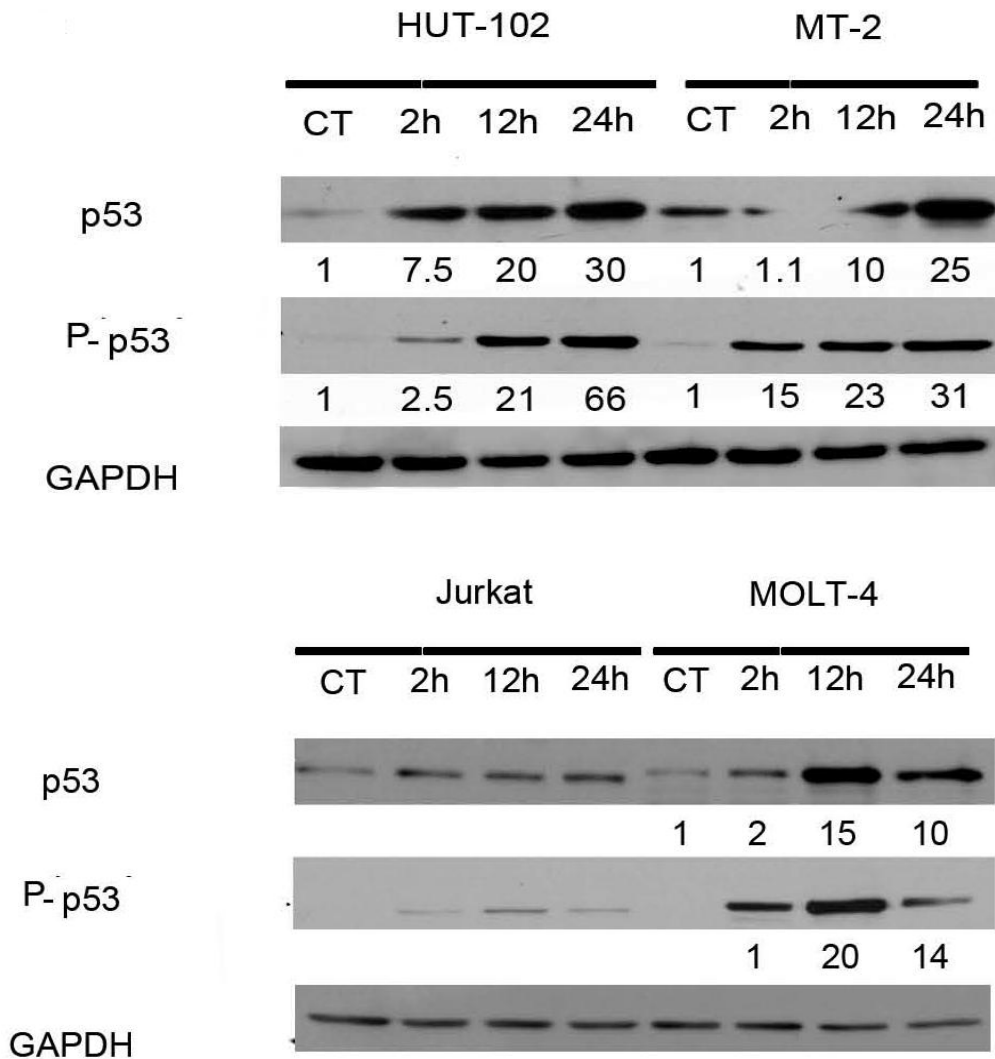


Figure 14. ST1926 upregulates p53 and its phosphorylated form in HTLV-1 positive cells and HTLV-1 negative cells. Cells were seeded at a density of  $2 \times 10^5$  cells/ml and then treated with  $1 \times 10^{-6}$  M ST1926 for 2, 12 and 24 h. Whole SDS protein lysates (50  $\mu$ g/lane) were prepared and immunoblotted against p53 and phosphorylated p53 antibodies. All blots were re-probed against GAPDH to ensure equal protein loading. Similar trends in protein levels were observed in three independent experiments. p53 and phosphorylated p53 bands were quantified and results are expressed relative to control cells (0.1% DMSO) or 2 h time point, respectively.

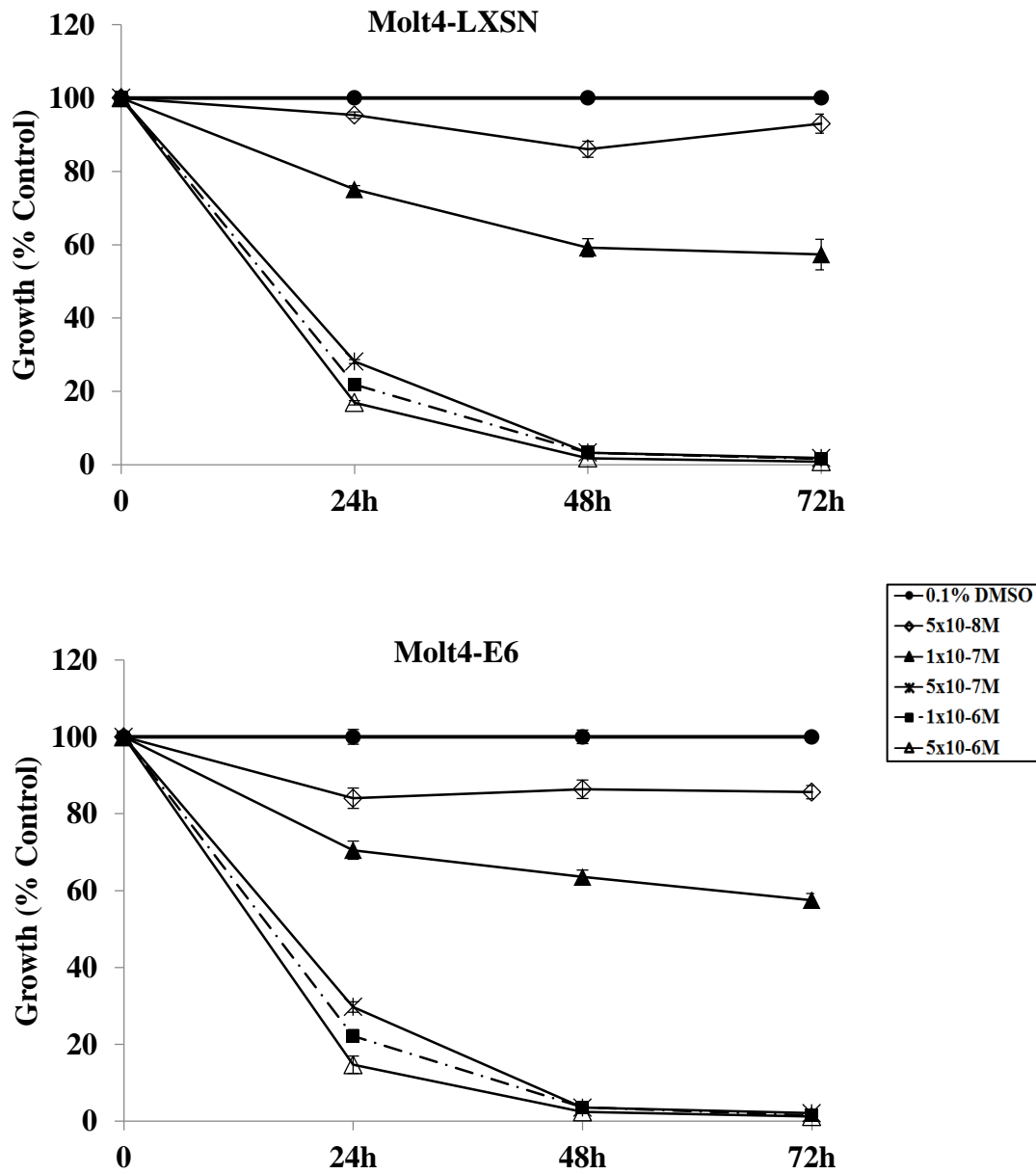


Figure 15. ST1926 growth suppressive effect is p53-independent in Molt-4 cells. Molt4-LXSN and Molt4-E6 were seeded at a density of  $2 \times 10^5$  cells/ml. Cell growth was assayed in quadruplicate wells with the CellTiter 96® nonradioactive cell proliferation kit. The results are expressed as percentage of control (0.1% DMSO), and represent the mean of the results obtained in at least three independent experiments ( $\pm$ ) SE.

#### **D. ST1926 Induces an Early Time-dependent Accumulation of Ceramide in Both HTLV-1 Positive and Negative Malignant T Cells**

As we have discussed earlier, ceramide plays a central role in sphingolipid metabolism. Moreover, multiple lines of evidence have established its anti-tumor properties in response to apoptotic stimuli (Huang 2011). We have previously determined that HPR and CD437 produce distinct ceramide responses in HTLV-1 positive and HTLV-1 negative malignant cells, with the former cell type having defect in accumulating ceramide (Darwiche 2005, unpublished data). Since 1  $\mu$ M ST1926 is a pharmacologically achievable and a non-cytotoxic concentration that causes more than 50% growth inhibition at 24 hours in all tested malignant T-cells with no effect on normal lymphocytes, we decided to test the effect of this concentration on ceramide accumulation. HTLV-1 positive (HuT-102 and MT-2) and HTLV-1 negative cells (Molt-4 and Jurkat) were treated with 1  $\mu$ M ST1926 for 2, 6, 12, 18, and 24 hours.

We tested the effect of 1  $\mu$ M ST1926 on the kinetics of ceramide accumulation in HTLV-1 positive, HuT-102 and MT-2 cells. Interestingly, our results confirm a time-dependent response in ceramide generation (Figure 16). The rise in ceramide levels started as two-fold increase at 12 hours, gradually increasing up to three-fold in HuT-102 and MT-2 cells. Remarkably, the sustained elevation in ceramide levels were observed prior to ST1926-induced cell death in the indicated cell lines (Figure 6 and data not shown).

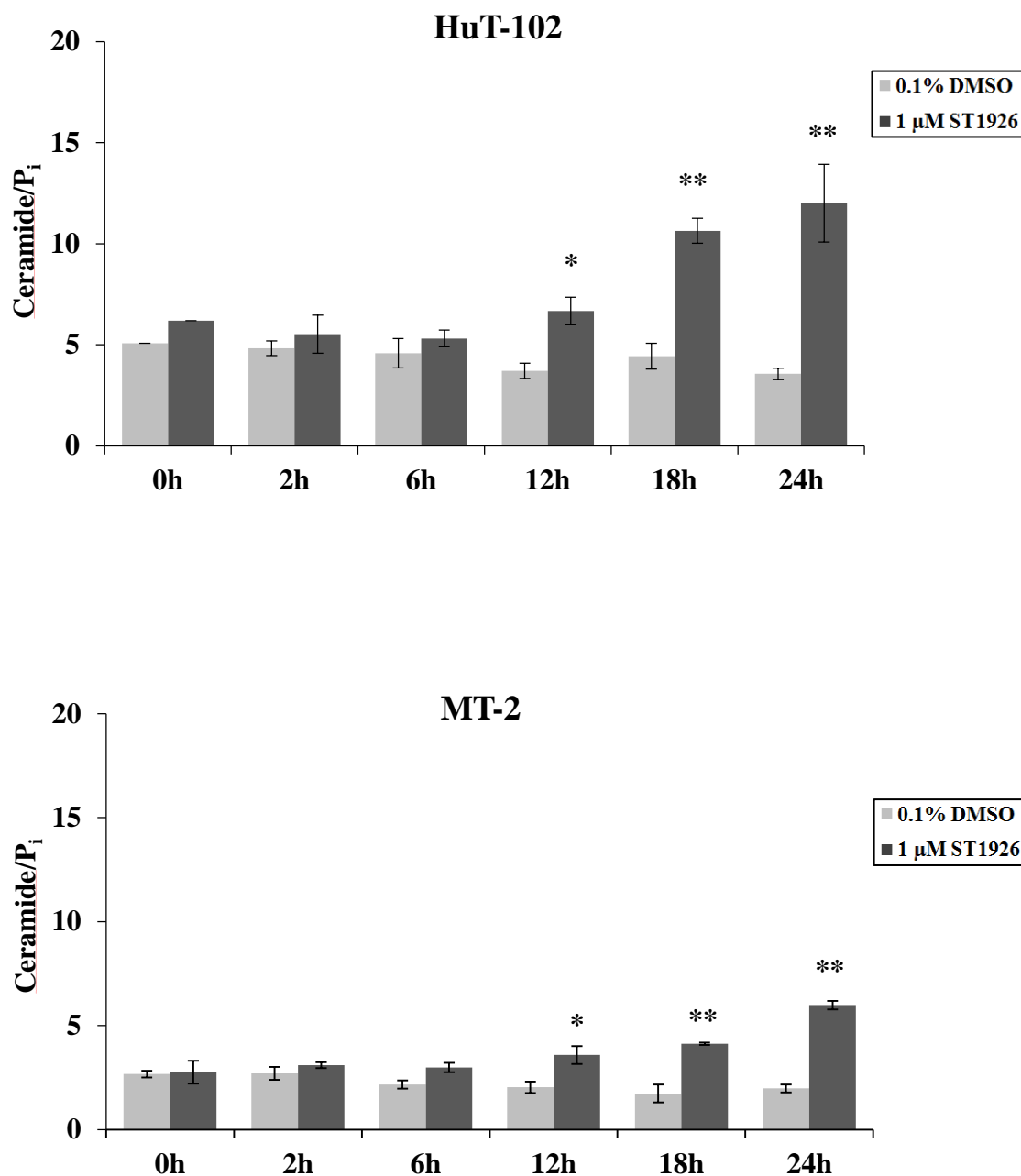


Figure 16. ST1926 treatment causes early accumulation in ceramide levels in HTLV-1 positive (HuT-102 and MT-2) human T-cell lines. Cells were seeded at a density of  $3.5 \times 10^5$  cells/ml and treated with 0.1 % DMSO as control or 1  $\mu$ M ST1926 for the indicated timepoints. Ceramide levels were determined in triplicates using the DGK assay as described in the Experimental Section and normalized to total cellular lipid phosphate levels. Data points represent the mean ( $\pm$  SD). Results are representative of two independent experiments. The asterisks \* and \*\* indicate statistically significant differences at  $p \leq 0.05$  or  $p \leq 0.01$ , respectively, *versus* control using the *t*-test.

We also tested the effect of ST1926 on ceramide generation in HTLV-1 negative, Jurkat and Molt-4 cells. Treatment with 1  $\mu$ M ST1926 stimulated a similar, but much more pronounced accumulation of ceramide in Molt-4 and Jurkat cells (Figure 17). The increase in ceramide was observed as two-fold at 6 hours in Jurkat and two fold at 12 hours in Molt-4 cells, reaching five-fold increase at 18 hours, and increasing up to at least ten-fold increase at 24 hours in Molt-4 and Jurkat cell lines (Figure 17). Notably, the sustained increase in ceramide levels preceded major ST1926-induced growth suppression and cell death in all tested HTLV-1 negative cell lines at the indicated concentrations (Figure 7 and data not shown).

In summary, our results indicate an early time-dependent accumulation of ceramide upon ST1926 treatment in both HTLV-1 positive and negative malignant T cells.

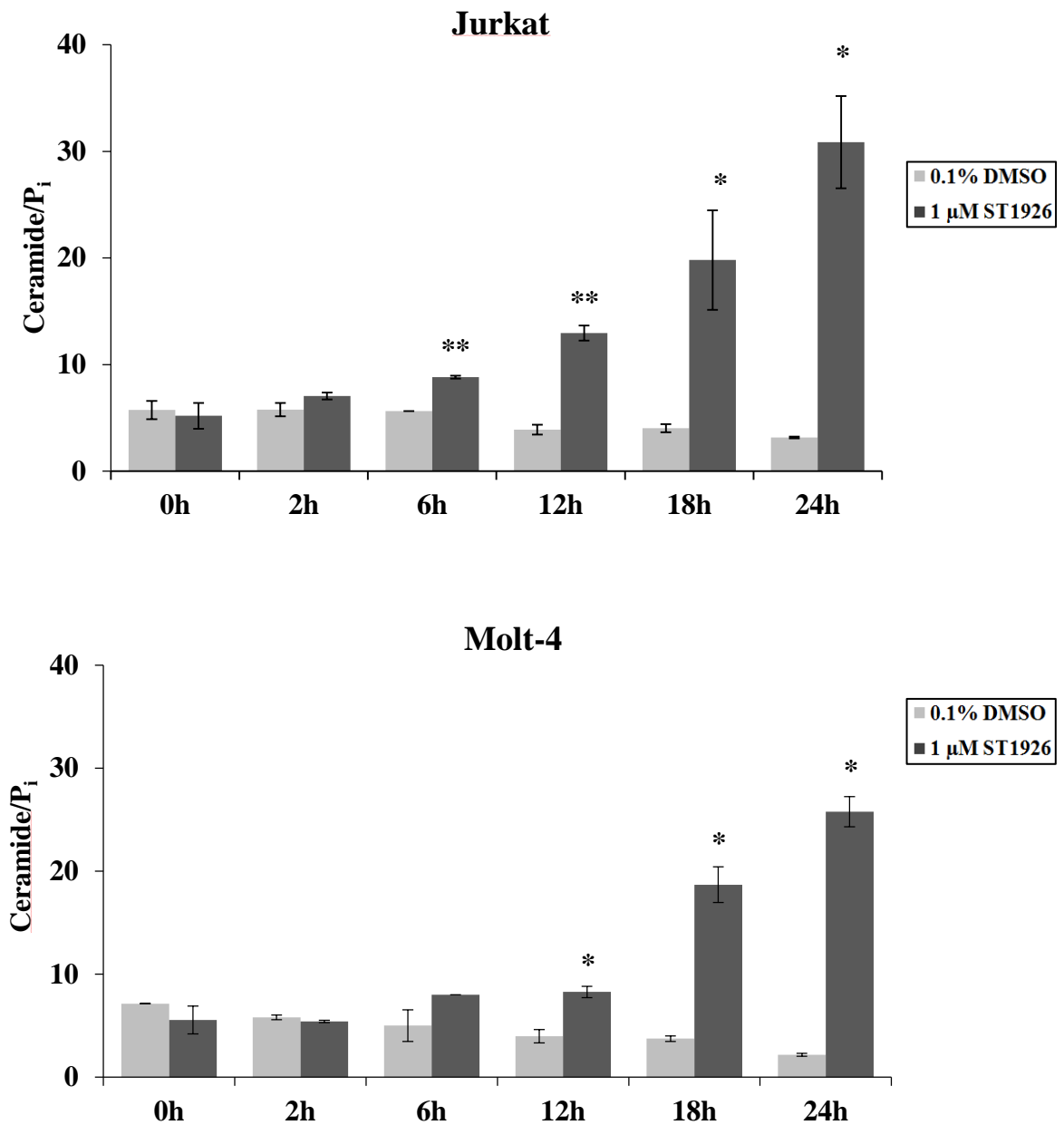


Figure 17. ST1926 treatment causes early accumulation in ceramide levels in HTLV-1 negative malignant cells (Jurkat and Molt-4). Cells were seeded at a density of  $3.5 \times 10^5$  cells/ml and treated with 0.1 % DMSO as control or 1  $\mu$ M ST1926 for the times indicated. Ceramide levels were determined in triplicates using the DGK assay as described in the Experimental Section and normalized to total cellular lipid phosphate levels. Data points represent the mean ( $\pm$  SD). Results are representative of two independent experiments. The asterisks \* and \*\* indicate statistically significant differences at  $p \leq 0.05$  or  $p \leq 0.01$ , respectively, *versus* control using the *t*-test.

### **E. ST1926 Stimulates a Dose-dependent Accumulation of Ceramide in HTLV-1 Transformed and Malignant T Cells**

The effect of ST1926 was further investigated in HTLV-1 positive (HuT-102 and MT-2), and negative malignant T cells (Molt-4 and Jurkat). A dose-dependent elevation of ceramide using ST1926 concentrations ranging from 0.05  $\mu\text{M}$  up to 5  $\mu\text{M}$  for 24 hours in HuT-102 and MT-2 cells (Figure 18). An increase of two-fold in ceramide levels was observed in HTLV-1 positive cells (HuT-102 and MT-2) following 24 hours of treatment with 0.1  $\mu\text{M}$  ST1926, and reaching a similar level with 1  $\mu\text{M}$  and 5  $\mu\text{M}$  concentrations of ST1926 (Figure 18).

Furthermore, a dose-dependent accumulation of ceramide was noted in Molt-4 at 24 hours with five-fold increase using 1  $\mu\text{M}$ , and nine-fold increase at 5  $\mu\text{M}$  ST1926 (Figure 19). Similarly, Jurkat cells have shown an increase of four-fold in ceramide levels following treatment for 24 hours with 1  $\mu\text{M}$  ST1926, and this level reached up to five-fold using a concentration of 5  $\mu\text{M}$  ST1926 (Figure 19).

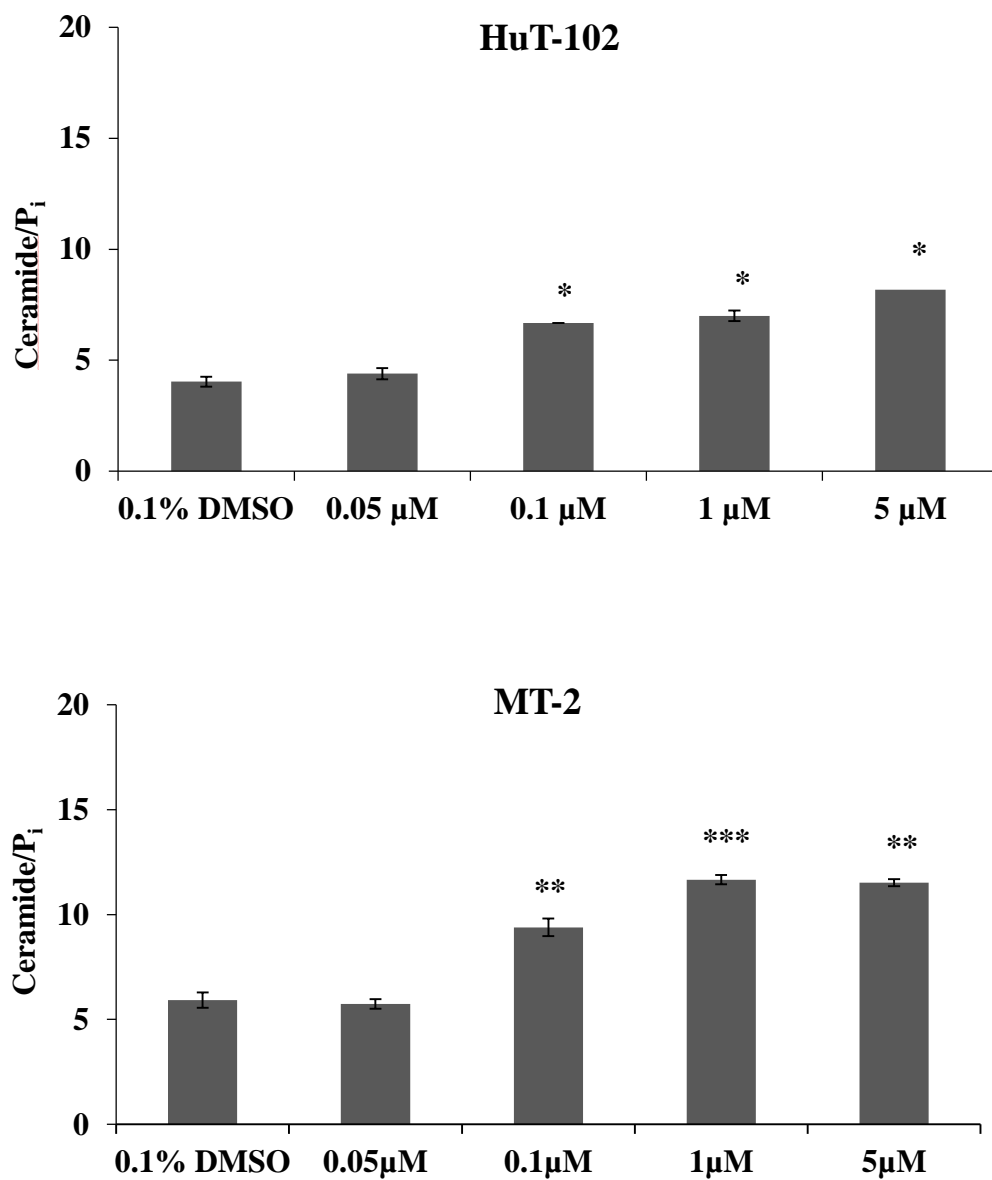


Figure 18. Dose-response to ST1926 treatment in HTLV-1 positive malignant cells. HuT-102 and MT-2 cells were seeded at a density of  $3.5 \times 10^5$  cells/ml and treated with the indicated concentrations of ST1926 for 24 h. Ceramide levels were determined in triplicates using DGK assay as described in the Experimental Section and normalized to total cellular lipid phosphate levels. Data points represent the mean ( $\pm$  SD). Results are representative of two independent experiments. The asterisks \*, \*\*, \*\*\* indicate statistically significant differences at  $p \leq 0.05$ ,  $p \leq 0.01$ , or  $p \leq 0.001$ , respectively, versus control using the *t*-test.



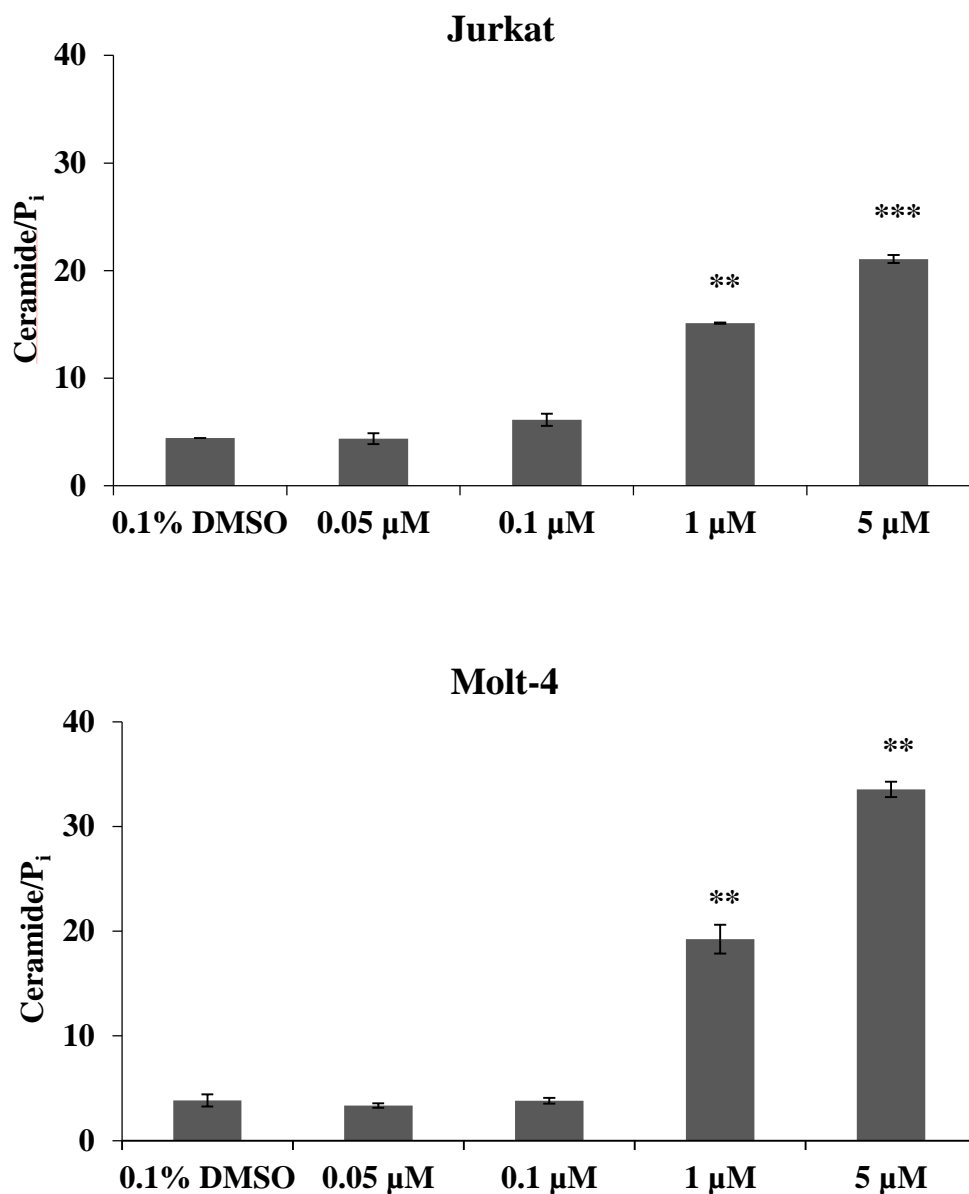


Figure 19. Dose-response to ST1926 treatment in HTLV-I-negative (Jurkat and Molt-4) human T-cells. Cells were seeded at a density of  $3.5 \times 10^5$  cells/ml and treated with the indicated concentrations of ST1926 for 24 h. Ceramide levels were determined in triplicates using DGK assay as described in the Experimental Section and normalized to total cellular lipid phosphate levels. Data points represent the mean ( $\pm$  SD). Results are representative of two independent experiments. The asterisks \*, \*\*, \*\*\* indicate statistically significant differences at  $p \leq 0.05$ ,  $p \leq 0.01$ , or  $p \leq 0.001$  respectively, *versus* control using the *t*-test.

## **F. ST1926 Induces Early *De Novo* Ceramide Synthesis in HTLV-1 Positive and HTLV-1 Negative Malignant T Cells**

We have previously demonstrated that HPR activates *de novo* pathway of ceramide synthesis in HTLV-1 negative human T-cells, but not in HTLV-1 transformed cells (Darwiche 2005). Moreover, this defect in ceramide synthesis upon HPR treatment was attributed to Tax inhibitory action on ceramide generation in HTLV-1 positive cells, as well as in Tax overexpressing Molt-4 and HeLa cells (Darwiche 2005). Therefore, we examined the contribution of *de novo* ceramide synthesis in HuT-102 and Molt-4 cells to elucidate the role of this pathway in ST1926-mediated ceramide accumulation in HTLV-1 positive and HTLV-1 negative malignant T cells, respectively.

HuT-102 and Molt-4 cells were treated with 1  $\mu$ M ST1926 for 6, 12, 18, and 24 hours, and *de novo* synthesized ceramide was measured by [ $^3$ H] palmitate incorporation. ST1926 treatment caused an early time-dependent increase in [ $^3$ H] ceramide in both cell lines, as early as 12 hours post treatment (Figure 20A). Remarkably, ST1926-induced *de novo* synthesis was more pronounced in Molt-4 *versus* HuT-102 cells reaching ten-fold increase *versus* two-fold increase at 24 hours post treatment, respectively (Figure 20A).

Interestingly, *de novo* ceramide accumulation in HuT-102 started at 12 hours which was preceded by earlier Tax protein degradation in HuT102 (Figure 20B). Moreover, we used Fumonisin B<sub>1</sub> (FB<sub>1</sub>), a potent ceramide synthase inhibitor, to distinguish between ceramide generated through *de novo* pathway and ceramide generated via sphingomyelin hydrolysis (Stiban 2010). FB<sub>1</sub> restored only one-third ceramide levels that accumulated upon ST1926, which confirms the major contribution of *de novo* pathway to endogenous ceramide accumulation upon ST1926 treatment (data not shown).

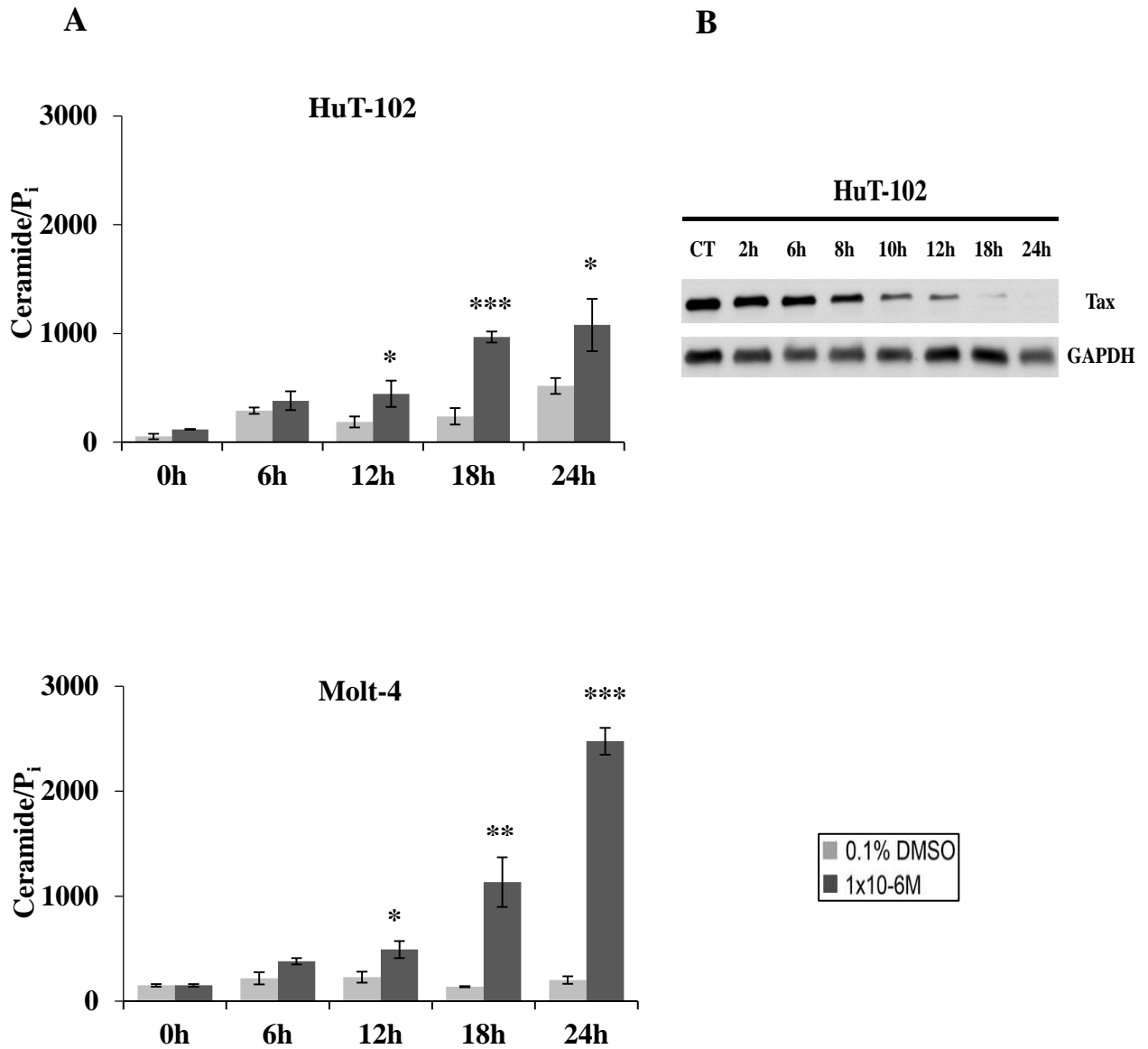


Figure 20. (A) ST1926 induces *de novo* ceramide synthesis in HTLV-1 positive (HuT102) and HTLV-1 negative malignant T-cells. HuT-102 and MT-2 cells were seeded at a density of  $3.5 \times 10^5$  cells/ml. *De novo* ceramide levels were determined in triplicates using the [ $^3$ H]palmitate incorporation method as described in the Experimental Section and normalized to total cellular lipid phosphate levels. Data points represent the mean ( $\pm$  SD). Results are representative of two independent experiments. The asterisks \*, \*\*, and \*\*\* indicate statistically significant differences at  $p \leq 0.05$ ,  $p \leq 0.01$ , or  $p \leq 0.001$ , respectively, *versus* control using the *t*-test. (B) ST1926 causes early degradation of Tax oncoprotein levels in HuT-102 cells. Cells were seeded at a density of  $2 \times 10^5$  cells/ml and then treated with  $1 \times 10^{-6}$  M ST1926 for 2, 12 and 24 h. Whole SDS protein lysates (50  $\mu$ g/lane) were prepared and immunoblotted against Tax antibody. The blot was re-probed against GAPDH to ensure equal protein loading.

### **G. Ceramide, but not Dihydroceramide Species, Predominantly Accumulate in Response to ST1926 Treatment in HTLV-1 Positive and HTLV-1 Negative Cells**

We have previously shown that HTLV-1 transformed cells have a defect in ceramide synthesis in response to HPR, and that the viral oncoprotein Tax was responsible for repressing the ceramide response in HTLV-1 positive human T-cell lines (Darwiche 2005). Therefore, HTLV-1 positive and HTLV-1 negative cells showed distinct ceramide response upon treatment with HPR, whereby Tax overexpression was sufficient to suppress ceramide synthase (s) activity, which is a crucial enzyme in *de novo* ceramide synthesis pathway (Darwiche 2005). Interestingly, dihydroceramide desaturase (DEGS1), the enzyme responsible for converting dihydroceramide to ceramide, was proven to be a direct target of HPR, which leads to accumulation of endogenous dihydroceramides rather than ceramides (Rahmaniyan 2011). Unlike ceramide, dihydroceramide is considered to be biologically inactive, at least in the context of cell death induction (Ogretmen and Hannun 2004).

To further explore the activity of ST1926 and its interplay with Tax in the regulation of ceramide metabolism, we performed Liquid Chromatography/Mass Spectrometric (LC/MS) analysis to differentiate the distinct ceramide (Cer)/dihydroceramide (dhCer) species that are generated upon ST1926 in HTLV-1 transformed and malignant T-cells. Basically, Liquid Chromatography (LC), is used to separate molecules in complex samples, such as biological fluids, based on their specific chemical and/or physical properties. Subsequently, this separation technique is coupled to mass spectrometry, which identifies and quantifies unknown species. Towards this end, HuT-102 and Molt-4 were treated with 1  $\mu$ M ST1926 for 12 and 24 hours.

Ceramide/dihydroceramide species were identified based on the fatty acyl- chain length that is introduced by different ceramide synthase (s) on the sphingoid base backbone of sphinganine. As such, ceramide species are categorized as medium long-chain (C14- C18), long-chain (C20- C22), and very long-chain (C24-C26).

Results confirm that ST1926 treatment induces a major accumulation of ceramide species relative to dihydroceramide species in response to 1  $\mu$ M ST1926 in both HuT-102 and Molt-4 cells after 12 hours (Table 2). Most importantly, this elevation was found to be consistent among all medium long-chain (Figure 21), long chain (Figure 22), and very-long chain (Figure 23) dihydroceramide and ceramide species. For instance, among medium long chain ceramides, accumulation of C16-ceramide constituted the most prominent increase among other species in this category in both HuT102 and Molt-4 cells (Figure 21). Similarly, there was a total increase in long-chain ceramides, of which C22-ceramide levels constituted the major increase among others in both cell lines (Figure 22). Also consistently, very-long chain ceramides were presented with similar trends of ceramide levels increase *versus* dihydroceramide; for example, C-24:1-ceramide levels were markedly increased among other species in this category in both treated HuT102 and Molt-4 cells (Figure 23).

Meanwhile, we also observed a minor dihydroceramide increase only 24 hours post- treatment in Molt-4 cells; however, HuT-102 cells accumulated higher levels of dihydroceramide species than Molt-4 cells did by 24 hours upon ST1926 treatment (Table 2). This could be clearly observed among medium long-chain dhCer/Cer species such as dhC14-Cer, dhC16-Cer, dhC18-Cer (Figure 21), among long-chain dhCer/Cer species, with the most prominent increase in the levels of dhC20-Cer and dhC22-Cer species (Figure 22),

and among very long-chain ceramides, such as dhC24-Cer and dhC24:1-Cer species (Figure 23). Interestingly, the major accumulation of dhCer and Cer levels in both cell lines was clearly observed among medium long-chain ceramides, followed by very long-chain ceramides, with least accumulation among long-chain ceramides (Table 3).

In conclusion, our analysis supports the results that ST1926 induces early *de novo* ceramide synthesis in both cell lines.

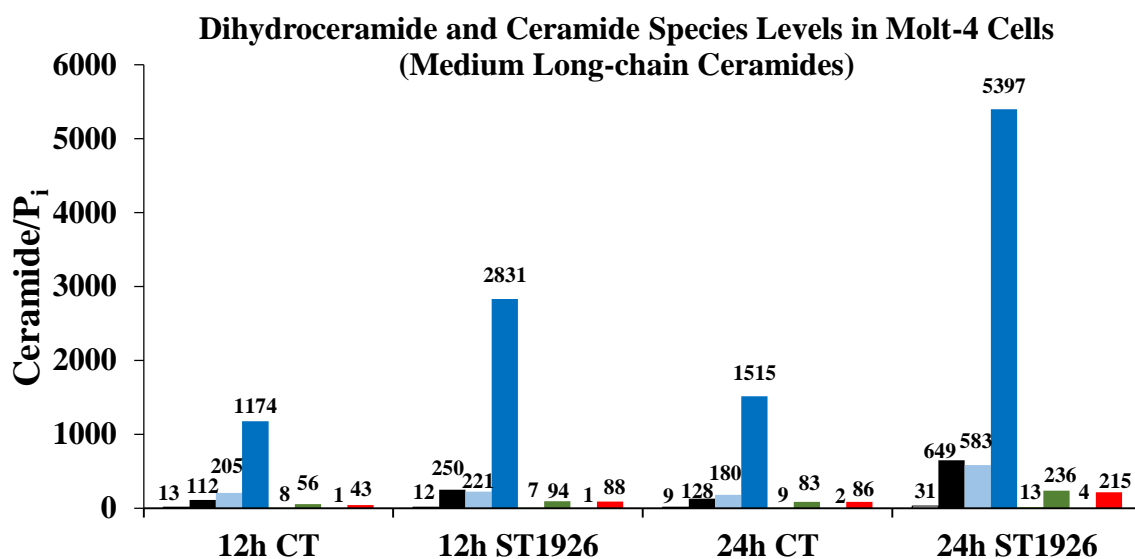
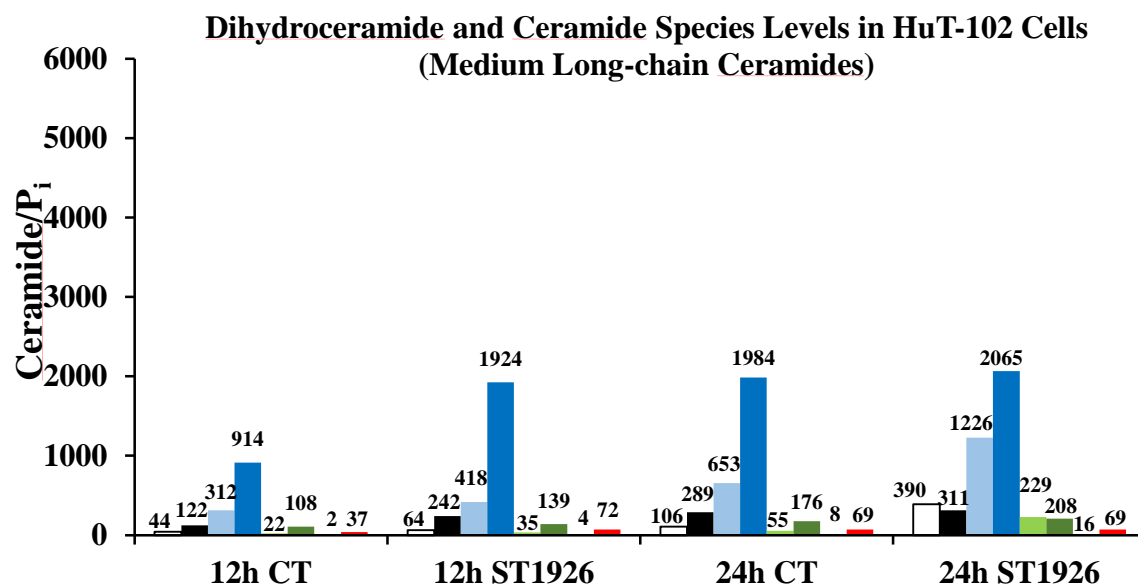
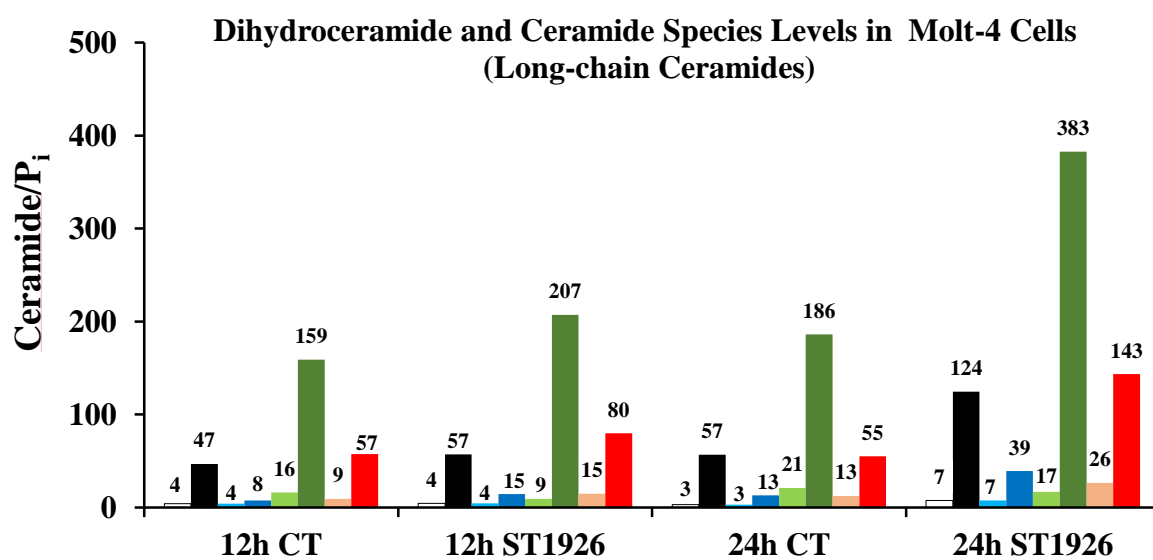
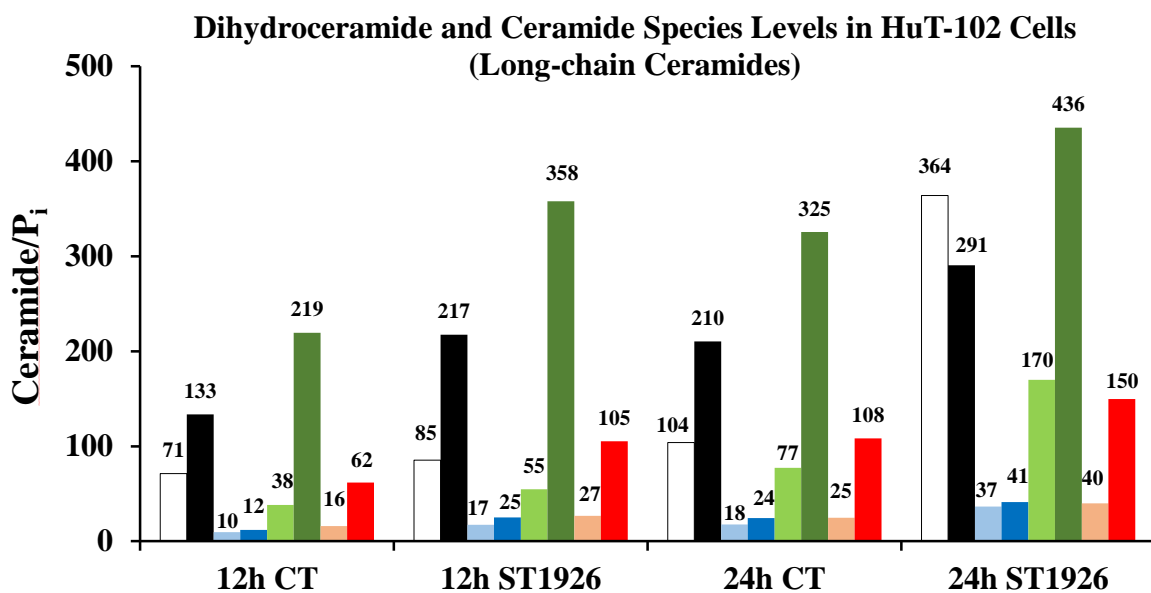


Figure 21. Medium-chain dihydroceramide/ceramide species levels in HTLV-1 positive and HTLV-1 negative cells in response to ST1926. HuT-102 and Molt-4 cells were seeded at a density of  $3.5 \times 10^5$  cells/ml and with treated with  $1 \mu\text{M}$  ST1926 for the indicated time points. DhCer/Cer species levels were measured in lyophilized samples in duplicates by LC/MS as described in Experimental Section and normalized to total cellular lipid phosphate levels.



■ dhC20-Cer ■ C20-Cer ■ dhC20:1-Cer ■ C20:1-Cer ■ dhC22-Cer ■ C22-Cer ■ dhC22:1-Cer ■ C22:1-Cer

Figure 22. Long-chain dihydroceramide/ceramide species levels in HTLV-1 positive and HTLV-1 negative cells in response to ST1926. HuT-102 and Molt-4 cells were seeded at a density of  $3.5 \times 10^5$  cells/ml and with treated with  $1 \mu\text{M}$  ST1926 for the indicated timepoints. DhCer/Cer species levels were measured in lyophilized samples in duplicates by LC/MS as described in Experimental Section and normalized to total cellular lipid phosphate levels.



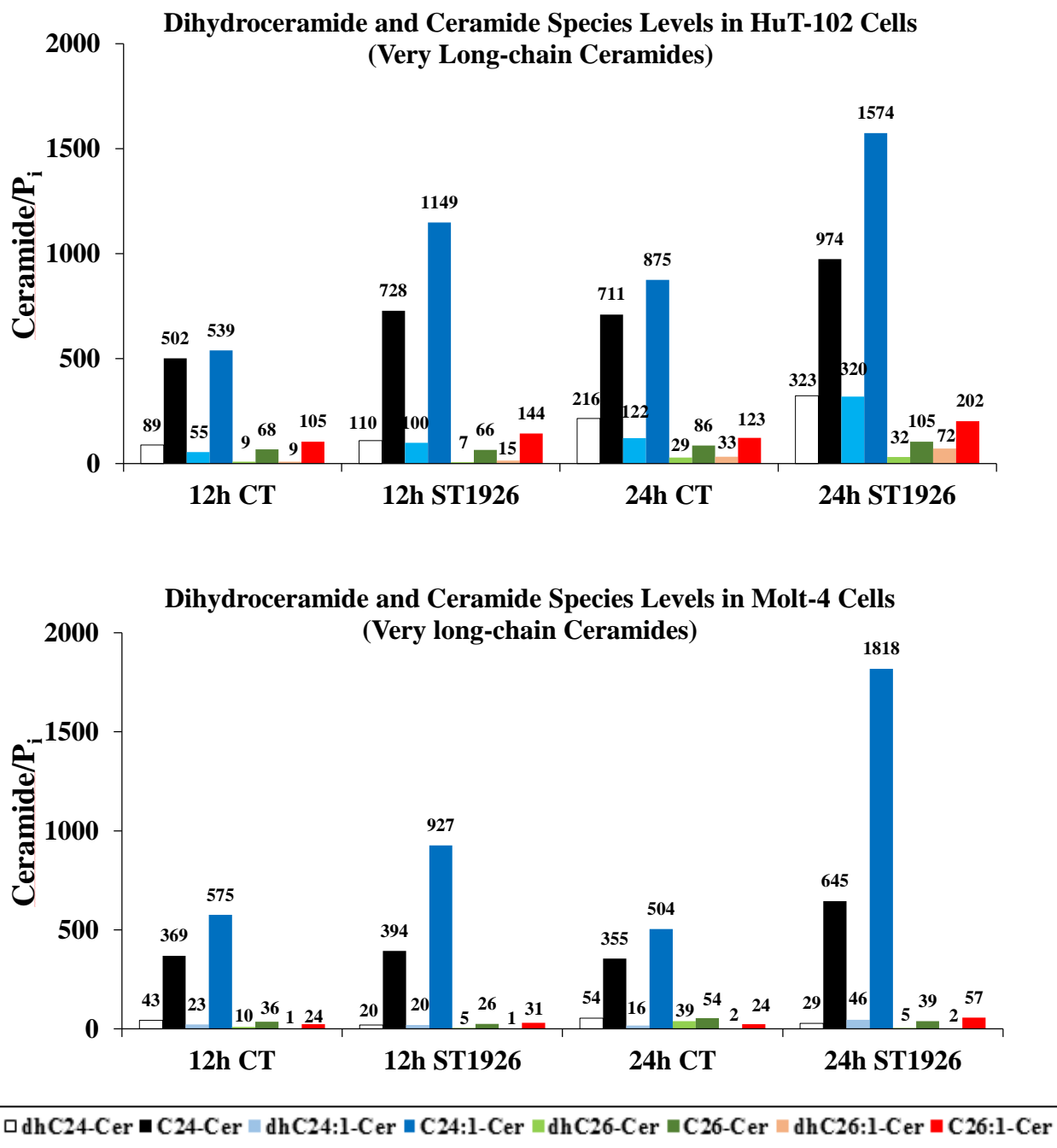


Figure 23. Very long-chain dihydroceramide/ceramide species levels in HTLV-1 positive and HTLV-1 negative cells in response to ST1926. HuT-102 and Molt-4 cells were seeded at a density of  $3.5 \times 10^5$  cells/ml and with treated with  $1 \mu\text{M}$  ST1926 for the indicated timepoints. DhCer/Cer species levels were measured in lyophilized samples in duplicates by LC/MS as described in Experimental Section and normalized to total cellular lipid phosphate levels.

**Table 2. Percent increase in total ceramide and dihydroceramide species in HuT-102 and Molt-4 cells**

<b>Cells</b>		<b>Total (dhCers +Cers)</b>	<b>Ceramide (% Total Cer)</b>	<b>Dihydroceramide (% Total Cer)</b>
<b>HuT-102</b>	<i>12 h</i>	2607	90	10
	<i>24 h</i>	3214	45	55
<b>Molt-4</b>	<i>12 h</i>	2321	100	0
	<i>24 h</i>	7103	94	6

Data are expressed as pmol/ $\mu$ g of total cellular lipid phosphate or percent, and are the mean of duplicates from one experiment.

**Table 3. Percent Increase of medium long chain (MLC), long chain (LC), and very long chain (VLC) ceramide and dihydroceramide species in HuT-102 and Molt-4 cells**

<b>Cells</b>		<b>Total Cer</b>	<b>MLC Cer (% Total Cer)</b>	<b>LC Cer (% Total Cer)</b>	<b>VLC Cer (% Total Cer)</b>
<b>HuT-102</b>	<i>12 h</i>	2607	51	13	36
	<i>24 h</i>	3214	36	20	44
<b>Molt-4</b>	<i>12 h</i>	2321	81	4	15
	<i>24 h</i>	7103	72	6	22

Data are expressed as pmol/ $\mu$ g of total cellular lipid phosphate or percent, and are the mean of duplicates from one experiment.

## **H. Bcl-2 Attenuates ST1926-Induced Cell Growth Arrest in Molt-4 cells**

We have previously shown that ST1926 treatment causes a major loss in mitochondrial membrane potential, and cause caspase 3 and PARP cleavage (Bariaa Khalil, MS Biology, AUB 2012). One of the earliest measurable changes in apoptosis occurs when the outer mitochondrial membrane becomes permeable and proteins located in the intermembrane space are released into the cytosol. A key regulator of apoptosis is the proto-oncogene *Bcl-2*, which was shown to play an inhibitory role in apoptosis initiated by several extracellular signals including chemotherapeutic drugs (Ogretmen and Hannun 2004). Therefore, we investigated whether Bcl-2 antagonizes ST1926-induced cell growth arrest in Molt-4 cells.

As we have demonstrated earlier, addition of ST1926 to malignant T cells induced significant growth suppression in a time- and dose-dependent manner. However, Molt-4 cells that overexpress Bcl-2 showed survival advantage over Molt-4 cells transfected with the control expression vector (MEP4) when challenged with ST1926 (Figure 24). Treatment with 1  $\mu$ M ST1926 caused 90% growth suppression in Molt4-MEP4 cells compared to 40% in Molt4-Bcl-2 cells.

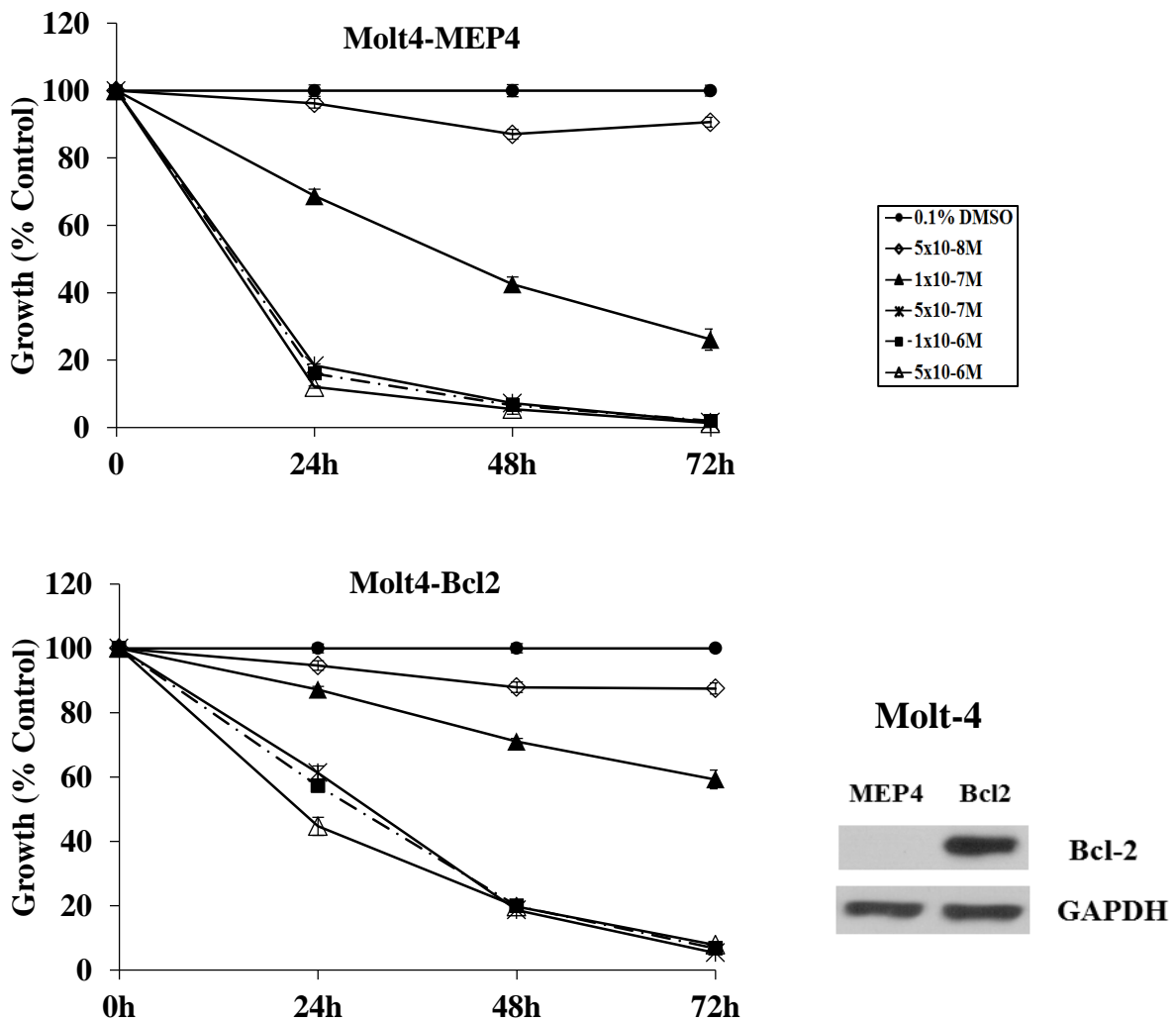


Figure 24. Bcl-2 attenuates ST1926-induced growth suppression in Molt-4 cells. Molt4-MEP4 and Molt4-Bcl2 were seeded at a density of  $2 \times 10^5$  cells/ml, and treated with 0.1% DMSO or with increasing concentrations of ST1926 ranging from  $5 \times 10^{-8}$  to  $5 \times 10^{-6}$  M up to three days. Cell growth was assayed in quadruplicate wells with the CellTiter 96® non-radioactive cell proliferation kit. The results are expressed as percentage of control (0.1% DMSO). Results are an average of three independent experiments ( $\pm$ SE).

## **I. Bcl-2 Delays Cell Death Response and Interferes with Ceramide Generation Mediated by ST1926 in Molt-4 Cells**

Although many downstream effector targets of ceramide apoptotic response are known, the way ceramide triggers these pathways still needs to be unveiled (Itoh 2003, Guenther 2008). Based on cell type and injury, the accumulated ceramide can either induce cell cycle arrest by activation of Rb protein, or induce apoptosis by a Bcl-2-regulated mechanism (Dbaiibo 1995, Dbaiibo 1997, El-Assaad 1998). Therefore, Bcl-2 acts as a downstream target of ceramide. Meanwhile, some of the pathways that lead to apoptotic cell death have been identified in haematological malignancies, whereby ceramide inhibitory action on Bcl2 phosphorylation is directly mediated by protein phosphatase 2A (PP2A) (Morad 2013). In other types of cancers and based on the treatment used, Bcl-2 inhibits ceramide accumulation. Moreover, it was previously shown that Bcl-2 prevents the ceramide mediated pathway of cell death in Molt-4 cells (Zhang 1996). For these reasons, it is noteworthy to delineate the role of Bcl-2 in ST1926-initiated ceramide production in cell death of malignant T cells.

We treated Molt-4 cells overexpressing Bcl-2 (Molt4-Bcl2) and Molt-4 containing the empty vector p-MEP4 (Molt4-MEP4) with 0.1  $\mu$ M and 1  $\mu$ M ST1926 for 12, 24, 48, and 72 hours. Cells were assayed for viability by trypan blue exclusion assay, while monitoring ceramide accumulation upon treatment with the indicated concentrations and time points. Bcl-2 attenuated the marked increase in accumulation of ceramide in Molt-4 starting 24 hours in response to ST1926 (Figure 25A). In particular, 0.1  $\mu$ M ST1926 caused 50% cell death at 72 hours, while no effect was observed in Bcl-2 overexpressing

cells. In addition, 1  $\mu$ M ST1926 caused 70% and 20% cell death in Molt4-MEP4 and Mol4-Bcl2 cells, respectively. Consistently, Bcl-2 interrupted early ceramide accumulation after 12 hours, as well as degree of accumulation up to 72 hours (Figure 25B). One  $\mu$ M ST1926 caused two- fold increase in ceramide as early as 12 hours in Molt4-MEP4, while the same effect was delayed and observed in Molt4-Bcl-2 cells only after 48 hours. Moreover, 0.1  $\mu$ M ST1926 resulted in no accumulation of ceramide up to 72 hours in Molt4-Bcl2 cells, while causing two-fold increase in Molt4-MEP4 cells.

Our results indicate that Bcl2 delays cell death-induced ST1926 treatment of malignant T cells and interferes with ceramide generation.

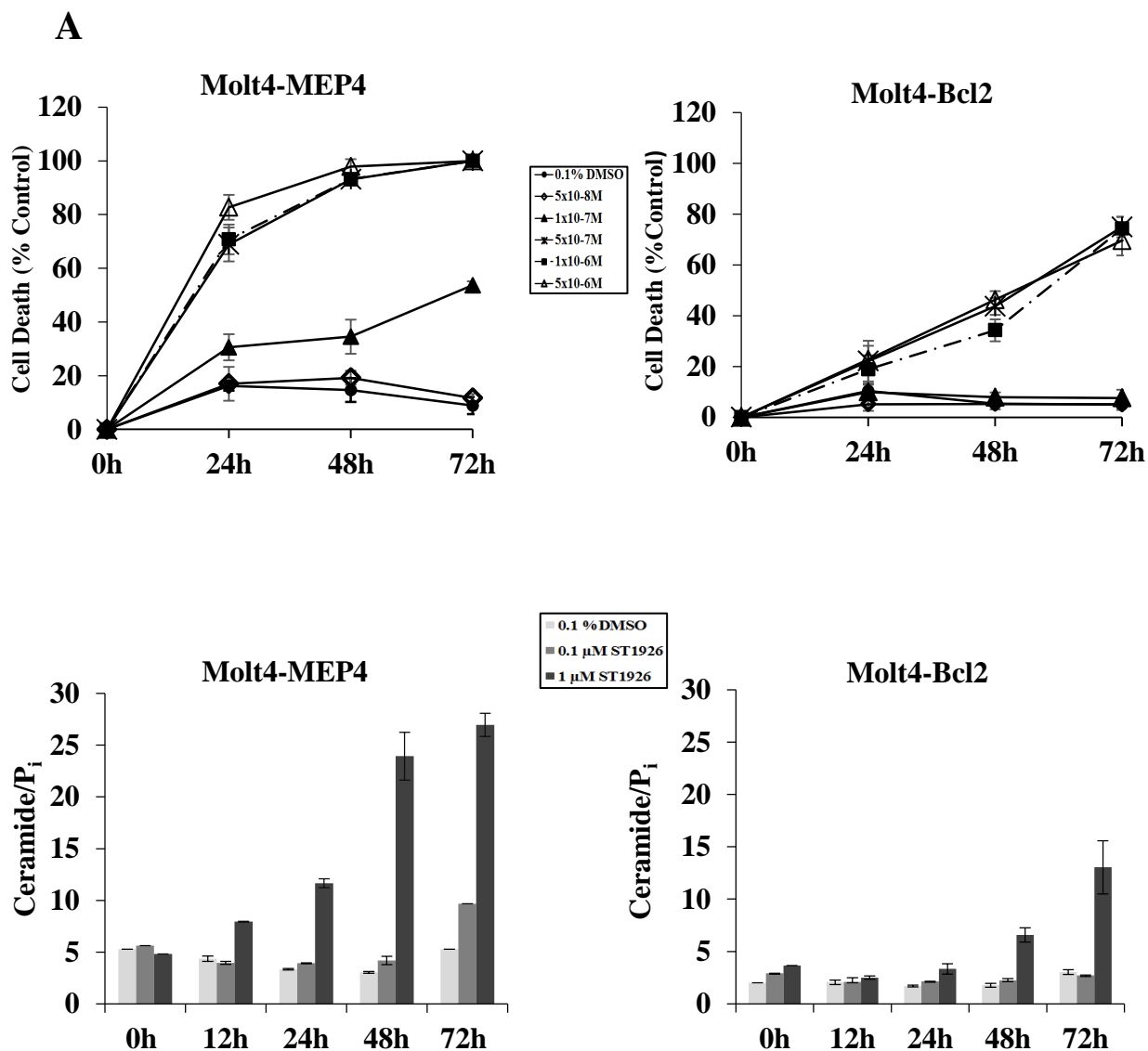


Figure 25. Bcl-2 interrupts ST1926-induced cell death and ceramide accumulation in Molt-4 cells. (A) Molt4-MEP4 and Molt4-Bcl2 were seeded at a density of  $2 \times 10^5$  cells/ml, treated with 0.1% DMSO or with increasing concentrations of ST1926 ranging from  $5 \times 10^{-8}$  to  $5 \times 10^{-6}$  M up to three days. Cells were assayed for death in quadruplicates using trypan blue exclusion assay. (B) Total ceramide levels in Molt4-MEP4 and Molt4-Bcl2 at the indicated timepoints treated with 0.1  $\mu$ M and 1  $\mu$ M ST1926. Ceramide levels were determined in duplicates using DGK assay as described in the Experimental Section and normalized to total cellular lipid phosphate levels. Data points represent the mean ( $\pm$  SD). Results are representative of two independent experiments.

## **J. Bcl-2 Inhibits *De Novo* Ceramide Synthesis in Response to ST1926 in Molt-4 Cells**

Since we have shown that ST1926 activates *de novo* pathway of ceramide production (Figure 20A), and that Bcl-2 interrupts ceramide accumulation upon ST1926 treatment (Figure 25B), we wanted to investigate whether Bcl-2 has an inhibitory action on *de novo* generated ceramide due to ST1926 treatment in Molt-4 cells. We have treated Molt4-MEP4 and Mol4-Bcl2 cells with 1  $\mu$ M ST1926 for 12, 24, and 48 hours (Figure 26). Results showed that Bcl-2 prevents *de novo* ceramide synthesis in response to ST1926, by lowering the magnitude as well as inhibiting early accumulation of ceramide after 12 hours (Figure 26).



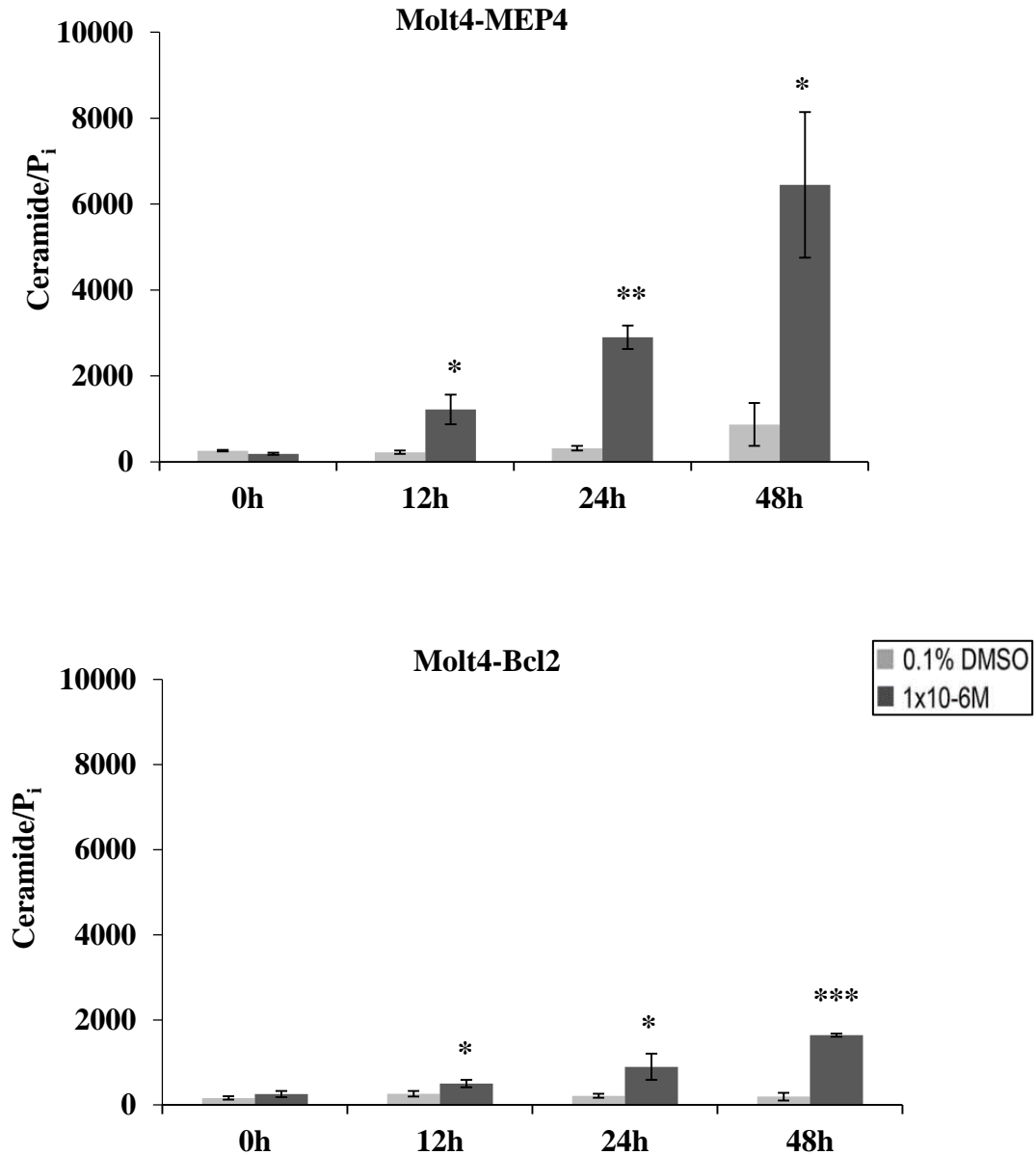


Figure 26. Bcl-2 inhibits ST1926-induced *de novo* synthesis of ceramide in Molt-4 cells. Cells were seeded at a density of  $3.5 \times 10^5$  cells/ml. *De novo* ceramide levels were determined in triplicates using the [ $^3$ H]palmitate incorporation method as described in the Experimental Section and normalized to total cellular lipid phosphate levels. Data points represent the mean ( $\pm$  SD). The asterisks \*, \*\*, and \*\*\* indicate statistically significant differences at  $p \leq 0.05$ ,  $p \leq 0.01$ , or  $p \leq 0.001$ , respectively, versus control using the *t*-test.

## CHAPTER IV

### DISCUSSION

The synthetic retinoid ST1926 is a strong inducer of cell death and apoptosis in several types of human cancers cells, including those that are ATRA-resistant. Here, we have determined that ST1926 exerts comparable growth inhibition and apoptosis of HTLV-1 positive and negative human malignant cells, while being resistant to ATRA treatment. ST1926-induced growth-suppressive effects were obtained at concentrations five to ten-fold lower than those previously used for other synthetic retinoids, namely HPR and CD437, in the same tested cell lines. A concentration of 1  $\mu\text{M}$  ST1926 resulted in at least 50 % growth suppression by 24 hours in all tested malignant cells. This concentration was shown to be the peak plasma concentration achieved in patients after oral administration of 200 mg ST1926/day (Valli 2008). Subsequently, primary cells, from the only three diagnosed ATL patients so far in Lebanon treated with 1  $\mu\text{M}$  and 5  $\mu\text{M}$  ST1926, were also responsive. Most notably, normal resting or activated circulating lymphocytes from three healthy donors were treated with a suprapharmacological concentration of 10  $\mu\text{M}$  ST1926 and these showed resistance to the drug. Furthermore, we have previously shown that HPR and CD437 induced growth inhibition,  $G_1$  arrest, and apoptosis in all tested malignant T cell lines at concentrations ranging from 0.5  $\mu\text{M}$  and 10  $\mu\text{M}$ . However, ST1926 effects were particularly more pronounced in the HTLV-1 positive cells. This may be due to the fact that ST1926 causes early downregulation of Tax protein levels whereas the other synthetic retinoids do not exert this effect (Darwiche 2004, unpublished data). Therefore, it would be

of particular and relevant interest to dissect the mechanism by which ST1926 induces Tax downregulation. For instance, recent studies have presented evidence regarding the role of the proteasome in the ST1926 induced apoptotic response in acute myeloid leukemia (Fratelli 2013).

Since in all tested cells, the pharmacologically achievable 1  $\mu$ M ST1926 resulted in at least 50 % growth suppression by 24 hours with no observed effect on normal lymphocytes, we have used this concentration to further investigate its effect on the cell death mechanisms in HTLV-1 positive and negative malignant T cells. Cell cycle analysis revealed a significantly high percentage of cells accumulating in the presumably apoptotic preG<sub>1</sub> phase in all tested malignant T cells with minor G<sub>1</sub> cell cycle arrest after 24 hours of treatment. To further confirm apoptosis induction by ST1926, we checked for DNA fragmentation, which occurs when nuclear enzymes become active and disrupt the normal chromatin structure of DNA. For this reason, we used the TUNEL assay that detects DNA fragmentation as a late apoptotic event. Treatment with 1  $\mu$ M ST1926 induced massive DNA fragmentation in all tested cells as early as 24 hours.

It has been previously shown that p53 functions are inactivated by Tax, whereby Tax-dependent activation of the NF- $\kappa$ B pathway plays a crucial role in this inhibition (Kfoury 2005). Furthermore, ST1926-induced apoptosis is mediated through p53-dependent or -independent pathways (Zuco 2005, Cincinelli 2003, Pisano 2007, Valli 2008, Fratelli 2013). Interestingly, our results have shown that ST1926 induces p53 activity by elevating the ratio of phosphorylated p53 over total p53 protein levels. Although the oncoprotein Tax suppresses p53 activity (Mulloy 1998), its early reduction by ST1926

suggests that upon ST1926 treatment, p53 activity is induced in the HTLV-1 positive HuT-102 and MT-2 cells. Meanwhile, p53-independent apoptosis was still clearly observed in Jurkat cells with mutant p53 as well as in Mol4-E6 transfected with human papillomavirus E6 which inhibits p53 function through direct binding (Bargonetti 1992). These results suggest that ST1926 anti-tumor activities could be mediated through both p53-dependent and -independent mechanisms. Of great interest to our study was to examine the expression profile of p21 upon ST1926 treatment in HTLV-1 positive and HTLV-1 negative cells. p21, a direct regulator of cyclin-dependent kinase (CDK) activity, is a mediator of p53- induced growth arrest, whose expression is induced during apoptosis and cellular senescence. Interestingly, p21 expression is elevated at both the mRNA and protein levels in HTLV-1-infected T-cells, as Tax was shown to transactivate the p21 promoter (Grassmann 2005). However, in ATL cells, elevated levels of p21 induce cell proliferation and inhibit cell death (Kawata 2003). Importantly, we found that ST1926 causes an early reduction in p21 protein expression levels in HTLV-1 positive cell lines, HuT-102 and MT-2, along with Tax downregulation in these cells (data not shown).

It is well established that ceramide acts as a lipid-tumor suppressor mediating anti proliferative effects such as differentiation, cell cycle arrest, and apoptosis in response to several extracellular signals including chemotherapeutic drugs (Lin 2006, Morad 2013). We have demonstrated that ST1926 elicits similar ceramide responses in both HTLV-1 positive and negative T cells. The kinetics and degree of ceramide production showed a unique response upon ST1926 treatment *versus* previous synthetic retinoids such as HPR and CD437 in all tested cell lines. We have previously shown that treatment with HPR or CD437 resulted in ceramide production only in HTLV-1 negative cells (Darwiche 2005,

unpublished results). Therefore, we used 1  $\mu$ M ST1926 to examine the time- and dose-dependent increase of ceramide in HTLV-1 positive and negative malignant T cells. Interestingly, 1  $\mu$ M ST1926 produced an earlier ceramide accumulation in Jurkat cells, compared to the same concentration of CD437 as early as 6 hours (unpublished results), followed by a persistent one fold and three fold increase at 12 and 24 hours, respectively. Similar results were also obtained with ST1926-treated Molt-4 cells. Most importantly, 1 $\mu$ M ST1926 revealed ceramide accumulation as early as 12 hours in HuT-102 and MT-2 cells, which preceded cell death, while previous results have indicated that treatment with 1  $\mu$ M CD437 shows no ceramide accumulation up to 24 hours (unpublished results). Additionally, only by increasing the concentration of HPR up to 5  $\mu$ M and after 48 hours, we observed a two fold increase in ceramide levels in HuT-102 cells which followed cell death (Darwiche 2005).

It was previously shown that HTLV-1 positive cells have a defect in ceramide synthesis in response to HPR (Darwiche 2005). Since in this study, we reported a similar ceramide accumulation response in both HTLV-1 positive and negative cells, we explored the effect of ST1926 on *de novo* ceramide synthesis pathway in these malignant T cells. Contrary to treatment with HPR, we showed that ST1926 activates *de novo* ceramide production in both HTLV-1 positive (HuT-102) and negative (Molt-4) cells as early as 12 hours. As discussed earlier, this could be attributed to the early reduction of Tax protein expression by ST1926, but not by HPR or CD437, and which preceded both cell death and ceramide accumulation in HTLV-1 positive, HuT-102 cells.

We have previously shown that the expression of Tax alone in cells not infected with HTLV-1 is sufficient and responsible for maintaining the impaired *de novo* ceramide

synthetic pathway in response to HPR or exogenous C6-ceramide (Darwiche 2005). Furthermore, there is accumulating evidence that cell permeant analogues of short-chain ceramides such as C2- and C6- could be used to emphasize apoptosis mediated by accumulation of endogenous cellular ceramide in response to extracellular signals including chemotherapeutic drugs (Mathias 1993, Cifone 1994, Tepper 1995, Bielawska 1993). We have previously shown that C2- and C6-ceramides induced growth-suppressive effects in both HTLV-1 positive and HTLV-1 negative cells in a time- and dose-dependent manner, with lower sensitivity in HTLV-1 positive cells (Darwiche 2005). This emphasizes the defect in ceramide synthesis in HTLV-1 positive cells, concomitant with decreased levels of ceramide, thus less sensitivity of HTLV-1 positive cells to exogenous C2- and C6-ceramide.

Furthermore, exogenous C6-ceramide was shown to induce *de novo* ceramide synthesis in A549 lung carcinoma cells, which was dependent on ceramide synthase to produce endogenous ceramides (Ogretmen 2002). In fact, ceramide sphingosine backbone becomes recycled after deacylation/reacylation into endogenous long-chain ceramides (Ogretmen 2002). We proved that both ceramide analogues induced *de novo* ceramide synthesis in both HTLV-1 positive and negative T cells, but was substantially lower in the former ones (Darwiche 2005). This suggests that ceramide synthase was inhibited in these cells. In addition, ceramide synthase is one of the crucial enzymes of this pathway that was found to be suppressed by Tax, which confers chemoresistance of HTLV-1 transformed cells (Darwiche 2004, Riebeling 2003). Since we proved ST1926 activates *de novo* pathway, it is noteworthy to investigate, using more *in vitro* enzymatic activity assays, whether this enzyme or other enzymes, such as serine palmitoyl CoA and dihydroceramide

desaturase, are modulated in response to ST1926 in HTLV-1 positive and negative cells. These investigations are crucial knowing that resistance to chemotherapeutic drugs could be attributed to a certain defect in ceramide synthesis and/or metabolism. For instance, Tamoxifen blocks the conversion of ceramide to glucosylceramide, thus, bypassing drug resistance by increasing endogenous ceramide levels (Pandey 2007). In addition, HPR increases the levels of intracellular ceramide in drug-resistant neuroblastoma cell lines (Maurer 1999).

Surprisingly, LC-MS analysis of sphingolipids from HPR-treated cells have shown that dihydroceramide, and not ceramide, is accumulated upon HPR treatment, accompanied by simultaneous activation of serine palmitoyltransferase and/or (dihydro)ceramide synthase, concurrent with inhibition of dihydroceramide desaturase (Zheng 2006, Kravka 2007, Wang 2008). In fact, the latter enzyme is highly inhibited by HPR in cell-free enzymatic assays as well as in intact cells (Zheng 2006, Kravka 2007). Since ST1926 reduces the viral oncoprotein Tax and activates *de novo* ceramide synthesis, and knowing that HPR significantly inhibits dihydroceramide desaturase, we have performed a high throughput sphingolipidomics analysis using LC-MS to identify the ceramide/dihydroceramide molecular species that are modulated in response to ST1926 in HTLV-1 positive and HTLV-1 negative cells. Interestingly, we have observed an increase of total ceramide and dihydroceramide species in both cell types by 12 and 24 hours. However, HuT-102 cells treated with 0.1 % DMSO for 24 hours exhibited higher levels of ceramide and dihydroceramide species accumulation, which may be due to the stress condition of these tax-expressing cells. Moreover, we reported that both cell types markedly accumulated ceramide *versus* dihydroceramide molecular species after 12 hours of

treatment with 1  $\mu$ M ST1926, and was by far more pronounced in Molt-4 than in HuT-102 cells. This adds to the novelty of the mechanism of action of ST1926 compared to our previously tested synthetic retinoids HPR and CD437.

Our results indicate the involvement of *de novo* ceramide synthesis in ST1926-mediated growth-suppressive effects in both HuT-102 and Molt-4 cells, as indicated by the accumulation of total dihydroceramide and ceramide species. As discussed earlier, each ceramide synthase (CerS) is specific for the addition of relatively distinct lengths of fatty acyl-CoAs to produce ceramide species with different chain lengths (Stiban 2010). We have observed significant accumulation of C16, C22, and C24:1 ceramide species among others in both cell lines. It has been shown that CerS5 mostly use C16-CoA, and CerS6 mostly utilize C14, C16, and C18-CoA (Lahiri and Futerman 2005), while CerS2 preferably uses longer fatty acyl chains (C20-C26), as in our case C22 and C24:1 acyl CoAs (Laviad 2008). This suggests a plausible role for the involvement of CerS5 and CerS6, as well as CerS2. Moreover, accumulating evidence suggests the role of the different ceramide synthase (s) in regulating cell death (Stiban 2010). Indeed, certain ceramide species such as C16 and C18 ceramides has shown to have proapoptotic effects in human leukemia cells and hematopoietic cells, respectively (Grösch 2013). Therefore, it would be of particular interest to further investigate the role of these CerS subtypes in mediating the growth-suppressive effects upon ST1926 in HTLV-1 positive and HTLV-1 negative malignant T cells. In this regards, further gene knock-down assays of the corresponding enzymes through RNA interference and/or overexpression models would provide relevant and useful answers.



Furthermore, one of the apoptotic pathways that are coordinated by ceramide as a lipid tumor suppressor are members of Bcl-2 family of proteins (Taha 2006). We have shown that Bcl-2 attenuates ST1926-induced cell growth arrest in Molt-4 cells. In addition, exogenous C6-ceramide induced ceramide-dependent cell death in these cells (Zhang 1996). We have determined an early accumulation of ceramide levels in Molt-4 cells by 12 hours, which preceded cell death in these cells. However, Bcl-2 rescued Molt-4 cells from early ceramide accumulation and cell death. Our results suggest a ceramide-dependent mechanism of programmed cell death in response to ST1926 treatment, in which Bcl-2 acts upstream to prevent both ceramide accumulation and consequently, cell death in Molt-4 cells. This implicates that Bcl-2 and ceramide act in a common pathway of the cell death mechanism, most probably with ceramide acting in the “sensing” phase rather in the “execution” phase of apoptosis (Zhang 1996). Our results also shed light into a mitochondrial pathway of cell death, which is a critical step for committing a cell into apoptosis, in which Bcl-2 was shown to play an inhibitory role in ceramide production and cell death. Moreover, late ceramide accumulation was still observed although to a lower extent in Molt4-Bcl2 cells. Indeed, in some cancer systems, early ceramide accumulation occurs downstream of Bcl-2 action and mitochondrial pathway, whereas in others ceramide production occurs upstream of these actions.

The mechanism by which ceramide exerts its pro-apoptotic functions is not fully unveiled. However, one of the proposed pathways involves the generation of mitochondrial ceramide prior to the induction phase of apoptosis and forming ceramide channels in the outer mitochondrial membrane that facilitate the release of pro-apoptotic proteins from the intermembrane space into cytoplasm (Siskend 2005). *De novo* ceramide synthesis occurs

in the endoplasmic reticulum (ER) and in the mitochondria (Bionda 2004). This underscores the relevant importance of *de novo* ceramide pathway in the mitochondria, and suggests the involvement of Bcl-2 family members. In our study, we showed that Bcl-2 interrupted early *de novo* ceramide synthesis upon ST1926 treatment in Molt-4 cells. Indeed, it has been recently shown that enzymes responsible for *de novo* ceramide synthesis, specifically ceramide synthase, localizes in the outer mitochondrial membranes (Bionda 2004). Meanwhile, two of the proposed mechanisms by which Bcl-2 inhibitory actions could be mediated are through direct binding to ceramide channels and/or altering the activity of the enzymes responsible for ceramide synthesis (Siskend 2005). Thus, it would be of particular interest to further investigate how Bcl-2 protects from *de novo* ceramide-induced cell death in Molt-4 cells upon ST1926 treatment regarding mitochondrial ceramide-induced apoptosis. We have observed an early induction of *de novo* ceramide generation upon ST1926 treatment in Molt-4 cells coupled to LC-MS analysis that showed pronounced accumulation of specific ceramide species. However, Bcl-2 interrupted *de novo* ceramide synthesis. Altogether combined, this suggests the involvement and localization of certain ceramide synthase (s) to the mitochondria and the potential participation of specific species in ST1926-induced apoptosis. Yet, more experiments with pure mitochondrial extracts need to be done combined with enzymatic activity assays and LC-MS analyses in order to reach a solid conclusion. Finally, we have recently shown that ST1926 significantly prolongs the survival of ATL mice, and recapitulates the cell death mechanisms that were tested in our *in vitro* model (data not shown). It would be crucial to identify the mechanisms of ceramide-mediated action upon

ST1926 treatment *in vivo*, eventually, identifying the enzyme (s) that might be also involved in this retinoid treatment.

Chemoresistance is commonly observed in cancer therapeutics and is a complex process. Sphingolipids metabolism may play a crucial role in cancer sensitivity or resistance to several commonly used anticancer drugs. Our results provide evidence that ST1926 is a strong inducer of ceramide in malignant T cells and support for the use of this drug in chemoresistant cancer cells whether alone or in combination treatment.

## REFERENCES

Adyan N, and Giam CZ. "Distinct regions in human T-cell lymphotropic virus type I tax mediate interactions with activator protein CREB and basal transcription factors." *Journal of virology* 69 (1995): 1834-1841.

Allouche M, Bettaieb A, Vindis C, Rousse A, Grignon C, and Laurent G. "Influence of Bcl-2 overexpression on the ceramide pathway in daunorubicin-induced apoptosis of leukemic cells." *Oncogene* 14 (1997).

Amaral JD Xavier JM, Steer CJ, Rodrigues CM. "The role of p53 in apoptosis." *Discov. Med.* 9 (2010): 145–152.

Antoine KZ, Hussain H, Dongo E, Kouam SF, Schulz B, and Krohn K. "Cameroonemide A: a new ceramide from *Helichrysum cameroonense*." *Journal of Asian natural products research* 12 (2010): 629-633.

Ardail D, Popa I, Alcantara K, Pons A, Zanetta JP, Louisot P, Thomas L, and Portoukalian J. "Occurrence of ceramides and neutral glycolipids with unusual long-chain base composition in purified rat liver mitochondria." *FEBS letters* 488 (2001): 160-164.

Bartke N, and Hannun YA. "Bioactive sphingolipids: metabolism and function." *Journal of lipid research* 50 (2009): S91-S96.

Baydoun HH, Bellon M, Nicot C. "HTLV-1 Yin and Yang: Rex and p30 master regulators of viral mRNA trafficking." *AIDS Rev* 10 (2008): 195–204.

Bazarbachi A, Ghez D, Lepelletier Y, Nasr R, de Thé H, El-Sabban M, and Hermine O. "New therapeutic approaches for adult T-cell leukemia." *Oncology* 5 (2004): 664 – 672.

Bazarbachi A, and Hermine O. "Treatment with a combination of zidovudine and  $\alpha$ -interferon in naive and pretreated adult T-cell leukemia/lymphoma patients." *JAIDS Journal of Acquired Immune Deficiency Syndromes* 13 (1996): S186-S190.

Bazarbachi A, Nasr R, El-Sabban ME, Mahe A, Mahieux R, Gessain A, Darwiche N et al. "Evidence against a direct cytotoxic effect of alpha interferon and zidovudine in HTLV-I associated adult T cell leukemia/lymphoma." *Leukemia* 14 (2000).

Bazarbachi A, Suarez F, Fields P, and Hermine O. "How I treat adult T-cell leukemia/lymphoma." *Blood* 118 (2011): 1736-1745.

Bernard BA, Bernardon JM, Delescluse C, Martin B, Lenoir MC, Maignan J, Charpentier B, Pilgrim WR, Reichert U, and Shroot B. "Identification of synthetic retinoids with selectivity for human nuclear retinoic acid receptor  $\gamma$ ." *Biochemical and biophysical research communications* 186 (1992): 977-983.

Bielawska A, Perry DK, and Hannun YA. "Determination of ceramides and diglycerides by the diglyceride kinase assay." *Analytical biochemistry* 298 (2001): 141-150.

Bielawski J, Pierce JS, Snider J, Rembiesa B, Szulc ZM, and Bielawska A. "Sphingolipid analysis by high performance liquid chromatography-tandem mass spectrometry (HPLC-MS/MS)." In *Sphingolipids as Signaling and Regulatory Molecules*, pp. 46-59. Springer New York, 2010.

Bionda C, Portoukalian J, Schmitt D, Rodriguez-Lafrasse C, and Ardail D. "Subcellular compartmentalization of ceramide metabolism: MAM (mitochondria-associated membrane) and/or mitochondria?" *Biochem. J* 382 (2004): 527-533.

Birbes H, El Bawab S, Hannun YA, and Obeid LM. "Selective hydrolysis of a mitochondrial pool of sphingomyelin induces apoptosis." *The FASEB Journal* 15 (2001): 2669-2679.

Birbes H, Luberto C, Hsu Y, El Bawab S, Hannun YA, and Obeid LM. "A mitochondrial pool of sphingomyelin is involved in TNF $\alpha$ -induced Bax translocation to mitochondria." *Biochem. J* 386 (2005): 445-451.

Bitar N, El Hajj H, Houmani Z, Sabbah A, Otrock Z, Mahfouz R, Zaatari G, Bazarbachi A. "Adult T-cell leukemia/lymphoma in the Middle East: first report of two cases from Lebanon." *Transfusion* 49 (2009):1859-64.

Bligh EG, and Dyer WJ. "A rapid method of total lipid extraction and purification." *Canadian journal of biochemistry and physiology* 37 (1959): 911-917.

Bose R, Verheij M, Haimovitz-Friedman A, Scotto K, Fuks Z, and Kolesnick R. "Ceramide synthase mediates daunorubicin-induced apoptosis: an alternative mechanism for generating death signals." *Cell* 82 (1995): 405-414.

Brockman JA., Scherer DC, McKinsey TA, Hall SM, Qi X, Lee WY, and Ballard DW. "Coupling of a signal response domain in I kappa B alpha to multiple pathways for NF-kappa B activation." *Molecular and Cellular Biology* 15 (1995): 2809-2818.

Cai Z, Bettaieb A, El Mahdani N, Legrès LG, Stancou R, Masliah J, and Chouaib S. "Alteration of the sphingomyelin/ceramide pathway is associated with resistance of human breast carcinoma MCF7 cells to tumor necrosis factor- $\alpha$ -mediated cytotoxicity." *Journal of Biological Chemistry* 272 (1997): 6918-6926.

Carvalho EM., and Da Fonseca Porto A. "Epidemiological and clinical interaction between HTLV-1 and *Strongyloides stercoralis*." *Parasite immunology* 26 (2004): 487-497.

Chalfant CE, Ogretmen B, Galadari S, Kroesen BJ, Pettus BJ, and Hannun YA. "FAS activation induces dephosphorylation of SR proteins dependence on the de novo generation of ceramide and activation of protein phosphatase 1." *Journal of Biological Chemistry* 276 (2001): 44848-44855.

Chalfant CE, Rathman K, Pinkerman RL, Wood RE, Obeid LM, Ogretmen B, and Hannun YA. "De novo ceramide regulates the alternative splicing of caspase 9 and Bcl-x in A549 lung adenocarcinoma cells Dependence on protein phosphatase-1." *Journal of Biological Chemistry* 277 (2002): 12587-12595.

Chambon P. "The nuclear receptor superfamily: a personal retrospect on the first two decades." *Molecular Endocrinology* 19 (2005): 1418-1428.

Chandhasin C, Ducu RI, Berkovich E, Kastan MB, and Marriott SJ. "Human T-cell leukemia virus type 1 tax attenuates the ATM-mediated cellular DNA damage response." *Journal of virology* 82 (2008): 6952-6961.

Chao TY, Jiang SY, Shyu RY, Yeh MY, and Chu TM. "All-trans retinoic acid decreases susceptibility of a gastric cancer cell line to lymphokine-activated killer cytotoxicity." *British journal of cancer* 75 (1997): 1284.

Chen LF, and Greene WC. "Shaping the nuclear action of NF- $\kappa$ B." *Nature Reviews Molecular Cell Biology* 5 (2004): 392-401.

Chmura SJ, Nodzenski E, Beckett MA, Kufe DW, Quintans J, and Weichselbaum RR. "Loss of ceramide production confers resistance to radiation-induced apoptosis." *Cancer research* 57 (1997): 1270-1275.

Chrivia, JC, Kwok RPS, Lamb N, Hagiwara M, Montminy MR, and Goodman RH. "Phosphorylated CREB binds specifically to the nuclear protein CBP." *Nature* 365 (1995): 855-859.

Chu ZL, DiDonato JA, Hawiger J, and Ballard DW. "The Tax oncoprotein of human T-cell leukemia virus type 1 associates with and persistently activates I $\kappa$ B kinases containing IKK $\alpha$  and IKK $\beta$ ." *Journal of Biological Chemistry* 273 (1998): 15891-15894.

Cincinelli R, Dallavalle S, Merlini L, Penco S, Pisano C, Carminati P, Giannini G, Vesci L, Gaetano C, Illy B, et al. "A novel atypical retinoid endowed with proapoptotic and antitumor activity." *J Med Chem.* 46 (2003):909-912.

Collins SJ. "Retinoic acid receptors, hematopoiesis and leukemogenesis." *Curr Opin Hematol.* Jul 15 (2008): 346-51.

Colombini M. "Ceramide channels and their role in mitochondria-mediated apoptosis." *Biochimica et Biophysica Acta (BBA)-Bioenergetics* 1797 (2010): 1239-1244.

Crowe DL. "Receptor selective synthetic retinoids as potential cancer chemotherapy agents." *Current cancer drug targets* 2 (2002): 77-86.

Dai Q, Liu J, Chen J, Durrant D, McIntyre TM, and Lee RM. "Mitochondrial ceramide increases in UV-irradiated HeLa cells and is mainly derived from hydrolysis of sphingomyelin." *Oncogene* 23 (2004): 3650-3658.

Darwiche N, Abou-Lteif G, and Bazarbachi A. "Reactive oxygen species mediate N-(4-hydroxyphenyl) retinamide-induced cell death in malignant T cells and are inhibited by the HTLV-I oncoprotein Tax." *Leukemia* 21 (2007): 261-269.

Darwiche N, Abou-Lteif G, Najdi T, Kozhaya L, Abou TA, Bazarbachi A, and Dbaiibo G. "Human T-cell lymphotropic virus type I-transformed T-cells have a partial defect in ceramide synthesis in response to N-(4-hydroxyphenyl) retinamide." *Biochem. J* 392 (2005): 231-239.

Darwiche N, El-Sabban M, Bazzi R, Nasr R, Al-Hashimi S, Hermine O, de The H, Bazarbachi A. "Retinoic acid dramatically enhances the arsenic trioxide-induced cell cycle arrest and apoptosis in retinoic acid receptor alpha-positive human T-cell lymphotropic virus type-I transformed cells." *Hematol J.* 2 (2001):127-135.

Darwiche N, Hatoum A, Dbaiibo G, Kadara H, Nasr R, Abou-Lteif G. "N-(4-hydroxyphenyl) retinamide induces growth arrest and apoptosis in HTLV-1-transformed cells." *Leukemia* 18 (2004): 607-615.

Dbaiibo GS, Pushkareva MY, Rachid RA, Alter N, Smyth MJ, Obeid LM, and Hannun YA. "p53-dependent ceramide response to genotoxic stress." *Journal of Clinical Investigation* 102 (1998): 329.

De Thé H, Chomienne C, Lanotte M, Degos L, Dejean A. "The t(15;17) translocation of acute promyelocytic leukaemia fuses the retinoic acid receptor alpha gene to a novel transcribed locus." *Nature* 343 (1990):58-6.



Di Francesco AM, Meco D, Torella AR, Barone G, D'Incalci M, Pisano C, Carminati P, and Riccardi R. "The novel atypical retinoid ST1926 is active in ATRA resistant neuroblastoma cells acting by a different mechanism." *Biochemical pharmacology* 73 (2007): 643-655.

Di Paola M, Cocco T, and Lorusso M. "Ceramide interaction with the respiratory chain of heart mitochondria." *Biochemistry* 39 (2000): 6660-6668.

El Hajj H, El-Sabban ME, Hasegawa H, Zaatari G, Ablain J, Saab ST, Janin A et al. "Therapy-induced selective loss of leukemia-initiating activity in murine adult T cell leukemia." *The Journal of experimental medicine* 207 (2010): 2785-2792.

El-Sabban ME, Abou Merhi R, Abi Haidar H, Arnulf B, Khoury H, Basbous J, Nijmeh J, Hermine O, and Bazarbachi A. "Human T-cell lymphotropic virus type 1-transformed cells induce angiogenesis and establish functional gap junctions with endothelial cells." *Blood* 99 (2002): 3383-3389.

El-Sabban ME, Nasr R, Dbaibo G, Hermine O, Abboushi N, Quignon F, Ameisen JC, Bex F, and Bazarbachi A. "Arsenic-interferon- $\alpha$ -triggered apoptosis in HTLV-I transformed cells is associated with Tax down-regulation and reversal of NF- $\kappa$ B activation." *Blood* 96 (2000): 2849-2855.

Eto M, Bennouna J, Hunter OC, Hershberger PA, Kanto T, Johnson CS, Lotze MT, and Amoscato AA. "C16 ceramide accumulates following androgen ablation in LNCaP prostate cancer cells." *The Prostate* 57 (2003): 66-79.

Fenaux P, Wang ZZ, and Degos L. "Treatment of acute promyelocytic leukemia by retinoids." In *Acute Promyelocytic Leukemia* (2007) 101-128.

Foley GE, Lazarus G, Farber S, Uzman BG, Boone BA, and McCarthy RE. "Continuous culture of human lymphoblasts from peripheral blood of a child with acute leukemia." *Cancer* 18 (1965): 522-529.

Feng X, Heyden NV, and Ratner L. "Alpha interferon inhibits human T-cell leukemia virus type 1 assembly by preventing Gag interaction with rafts." *Journal of virology* 77 (2003): 13389-13395.

Fontana J, *et al.* "Classical and novel retinoids: their targets in cancer therapy." *Leukemia* 16 (2002): 463-472.

Fratelli M, Fisher JN, Paroni G, Di Francesco AM, Pierri F, Pisano C, Godl K *et al.* "New insights into the molecular mechanisms underlying sensitivity/resistance to the atypical retinoid ST1926 in acute myeloid leukaemia cells: The role of histone H2A, Z, cAMP-dependent protein kinase A and the proteasome." *European Journal of Cancer* 49 (2013): 1491-1500.

Freemantle SJ, Spinella MJ, and Dmitrovsky E. "Retinoids in cancer therapy and chemoprevention: promise meets resistance." *Oncogene* 22 (2003): 7305-7315.

Fu, DX, Kuo YL, Liu BY, Jeang KT, and Giam CZ. "Human T-lymphotropic virus type I tax activates I- $\kappa$ B kinase by inhibiting I- $\kappa$ B kinase-associated serine/threonine protein phosphatase 2A." *Journal of Biological Chemistry* 278 (2003): 1487-1493.

Gabet AS, Mortreux F, Charneau P, Riou P, Duc-Dodon M, Wu Y, Jeang KT, and Wattel E. "Inactivation of hTERT transcription by Tax." *Oncogene* 22 (2003): 3734-3741.

Gallo RC. "The Discovery of the first human retroviruse: HTLV-I and HTLV-2." *Retrovirology* 2 (2005): 17.

Garattini E and Terao M. "Atypical retinoids: an expanding series of antileukemia and anti-cancer agents endowed with selective apoptotic activity." *J Chemother* 16 (2004):70–73.

Gartenhaus RB, Wang P, and Hoffmann P. "Induction of the WAF1/CIP1 protein and apoptosis in human T-cell leukemia virus type I-transformed lymphocytes after treatment with adriamycin by using a p53-independent pathway." *Proceedings of the National Academy of Sciences* 93 (1996): 265-268.

Germain P, Chambon P, Eichele G, Evans RM, Lazar MA, Leid M, De Lera AR, Lotan R, Mangelsdorf DJ, and Gronemeyer H. "International union of pharmacology. LXIII. Retinoid X receptors." *Pharmacological reviews* 58 (2006): 760-772.

Goodbourn S, Didcock L, and Randall RE. "Interferons: cell signalling, immune modulation, antiviral response and virus countermeasures." *Journal of General Virology* 81 (2000): 2341-2364.

Grassmann R, Aboud M, and Jeang KT. "Molecular mechanisms of cellular transformation by HTLV-1 Tax." *Oncogene* 24 (2005): 5976-5985.

Grösch S, Schiffmann S, and Geisslinger G. "Chain length-specific properties of ceramides." *Progress in lipid research* 51 (2012): 50-62.

Gottschalk AR, McShan CL, Kilkus J, Dawson G, and Quintáns J. "Resistance to anti-IgM-induced apoptosis in a WEHI-231 subline is due to insufficient production of ceramide." *European journal of immunology* 25 (1995): 1032-1038.

Hanada K, Kumagai K, Yasuda S, Miura Y, Kawano M, Fukasawa M, and Nishijima M. "Molecular machinery for non-vesicular trafficking of ceramide." *Nature* 426 (2003): 803-809.

Hannun YA, and Obeid LM. "Principles of bioactive lipid signalling: lessons from sphingolipids." *Nature reviews Molecular cell biology* 9 (2008): 139-150.

Hannun YA, and Obeid LM. "Many ceramides." *Journal of Biological Chemistry* 286 (2011): 27855-27862.

Heinrich M, Neumeyer J, Jakob M, Hallas C, Tchikov V, Winoto-Morbach S, Wickel M et al. "Cathepsin D links TNF-induced acid sphingomyelinase to Bid-mediated caspase-9 and -3 activation." *Cell Death & Differentiation* 11 (2004): 550-563.

Huang WC, Chen CL, Lin YS, and Lin CF. "Apoptotic sphingolipid ceramide in cancer therapy." *Journal of lipids* (2011).

Isono T, Ogawa K, and Seto K. "Antiviral effect of zidovudine in the experimental model of adult T cell leukemia in rabbits." *Leukemia research* 14 (1990): 841-847.

Jeang KT, Giam CZ, Majone F, Aboud M. "Life, death, and tax: Role of HTLV-1 oncoprotein in genetic instability and cellular transformation." *J Bio Chem* (2004) 279: 31991-31994.

Kashkar H, Wiegmann K, Yazdanpanah B, Haubert D, and Krönke M. "Acid sphingomyelinase is indispensable for UV light-induced Bax conformational change at the mitochondrial membrane." *Journal of Biological Chemistry* 280 (2005): 20804-20813.

Kawakami K, Miyazato A, Iwakura Y, and Saito A. "Induction of lymphocytic inflammatory changes in lung interstitium by human T lymphotropic virus type I." *American journal of respiratory and critical care medicine* 160 (1999): 995-1000.

Kawatani M, Uchi M, Simizu S, Osada H, and Imoto M. "Transmembrane domain of Bcl-2 is required for inhibition of ceramide synthesis, but not cytochrome c release in the pathway of inostamycin-induced apoptosis." *Experimental cell research* 286 (2003): 57-66.

Kfoury Y, Nasr R, Hermine O, De The H, & Bazarbachi A. "Proapoptotic regimes for HTLV-I-transformed cells: targeting Tax and the NF- $\kappa$ B pathway." *Cell Death & Differentiation* 12 (2005): 871-877.

Kroesen BJ, Pettus B, Luberto C, Busman M, Sietsma H, de Leij L, and Hannun YA. "Induction of apoptosis through B-cell receptor cross-linking occurs via de novo generated C16-ceramide and involves mitochondria." *Journal of Biological Chemistry* 276 (2001): 13606-13614.

Kroemer G, Galluzzi L, Vicencio JM, Kepp O, Tasdemir E, and Maiuri MC. "To die or not to die: that is the autophagic question." *Current molecular medicine* 8 (2008): 78-91.

Kuwazuru Y, Yoshimura A, Hanada S, Utsunomiya A, Makino T, Ishibashi K, Kodama M, Iwahashi M, Arima T, Akiyama S. "Expression of the multidrug transporter, P-

glycoprotein, in acute leukemia cells and correlation to clinical drug resistance." *Cancer* 6 (1990):868–873.

Lau A, Nightingale S, Taylor GP, Gant TW, and Cann AJ. "Enhanced MDR1 gene expression in human T-cell leukemia virus-I–infected patients offers new prospects for therapy." *Blood* 91 (1998): 2467-2474.

Lavie Y, Caov HT, Volner A, Lucci A, Han TY, Geffen V, Giuliano AE, and Cabot MC. "Agents that reverse multidrug resistance, tamoxifen, verapamil, and cyclosporin A, block glycosphingolipid metabolism by inhibiting ceramide glycosylation in human cancer cells." *Journal of Biological Chemistry* 272 (1997): 1682-1687.

Lin RJ, Egan DA, and Evans RM. "Molecular genetics of acute promyelocytic leukemia." *Trends in Genetics* 15 (1999): 179-184.

Maeda N, Fan H, and Yoshikai Y. "Oncogenesis by retroviruses: old and new paradigms." *Reviews in medical virology* 18 (2008): 387-405.

Majone F, Semmes OJ, and Jeang KT. "Induction of micronuclei by HTLV-I Tax: a cellular assay for function." *Virology* 193 (1993): 456-459.

Majone F and Jeang KT. "Clastogenic effect of the human T-cell leukemia virus type I Tax oncoprotein correlates with unstabilized DNA breaks." *Journal of Biological Chemistry* 275 (2000): 32906-32910.

Marçais A, Suarez F, Sibon D, Bazarbachi A, and Hermine O. "Clinical trials of adult T-cell leukaemia/lymphoma treatment." *Leukemia research and treatment* 2012 (2012).

Marçais, A, Suarez F, Sibon D, Frenzel L, Hermine O, and Bazarbachi A. "Therapeutic options for adult T-cell leukemia/lymphoma." *Current oncology reports* 15 (2013): 457-464.

Matsuoka M. "Human T-cell leukemia virus type I and adult T-cell leukemia." *Oncogene* 22 (2003): 5131-5140.

Merrill AH, Schmelz EM, Dillehay DL, Spiegel S, Shayman JA, Schroeder JJ, Riley RT, Voss KA, and Wang E. "Sphingolipids—the enigmatic lipid class: biochemistry, physiology, and pathophysiology." *Toxicology and applied pharmacology* 142 (1997): 208-225.

Michael JM, Lavin MF, and Watters DJ. "Resistance to radiation-induced apoptosis in Burkitt's lymphoma cells is associated with defective ceramide signaling." *Cancer research* 57 (1997): 3600-3605.

Morad SAF, Madigan JP, Levin JC, Abdelmageed N, Karimi R, Rosenberg DW, Kester M, Shanmugavelandy SS, and Cabot MC. "Tamoxifen magnifies therapeutic impact of ceramide in human colorectal cancer cells independent of p53." *Biochemical pharmacology* 85, no. 8 (2013): 1057-1065.

Mori N, Fujii M, Cheng G, Ikeda S, Yamasaki Y, Yamada Y, Tomonaga M, and Yamamoto N. "Human T-cell leukemia virus type I tax protein induces the expression of anti-apoptotic gene Bcl-xL in human T-cells through nuclear factor- $\kappa$ B and c-AMP responsive element binding protein pathways." *Virus genes* 22 (2001): 279-287.

Mullen TD, Jenkins RW, Clarke CJ, Bielawski J, Hannun YA, and Obeid LM. "Ceramide Synthase-dependent Ceramide Generation and Programmed Cell Death Involvement of Salvage Pathway in Regulating Postmitochondrial Events." *Journal of Biological Chemistry* 286 (2011): 15929-15942.

Nasr R, El Hajj H, Kfoury Y, de The H, Hermine O, Bazarbachi A. "Controversies in Targeted Therapy of Adult T cell Leukemia/Lymphoma: ON Target or OFF Target Effects?" *Viruses* 3 (2011): 750-769.

Nasr R, Guillemin MC, Ferhi O, Soilhi H, Peres L, Berthier C, Rousselot P et al. "Eradication of acute promyelocytic leukemia-initiating cells through PML-RARA degradation." *Nature medicine* 14 (2008): 1333-1342.

Nasr R, Rosenwald A, El-Sabban ME, Arnulf B, Zalloua P, Lepelletier Y, Bex F, Hermine O, Staudt L, and Bazarbachi A. "Arsenic/interferon specifically reverses 2 distinct gene networks critical for the survival of HTLV-1-infected leukemic cells." *Blood* 101 (2003): 4576-4582.

O' Driscoll M, and Jeggo PJ. "The role of double-strand break repair—insights from human genetics." *Nature Reviews Genetics* 7 (2006): 45-54.

Ogretmen B, and Hannun YA. "Biologically active sphingolipids in cancer pathogenesis and treatment." *Nature Reviews Cancer* 4 (2004): 604-616.

Parrella E, Gianni` M, Fratelli M et al. "Antitumor activity of the retinoid-related molecules (E) 3-(4-hydroxy-3-adamantylbiphenyl-4-yl)acrylic acid (ST1926) and 6-[3-(1-adamantyl)-4-hydroxyphenyl]-2-naphthalene carboxylic acid (CD437) in F9 teratocarcinoma: role of retinoic acid receptor c and retinoid-independent pathways." *Mol Pharmacol* 70 (2006): 909-924.

Perry DK. "Serine palmitoyltransferase: role in apoptotic de novo ceramide synthesis and other stress responses." *Biochimica et Biophysica Acta (BBA)-Molecular and Cell Biology of Lipids* 1585 (2002): 146-152.

Pinton P, Ferrari D, Rapizzi E, Di Virgilio F, Pozzan T, and Rizzuto R. "The Ca<sup>2+</sup> concentration of the endoplasmic reticulum is a key determinant of ceramide-induced apoptosis: significance for the molecular mechanism of Bcl-2 action." *The EMBO journal* 20 (2001): 2690-2701.

Pise-Masison CA, Mahieux R, Jiang H, Ashcroft M, Radonovich M, Duvall J, Guillerm C, and Brady JN. "Inactivation of p53 by human T-cell lymphotropic virus type 1 Tax requires activation of the NF-κB pathway and is dependent on p53 phosphorylation." *Molecular and cellular biology* 20 (2000): 3377-3386.

Pise-Masison CA, Mahieux R, Radonovich M, Jiang H, and Brady JN. "Human T-lymphotropic virus type I Tax protein utilizes distinct pathways for p53 inhibition that are cell type-dependent." *Journal of Biological Chemistry* 276 (2001): 200-205.

Pise-Masison CA, Radonovich M, Sakaguchi K, Appella E, and Brady JN. "Phosphorylation of p53: a novel pathway for p53 inactivation in human T-cell lymphotropic virus type 1-transformed cells." *Journal of virology* 72 (1998): 6348-6355.

Pettus BJ, Chalfant CE, and Hannun YA. "Ceramide in apoptosis: an overview and current perspectives." *Biochimica et Biophysica Acta (BBA)-Molecular and Cell Biology of Lipids* 1585 (2002): 114-125.

Pisano C, Merlini L, Penco S et al. "Cellular and pharmacological bases of the antitumor activity of a novel adamantyl retinoid, ST1926." *J Chemother* 16 (2004): 74-76.

Ponnusamy S, Meyers-Needham M, Senkal CE, Saddoughi SA, Sentelle D, Selvam SP, Salas A, and Ogretmen B. "Sphingolipids and cancer: ceramide and sphingosine-1-phosphate in the regulation of cell death and drug resistance." *Future oncology* (2010): 1603-1624.

Pryor K and Marriott SJ. "Pleiotropic Functions of HTLV-1 Tax Contribute to Cellular Transformation." (2013).

Radin N. "Killing tumours by ceramide-induced apoptosis: a critique of available drugs." *Biochem. J* 371 (2003): 243-256.

Rahmaniyan M, Curley RM, Obeid LM, Hannun YA, and Kraveka JM. "Identification of dihydroceramide desaturase as a direct in vitro target for fenretinide." *Journal of Biological Chemistry* 286 (2011): 24754-24764.

Reynolds CP, Maurer BJ, and Kolesnick RN. "Ceramide synthesis and metabolism as a target for cancer therapy." *Cancer letters* 206 (2004): 169-180.

Sakashita A, Hattori T, Miller CW, Suzushima H, Asou N, Takatsuki K, and Koeffler HP. "Mutations of the p53 gene in adult T-cell leukemia." *Blood* 79 (1992): 477-480.

Sala F, Zucchetti M, Bagnati R, D'Incalci M, Pace S, Capocasa F, Marangon E. "Development and validation of a liquid chromatography-tandem mass spectrometry method for the determination of ST1926, a novel oral antitumor agent, adamantyl retinoid derivative, in plasma of patients in a Phase I study." *J Chromatogr B Analyt Technol Biomed Life Sci.* 1877 (2009): 3118-26.



Satou Y, and Matsuoka M. "Molecular and Cellular Mechanism of Leukemogenesis of ATL: Emergent Evidence of a Significant Role for HBZ in bHTLV-1-Induced Pathogenesis." *Leukemia Research and Treatment* 2012.

Siskind LJ. "Mitochondrial ceramide and the induction of apoptosis." *Journal of bioenergetics and biomembranes* 37 (2005): 143-153.

Siskind LJ, Kolesnick RN, and Colombini M. "Ceramide channels increase the permeability of the mitochondrial outer membrane to small proteins." *Journal of Biological Chemistry* 277 (2002): 26796-26803.

Stiban J, Tidhar R, and Futerman AH. "Ceramide synthases: roles in cell physiology and signaling." In *Sphingolipids as Signaling and Regulatory Molecules*, pp. 60-71. Springer New York, 2010.

Sun, SC, and Xiao G. "Deregulation of NF- $\kappa$ B and its upstream kinases in cancer." *Cancer and Metastasis Reviews* 22 (2003): 405-422.

Sun SY, Yue P, Lotan R. "Implication of multiple mechanisms in apoptosis induced by the synthetic retinoid CD437 in human prostate carcinoma cells." *Oncogene* 19 (2000): 4513-4522.

Suzuki T, and Yoshida M. "HTLV-1 Tax protein interacts with cyclin-dependent kinase inhibitor p16Ink4a and counteracts its inhibitory activity to CDK4." *Leukemia* (1997) 11.

Taha TA, Mullen TD, and Obeid LM. "A house divided: ceramide, sphingosine, and sphingosine-1-phosphate in programmed cell death." *Biochimica et Biophysica Acta (BBA)-Biomembranes* 1758 (2006): 2027-2036.

Tang XH, and Gudas LJ. "Retinoids, retinoic acid receptors, and cancer." *Annual Review of Pathology: Mechanisms of Disease* 6 (2011): 345-364.

Taylor GP, and Matsuoka M. "Natural history of adult T-cell leukemia/lymphoma and approaches to therapy." *Oncogene* 24 (2005): 6047-6057.

Tepper AD, de Vries E, van Blitterswijk WJ, and Borst J. "Ordering of ceramide formation, caspase activation, and mitochondrial changes during CD95- and DNA damage-induced apoptosis." *Journal of Clinical Investigation* 103 (1999): 971-978.

Tsukazaki K. "Adult T-cell leukemia-lymphoma." *Hematology* 17 (2012): 32-35.

Tsukazaki K, and Tobinai K. "Biology and Treatment of HTLV-1 associated T-cell lymphomas." *Best Practice & Research Clinical Haematology* 26 (2013): 3-14.

Valli, C. *et al.* "Atypical retinoids ST1926 and CD437 are S-phase-specific agents causing DNA double-strand breaks: significance for the cytotoxic and antiproliferative activity." *Molecular Cancer Therapeutics* 7 (2008): 2941- 2954.

Valsecchi M, Aureli M, Mauri L, Illuzzi G, Chigorno V, Prinetti A and Sonnino S. "Sphingolipidomics of A2780 human ovarian carcinoma cells treated with synthetic retinoids." *Journal of lipid research* 51 (2010): 1832-1840.

Wang G, Silva J, Dasgupta S, and Bieberich E. "Long-chain ceramide is elevated in presenilin 1 (PS1M146V) mouse brain and induces apoptosis in PS1 astrocytes." *Glia* 56 (2008): 449-456.

Wang H, Maurer BJ, Reynolds CP, and Cabot MC. "N-(4-hydroxyphenyl) retinamide elevates ceramide in neuroblastoma cell lines by coordinate activation of serine palmitoyltransferase and ceramide synthase." *Cancer research* 61 (2001): 5102-5105.

Wang ZY. "Arsenic compounds as anticancer agents." *Cancer chemotherapy and pharmacology* 48 (2001): S72-S76.

Wiesner DA, Kilkus JP, Gottschalk AR, Quintáns J, and Dawson G. "Anti-immunoglobulin-induced apoptosis in WEHI 231 cells involves the slow formation of ceramide from sphingomyelin and is blocked by bcl-XL." *Journal of Biological Chemistry* 272 (1997): 9868-9876.

Yasunaga J, and Matsuoka M. "Human T-Cell Leukemia Virus Type I Induces Adult T-Cell Leukemia: From Clinical Aspects to Molecular Mechanisms." *Cancer Control* 14 (2007): 133-140.

Yoshida M. "Multiple viral strategies of HTLV-1 for dysregulation of cell growth control." *Annu Rev Immunol* 19 (2001): 475-96.

Yoshimura S, Banno Y, Nakashima Y, Takenaka K, Sakai H, Nishimura Y, Sakai N et al. "Ceramide Formation Leads to Caspase-3 Activation during Hypoxic PC12 Cell Death Inhibitory Effects of Bcl-2 on Ceramide Formation and Caspase-3 Activation." *Journal of Biological Chemistry* 273, (1998): 6921-6927.

Zhang J, Alter N, Reed JC, Borner C, Obeid LM, and Hannun YA. "Bcl-2 interrupts the ceramide-mediated pathway of cell death." *Proceedings of the National Academy of Sciences* 93 (1996): 5325-5328.

Zhang Y, Rishi AK, Dawson MI, Tschang R, Farhana L, Boyanapalli M, Reichert U, Shroot B, Buren ECV, and Fontana JA. "S-phase arrest and apoptosis induced in normal mammary epithelial cells by a novel retinoid." *Cancer research* 60 (2000): 2025-2032.

Zheng W, Kollmeyer J, Symolon H, Momin A, Munter E, Wang E, Kelly S et al. "Ceramides and other bioactive sphingolipid backbones in health and disease: lipidomic analysis, metabolism and roles in membrane structure, dynamics, signaling and autophagy." *Biochimica et Biophysica Acta (BBA)-Biomembranes* 1758 (2006): 1864-1884.

Zuco V, Benedetti V, De Cesare M, and Zunino F. "Sensitization of ovarian carcinoma cells to the atypical retinoid ST1926 by the histone deacetylase inhibitor, RC307: enhanced DNA damage response." *International Journal of Cancer* 126 (2010): 1246-1255.

Zuco V, Zanchi C, Cassinelli G, Lanzi C, Supino R, Pisano C, Zanier R, Giordano V, Garattini E, and Zunino F. "Induction of apoptosis and stress response in ovarian carcinoma cell lines treated with ST1926, an atypical retinoid." *Cell Death & Differentiation* 11 (2004): 280-289.